HAL
open science

New Optimized Electrical Architectures of a Photovoltaic Generators with High Conversion Efficiency

Aloña Berasategi Arostegi

To cite this version:

Aloña Berasategi Arostegi. New Optimized Electrical Architectures of a Photovoltaic Generators with High Conversion Efficiency. Electronics. Université Paul Sabatier - Toulouse III, 2013. English. NNT : . tel-00849028

HAL Id: tel-00849028

https://theses.hal.science/tel-00849028v1

Submitted on 29 Jul 2013

HAL is a multi-disciplinary open access archive for the deposit and dissemination of scientific research documents, whether they are published or not. The documents may come from teaching and research institutions in France or abroad, or from public or private research centers.

L'archive ouverte pluridisciplinaire **HAL**, est destinée au dépôt et à la diffusion de documents scientifiques de niveau recherche, publiés ou non, émanant des établissements d'enseignement et de recherche français ou étrangers, des laboratoires publics ou privés.

Université de Toulouse

THÈSE

En vue de l'obtention du

DOCTORAT DE L'UNIVERSITÉ DE TOULOUSE

Délivré par :

Université Toulouse 3 Paul Sabatier (UT3 Paul Sabatier)

Présentée et soutenue par :
Aloña Berasategi Arostegi

le mardi 11 juin 2013

Titre :

New Optimized Electrical Architectures of Photovoltaic Generators with High Conversion Efficiency

---

École doctorale et discipline ou spécialité :

ED GEET : Génie Electrique

Unité de recherche :

LAAS-CNRS & TOTAL

Directeur(s) de Thèse :

Mme. Corinne ALONSO, Directrice de thèse
M. Bruno ESTIBALS, Co-directeur de thèse

Jury :

M. Christian SCHAEFFER, Président
M. Angel CID-PASTOR, Rapporteur
M. Michel AILLERIE, Rapporteur
M. Marc VERMEERSCH, Examinateur
M. Carlos CARREJO, Invité

ABSTRACT

This thesis focuses in the optimization of the efficiency of photovoltaic power conversion chain. In this way, different improvements have been proposed in the electrical architecture and its control algorithms in order to obtain high efficiency in a large rage of input power and long life-time of PV power conversion system. Using loss analysis, the benefits and drawbacks of parallel connection of power structures has been shown. This analysis has allowed the conception of a new optimized architecture constituted by parallelized power converters, called Multi-Phase Adaptive Converter (MPAC). The singularity of these power structures consists on the adaptation of the phases of the converter depending on the power production in real-time and looking for the most efficient configuration all time. In this way, the MPAC guarantees high conversion efficiency for all power ranges. Another control law is also implemented which guarantees a rotation of the phases to keep their working time uniform. Thus, the stress of the components of all the phases is kept homogenous, assuring a homogeneous aging of the phases. Since the global stress of the component is lower, the MPAC presents a longer life-time. The improvements in the power conversion stage are shown by experimental prototypes. Experimental tests have been done for global validation. Comparison with a classical power conversion stage shows the improvement in the global conversion efficiency.

AKNOWLEDGMENT – RÉMERCIMENTS

After all those years of work, there is a long list of people who have contribute in one or another way in this thesis and I would like to express them my gratitude.

First of all, I would like to thank Prof. Corinne Alonso and Prof. Bruno Estibals, my scientific directors in the LAAS-CNRS, who give me the opportunity to integrate this PV team as well as to Dr. Marc Vermeersch, my industrial director, who give me the opportunity to carry out this research work for Total group. I thank them for their advices and their encouragement along these hard years of work.

I also want to express my gratitude to my reviewers Prof. Michel Aillerie and Dr. Angel Cid-Pastor for their notable recommendation as well as to Prof. Christian Schaeffer for evaluating this work.

A special thank to Dr. Cedric Cabal. I jointed this group because he trusts in me, giving me the chance to do my internship in his orders and transmitting me his knowledge about PV and other subjects. He had been an important help in my first years of thesis. And of course, another special thank to Dr. Youssef El Barsi, who had also been an important colleague support throughout all the thesis years and helps me either in research and technical task or in human aspects.

I would also like to thank all my colleagues for their help, comradeship and endless patience. The list of people who had crossed in my way in these years is very long, all of them helped me in a smaller or bigger way: thanks to the group who take me in my arrival (Stéphane, Adan, Jean-François, Olivier, Lionel, Cyril, Pierre …), to those one that had supported me as officemate (Marcos, Zhongda, Elias, Florence, Julie, Peihua, Emilie, …), to my colleagues of lasts months (Adrien, Carlos, Valérie, Bruno, Olivier, all the *stagieres*…) and these ones that have accompanied me in coffee breaks one or another day. Thank to all of you and some others that I might forgot!

Nuria, Montse, Carlos, Martí, Isidre, Roger, Josu, Maialen, Ane, Idoia. *No puc oblidar de la meva nova família basc-catalana. Les pauses cafè, els dinars de la desesperació o de catalans i els sopars setmanals han estat un gran suport durant aquests últims mesos i no s'esborraran de la meva memòria. Moltes Gràcies!* Ezin dut nire euskal-katalan familia berria ahaztu. Kafe etenaldiak eta asteroko afari gastronomikoak laguntza handia izan dira azken hilabete hauetan eta ez ditut inoiz ahaztuko. Eskerrikasko!

Y tampoco me olvidaré de mis amigos latinoamericanos, sobre todo de Sandra, mi compañera de despacho y sufrimiento, pero también gracias a Miguel, Oswaldo y Carlos. Las comidas con ustedes fueron muy enriquecedoras.

Finally, a big thank to all my friends in Toulouse that do not exactly know what I am doing, but give me the encouragement to continue and finish this work: for those who already left la Ville Rose (Cesc, Javi, Nico,…) or are still here, in special to *les filles* (Marta, Idoia and Aitzi), *los Tulusanos*, Victoria, *ma coloc* Laura and of course, *Toulouseko euskal komunitate guztia (euskara ikasleak ere bai!)* that help me to feel as at home! *Merci, Gracias,* Gràcies*, Eskerrikasko*!

Bukatzeko, esker oso berezia Euskal Herriko familiari: batez ere nire amari baino baita ere etxekoei (Jose Luis, Joanes, Unai, Beñat), gainerako familiari eta lagunei. Nahiz eta distantziaz ez alboan izan zuen sostengurik gabe ezin izango nuen amaierara iritsi. Eskerrikasko benetan!

.

CONTENTS

Abstract I
Aknowledgment – Rémerciments III
List of Figures IX
List of Tables XIII
List of Acronyms XV

1 GENERAL INTRODUCTION 1

2 GENERALITIES: PHOTOVOLTAIC CONVERSION CHAIN 7

2.1 Introduction 9

2.2 Photovoltaic generator 10
2.2.1 Photovoltaic cell 10
2.2.2 Photovoltaic panel or module 13
2.2.3 PV cell or panel efficiency 15
2.2.4 Temperature and irradiance influences in the PV characteristics 15
2.2.5 PV cell technologies 16
2.2.6 Protections included in a photovoltaic generator 20

2.3 Power Conditioning Units 23
2.3.1 Classification of photovoltaic systems 24
2.3.1.1 On grid applications 25
2.3.1.2 Stand-alone systems 26
2.3.2 Maximum Power Point Control Tracking 27
2.3.3 MPPT efficiency 33
2.3.4 Power static converter used for matching stage 34

2.4 Definition of efficiencies in photovoltaic chains 35
2.4.1 Notion of total efficiency 36
2.4.2 Power converter efficiency 37
2.4.3 CEC and EURO weighted efficiencies 38
2.4.1 Synthesis 40

2.5 Conclusion 41

3 EVOLUTION OF PHOTOVOLTAIC CONVERSION CHAINS 43

3.1 Introduction 45

3.2 On-grid photovoltaic systems particularities 45
3.2.1 Properties of a grid connection 46
3.2.2 A static power converter concept 48
3.2.3 Main structures of power inverters used for matching PV stages 50
3.2.3.1 Number of power processing stages 50
3.2.3.2 Power inverters with Transformer 51
3.2.3.3 The H-bridge inverter 51

3.3 Power architectures of PV systems 52
3.3.1 Main grid-tied photovoltaic systems 53
3.3.1.1 String level energy management solution 54
3.3.1.2 Module Level Power Management (MLPM) photovoltaic solutions 54
3.3.2 DC-DC structures in PV systems 56
3.3.2.1 Study of classical DC-DC boost converter 57
3.3.2.2 Other DC-DC converter structures used in DC optimizers 66
3.3.3 Synthesis 71

3.4 Association of power converters 72
3.4.1 Cascaded power converters 73
3.4.2 Series connection 74
3.4.3 Parallel connection 76

3.5 Conclusion 79

4 MULTI-PHASE ADAPTIVE CONVERTER 81

4.1 Introduction 83

4.2 Study of Different control strategies 84
4.2.1 Efficiency improvement by Interleaving control mode 84
4.2.1.1 Interleaved mode 86
4.2.1.2 Current distribution control 87
4.2.1.3 Experimental prototype and control laws 88
4.2.1.4 Validation of the experimental prototype 89
4.2.1.5 Comparatives experimental results 90
4.2.2 Multi-Phase Adaptive Converter 92
4.2.2.1 Efficiency improvement by Phase adaptation 92
4.2.2.2 Example of design of a MPAC 96
4.2.2.3 Determination of power ranges 99
4.2.2.4 Phase adaptation control law 101
4.2.2.5 Life-time improvement by phase rotation 101
4.2.2.6 Other functionalities 102
4.2.2.7 Design of complete algorithm and its integrations 103
4.2.2.8 Experimental prototypes 104
4.2.2.9 Experimental results 105
4.2.2.10 Comparatives tests 107
4.2.3 Control of a MPAC based on a Look-up Table integrating an adaptive control law 113
4.2.3.1 Effects in efficiency due to working parameter of the system 113
4.2.3.2 Definition of a look up table 116
4.2.3.3 Determining optimal Pn values 116
4.2.3.4 Design of optimal look-up tables dedicated for a PV multi-phase converter like the MPAC ... 118
4.2.3.5 Experimental results done with a tri-phase boost MPAC 120

4.3 Advanced control strategies 122
4.3.1 Meteorological effects..... 122
4.3.2 Converter redundancy and over-sizing..... 123
4.3.3 Effects of temperature in electronics lifetime..... 125
4.3.4 Experimental tests: temperature profiles 126
4.4 Conclusion 129
5 CONCLUSION AND FUTURE WORKS 131
6 REFERENCES:..... 137

LIST OF FIGURES

Fig. 2.1. A schematic of a simple conventional photovoltaic cell constituted by inorganic material. Establishment of electron-hole pairs [12]. 11
Fig. 2.2. The simplest electrical representation of a PV cell. 12
Fig. 2.3. Characteristic curves of a PV cell: $I = f(V)$ in black and $P = f(V)$ in red. 12
Fig. 2.4. The *I(V)* characteristics of a PV cells compared to one PV module. a) a *n* PV cells parallel connexion and b) a *p* PV cells series connexion. 14
Fig. 2.5. A typical Photovoltaic Cell, module and array for first PV cells generation of micro-crystalline silicon material 14
Fig. 2.6. *I(V)* characteristics of a 125W_P PW6 module of Photowatt manufacturer [13] for a) different temperature levels for a constant irradiance and b) different irradiance levels with constant temperature. 16
Fig. 2.7. Evolution of different photovoltaic technologies in the last decades [14]. 17
Fig. 2.8. Example of a multijunction solar cell and its spectral irradiance absorption [31] 20
Fig. 2.9. The typical electric protections in a PV module: D_B, the blocking diode and D_{BP} the by-pass diodes 21
Fig. 2.10. Blocking diodes do not let leakage and reverse current to go into the PV module....22
Fig. 2.11. Effect of a shadow on the *I(V)* and the *P(V)* characteristics of a PVG a) with its by-pass diodes protections b) without protections. 22
Fig. 2.12. By-pass diodes allowing the circulation of the current produced by the PV module in case of shadowing conditions. 23
Fig. 2.13. *I(V)* characteristics of a PVG and the different kinds of loads that can be connected to it.24
Fig. 2.14. Simplest electrical scheme block of a typical power conversion chain. 24
Fig. 2.15. Grid connected photovoltaic system 25
Fig. 2.16. Grid connected photovoltaic system with storage system. 26
Fig. 2.17. Example of Isolated or off-grid photovoltaic system for domestic applications 27
Fig. 2.18. The algorithm of the Incremental Conductance MPPT method [42] 30
Fig. 2.19. Algorithm of the P&O MPPT method [50]. 31
Fig. 2.20. Membership function for inputs and output of fuzzy logic controller....32
Fig. 2.21. Example of a neural networks....33
Fig. 2.22. Typical efficiency characteristic of a power converter in relation with increasing input power. 38

Fig. 2.23. Representation of PV power productions profiles of 85 W_P PV module during a sunny and cloudy day (top) and the production of 1.5 W_P PV module during different seasons (bottom). 39
Fig. 2.24. Representation of the European efficiency expression as well as the efficiency characteristic evolution of a classical Boost. 40

Fig. 3. 1. PV conversion chain 46
Fig. 3. 2. Cumulative installed capacity between 1992 and 2009 in the IEA-PVPS reporting countries 46
Fig. 3. 3. Schema blocks of a) DC-DC converter and b) DC-AC inverter 48
Fig. 3. 4. Schematised energy transfer though a power converter. 49
Fig. 3. 5. Two types of PV inverter depending in number of processing stages: a) single-stage inverter and b) dual-stage inverter 50
Fig. 3. 6. Electric schema of the H-bridge inverter. 51
Fig. 3. 7. Photovoltaic system based in centralized architecture 53
Fig. 3. 8. String level energy management photovoltaic architectures: a) string topology and b) multi-string topology. 54
Fig. 3. 9. Micro-inverter, DC-optimizer and MLPM PV system installation forecast [86] 55
Fig. 3. 10. Distributed PV architectures: a) AC module and b) DC optimizer connected to DC bus and Grid-tied inverter 56
Fig. 3. 11. Two example of DC-DC structures in a distributed PV system 57
Fig. 3. 12. Electric structure of the boost power converter 58
Fig. 3. 13. ON and OFF state of a boost converter 58
Fig. 3. 14. Representation of a boost DC-DC converter by a DC transformer (a) and its equivalent circuit in primary side (b) 60
Fig. 3. 15. Equivalent model of inductor representing copper losses by series resistor RL 60
Fig. 3. 16. Boost converter circuit: when MOSFET conducts (on state), et when diode conducts (off state) 60
Fig. 3. 17. Equivalent circuit model of boost convert including an ideal transformer, diodes and MOSFET losses. 61
Fig. 3. 18. AC Current through an inductor in a typical DC-DC converter 62
Fig. 3. 19. a)The electrical representation of a MOSFET device with its parasite elements; and b) switching losses evaluation, ...63
Fig. 3. 20. Efficiency simulation of a boost converter 66
Fig. 3. 21. Three level boost DC-DC conversion structure 67
Fig. 3. 22. Two cascade boost power structure 68
Fig. 3. 23. Quadratic boost structure 68
Fig. 3. 24. Coupled-inductor DC-DC power converter 69
Fig. 3. 25. Two structure of N-stage high-step-up converters with switched capacitors. 69
Fig. 3. 26. Electric structure of a high-step-power converter with multilevel cells. 70
Fig. 3. 27. Electric structure of a resonant DC-DC converter with galvanic isolation for DC module applications 71
Fig. 3. 28. Three type of power converter connections: a) Paralleled connection, b) Series connection, and c) Cascaded connection. 73
Fig. 3. 29. Example of cascaded converters with a boost converter and H-bridge inverter. 73

Fig. 3. 30. The schema block of DC-DC series connected converters for PV application 75
Fig. 3. 31. Electric structure of the FSBB with its associated control.....76
Fig. 3. 32. Schema block of the PIPO structure.....76
Fig. 3. 33. The structure of SolarMax 4200C and 6000C inverters using Master-Slave control. 78
Fig. 3. 34. The three possible configuration of MIX system for three paralleled inverters PV system. 78
Fig. 3. 35. Comparison of conversion efficiency depending on voltage input voltage between traditional systems and Fronius IG Plus inverter with MIX system [130] 79

Fig. 4. 1. Simplest evalutaion of losses in a MOSFET 85
Fig. 4. 2. Waveforms of the output capacity tension and the inductor current for a classical Boost (a) and three Boost operating in interleaving mode. 87
Fig. 4. 3. Schema of the three paralleled Boost system with interleaved current control for PV application 89
Fig. 4. 4. Steady state behaviour of photovoltaic conversion chain (a), zoom on inductor currents (IL1, IL2 and IL3) and photovoltaic current (IPV). 89
Fig. 4. 5. Dynamic response during a solar radiation increase (a), and decrease (b). 90
Fig. 4. 6. Scheme of paralleling 3 Boost converter and a classical Boost converter for the realisation of the tests.....91
Fig. 4. 7. Daily comparison of power an efficiency between three cells interleaved Boosts converter and a classical Boost converter 91
Fig. 4. 8. Schema block of the n parallelized converters 93
Fig. 4. 9. Efficiency curves for 1,2 and 3 phases operating mode and for an algorithm based on the adaptation done for 1/3 and 2/3 of nominal power. 94
Fig. 4. 10. Efficiency curves for 1,2 and 3 phases operating mode and for the adaptation using predetermined optimal points. 94
Fig. 4. 11. Comparison of efficiencies with the two algorithms. 95
Fig. 4. 12. The working mode of N paralleled converter for a sunny day.....95
Fig. 4. 13. The electrical schema of a boost converter 96
Fig. 4. 14. Electric schema of N paralleled boost converters.....97
Fig. 4. 15. Power loss evolution for 1 and 3 phases parallelised boost converter. 99
Fig. 4. 16. Behaviour of the conversion efficiency of the MPAC operating during different configurations.....100
Fig. 4. 17. Algorithm for the converters number activation. 101
Fig. 4. 18. Algorithm of the rotation law of phases 102
Fig. 4. 19. Principle algorithm of the multi-phases converter. 103
Fig. 4. 20. Implementation of the function on the system for three static converters 104
Fig. 4. 21. Prototype of MPAC: a) User interface; b) Control; c) Power 105
Fig. 4. 22. Test of phase rotation algorithm.....106
Fig. 4. 23. Test of the algorithm for the converter number activation in interaction with the phase rotation algorithm. (SC : Static Converter) 106
Fig. 4. 24. Experimental results: a) Phase adaptation in decreasing power: from 2 to 1 active phase; b) Phase adaptation in power: from 3 to 2 active phases.....107
Fig. 4. 25. Comparison of one phase boost converter (a) and MPAC (b) energy production in a sunny day. 108

Fig. 4. 26. Comparison of efficiencies of one phase boost converter and three phase MPAC.....109
Fig. 4. 27. One phase boost converter (a) and MPAC (b) energy production in a sunny day.....109
Fig. 4. 28. Comparison of efficiencies of one phase boost converter and three phase MPAC.....110
Fig. 4. 29. One phase boost converter (a) and MPAC (b) energy production in a sunny day.....110
Fig. 4. 30. Comparison of of efficiencies between one phase boost converter and a three phase MPAC prototypes. 111
Fig. 4. 31. Experimental measurements of power production for a classical boost and for our MPAC converter. 112
Fig. 4. 32. Efficiency evolution for on phase for different inputs and outputs voltage levels. 114
Fig. 4. 33. Effects of the temperature in the value of RDS(on) resistance for IRFR024N MOSFET [139] 115
Fig. 4. 34. Effects of the of the temperature in the value of Voltage drop (Vf) for MBRD620CT Diode [140] 115
Fig. 4. 35. The experimental evolution of efficiency for different output voltage levels for respectively one, two and three phases working modes for three 100W phase paralleled converter. 117
Fig. 4. 36. Distribution of P_1 and P_2 values for different input and output voltage levels.....117
Fig. 4. 37. The structure of the Look-up table used for the MPAC takes into account three variables: input voltage, output voltage and temperature. 118
Fig. 4. 38. Schema of the simulated power of the power part in PSIM.....119
Fig. 4. 39. Schema of the MPAC using a look-up table as shown in fig. 4. 37.....119
Fig. 4. 40. Simulation results of the adaptive control for multi-phase converter based on look-up tables. 120
Fig. 4. 41. P1 and P2 variation according to the input voltage 120
Fig. 4. 42. Comparison between a fix and adaptive crossing points algorithms 121
Fig. 4. 43. Evolution of photovoltaic power production in a perturbed working day (a) and the principle of working of the anticipation algorithm (b and c). 123
Fig. 4. 44. Experimental prototype of MPAC where each phase is easily changeable in case of failure of one of them.....125
Fig. 4. 45. Electronic power device working in a) 25°C and b) 100°C 125
Fig. 4. 46. Micro-fissures in a wire bonding after N thermal cycles.....126
Fig. 4. 47. Image of power converter by thermal camera where the temperatures has been measured.....126
Fig. 4. 48. Temperature comparison between the diodes of one phase structure and three phase structure for a simulated sunny day. 127
Fig. 4. 49. Temperature comparison between the diodes of one phase structure and three phase structure for a simulated sunny day with sudden clouds or shadows.....128
Fig. 4. 50. Temperature comparison between the diodes of one phase structure and three phase structure for a simulated day. 129

LIST OF TABLES

Table. 2.1. Confirmed terrestrial module efficiencies under standard conditions. 20
Table. 2.2. Fuzzy rule base table [64] 32
Table. 2.3. Comparison of major characteristics of PV array MPPT techniques [34]. 34

Table 3.1. Values of individual harmonic voltages at the supply-terminals for orders up to 25. The THD of supply voltage, including all harmonics up to the order 40, shall be less than 8% [77]. 47
Table 3.2. EN 61000-3-2-A harmonic current limits [77]. 47
Table 3.3. Simulation parameter for efficiency calculus: 66
Table 3.4. Components parameter for the efficiency simulation 66
Table 3.5. Review of presented DC-DC converter structures: 71

Table 4.1. Electrical features of the photovoltaic array: 90
Table 4.2. Synthesis of one day of measures: 92
Table 4.3. Energy production of 5 days in December. 112
Table 4.4. P1 and P2 turning points variations Vs. VIN 121

LIST OF ACRONYMS

AC	Alternating current
A_{eff}	Effective Area
BMS	Battery Management System
CEC	California Energy Commission
D_B	Blocking Diode
DC	Direct Current
D_{PB}	By-pass Diode
E_e	Irradiance
EMI	ElectroMagnetical Interference
EURO	European
FSBB	Four-Switch Buck-Boost
G	Photon power for unity of surface
η_{MPPT}	MPPT control efficiency
η_{PV}	Photovoltaic Efficiency
η_{CEC}	California Energy Commission Efficiency
η_{Conv}	Converter Efficiency
η_{EURO}	European Efficiency
η_{PC}	Power Converter Efficiency
$\eta_{PVchain}$	Photovoltaic Conversion Chain Efficiency
η_{Total}	Total Efficiency
I	Current
I_{cell}	Cell current
I_D	Diode current
I_{IN}	Input Current
IncCond	Incremental Conductance
I_{opt}	Optimal Current

I_{OUT}	Output Current
I_{ph}	Photocurrent
I_{PV}	Photovoltaic Current
I_{ref}	Reference Current
I_{SC}	Short Circuit Current
I_{string}	String Current
K	Boltzmann Constant [$1.38*10^{-23}$ JK^{-1}]
L	Inductance
MLPM	Module Level Power Management
MPAC	Multi-Phase Adaptive Converter
MPP	Maximum Power Point
MPPT	Maximum Power Point Tracking
P	Power
P&O	Perturb and Observe
PCU	Power Conditioning Unit
P_{IN}	Input Power
PIPO	Parallel Input - Parallel Output
P_{Loss}	Power Losses
P_{MAX}	Maximal Power
P_{MPP}	Maximum Power Point Power
POL	Point of Load
P_{OUT}	Output Power
PV	PhotoVoltaic
PVG	PhotoVoltaic Generator
PWM	Pulse Width Modulation
R_{DSon}	Drain-Source Resistance
R_s	Series Resistor
R_{sh}	Shunt Resistor
SC	Static Converter
THD	Total Harmonic Distortion
UPS	Uninterruptable Power Supply
V	Voltage
V_{bat}	Battery Voltage
V_{cell}	Cell Voltage
V_{OC}	Open Circuit Voltage
V_{IN}	Input Voltage
V_{opt}	Optimal Voltage

V_{OUT}	Output Voltage
V_{PV}	PhotoVoltaic Voltage
V_{ref}	Reference Voltage
VRM	Voltage Regulator Module
ZCS	Zero Current Source
ZVS	Zero Voltage Source

CHAPTER 1

1 GENERAL INTRODUCTION

INTRODUCTION

The world energy consummation of electricity has been strongly linked to the industry and communication media development in the last decades. Nowadays, the most of consumed energy is produced by non renewable energies as carbon, natural gas, petrol or uranium. The recovery time of this type of energy source is extremely slow compared to the human life scale. Sooner or later, the high probability of end of these resources must be taken into account. Moreover, as the consumer energy demand does not stop increasing in all around the world, being day after day superior to the offered global energy, energies crisis can be periodically observed with more and more violence. The case of petroleum resources is the representation of a critical situation example, as shown by the high fluctuations in the global petrol price during the last fifty years.

In addition, this kind of energy consumption has important effects in the environments impact. Actually, the hydrocarbon and the carbon cause important emissions of greenhouse gas every day, which have direct relation in the climatic disorders and in the pollution increases. These worrying facts encourage more and more the research of innovative solutions which will limit the energetic deficit and negative impacts in the environment. In this way, a lot of governments and energy producers sustain since a long time the development of non polluting sources of energy.

For instance, in parallel of eating and health, developing renewable energies is one of the European Union's priority strategies to fight against climate warning and reduce dependency on fossil fuels. According to Kyoto's protocol which was signed by 191 states including France, the greenhouse effect gas emissions had to be reduced at least by 20% by 2020 compared of 1990 [1]. Countries as United States and Canada did not sign this petitions. Nevertheless, a regional initiative of North-Eastern United States and Eastern Canada regions has created the Regional Greenhouse Gas Initiative to reduce greenhouse gas emissions [2].

Solar, wind, geothermic, hydraulic or even biomass are said to be the renewable energy resources of the future. In contrary of fossil energies, these renewable energies are unlimited energy resources. The solar energy is abundantly available and it is not a greenhouse effect gas emitter. For this reason, it is considered as one of the most adapted solutions to the current needs of electrical energy production. In the last years, the three methods of solar energy exploitations, solar thermals, concentrated solar power and solar photovoltaic (PV), have undergone an important increase. In the global of European Union countries, for the year 2011, the solar thermals had reach the amount of 25 GW_P installed power, concentrated solar power produced 1959 MW_P and more than 51 GW_P of photovoltaic power were installed.

This thesis has been developed in a contractual context between Total SA and the laboratory LAAS-CNRS. Both organizations are sensitive with the development of renewable energies and they make special effort in the research and development of this kind of energy sources. In 2007, they decided to join their efforts to develop some innovative PV systems concepts. The solar PV energy production, and specially its conversion and optimization are the main subjects of this thesis made in this scientific context.

Although Total S.A. is actually a petrol enterprise, it is concerned with the future alternative energies. For this reason, the Total group has a relatively new group of new energies, which makes researches not only in all the elements of photovoltaic energy systems but also in solar concentrated, sea wave and biomass energies. TOTAL has been involved in photovoltaic energy research (crystalline silicon, thin film, organic PV and CSP) since 1983. Their interest in PV systems is more visible since the group acquired the 60% of the monocrystalline PV module manufacturer SunPower in 2011.

The Laboratory of Analysis and Architecture of Systems (LAAS) is a unit within the French National Center for Scientific Research (CNRS). It has a long history in photovoltaic research since its beginning in 1967. For more than 15 years, the study of PV systems has been increased in this laboratory either studying power conversion structures, storage systems or MPPT controls. Today, the laboratory has a new study platform named ADREAM to reach the researches. The collaboration between Total and LAAS began with ATOS ANR project, within the objective of optimize the coupling of thin film PV cell in Tandem modules. Since this project, the collaboration continues through other contract collaborations.

Even if solar photovoltaic energy is still a minor energy source compared to other sources, the last years it has been presented as an important potential of innovative and robust energy production source. In this way, the European Union supports and promotes the development of the solar energy field by financing research project. Moreover, many European governments offer help to users as feed-in tariffs (FIT), capital subsidies or tax credits to facilitate the accessibility of this energy. For these reasons, the photovoltaic field has presented the biggest annual growth rate between 2000 and 2010 [4] and this increasing tendency has a high percentage of probability to continue in following years.

Although this increasing tendency, the PV energy source has still insignificant presence compared to fossil energies, which gives an important growing margin. The presence of the PV energy production is still anecdotal in almost all around the world, and even more, in countries like France where the most part of the energy production is carried out by nuclear energy and the PV energy production only takes the 0.79% of total electrical energy production [3]. In fact, the PV energy is still expensive due to the price of its sensors (PV modules) and its lack of robustness compared to other energies. Today, the major reason of its development beyond its drawbacks resides in governmental subsidies helps. To overcome its constant development, it is important to increase the Photovoltaic power production and reduce drastically its global price.

Three parameters can be improved in order to reduce the price and make it more affordable to all users:

- the reduction of cost of each part of the PV system to decrease drastically the investment;
- the increase of efficiency of each component for a bigger power supply to the final user
- the enlargement of life-time to augment the power production time.

One of the first difficulties to improve the energy conversion efficiency in photovoltaic systems resides in the non lineal and extremely changeable characteristic of the power production of photovoltaic generators (PVG) linked to meteorological phenomena. In effect,

the solar irradiation and the temperature determine the power production of a PVG in each moment, and therefore the working condition of the power conversion system. The large amount of operating points that presents photovoltaic applied power converters complicates their design.

Another important issue in photovoltaic power conversion systems resides in its life-time. Nowadays, the life-time of photovoltaic sensors is guarantee for more than 25 years. Today, this is not the case of the electronic devices that are needed to connect PV arrays to a load. They do not satisfy users exigencies due to the high cost of the initial investment. Moreover, a failure in the power conversion element involves a stop in a high part of PV power production. To increase the PV energy production, the improvement of the life-time and the reliability are very important. Many factors accelerate the aging of power converter components. The electrical stress and thermal stress are two of the most important factors that must be reduced in order to improve life-time prevision.

The main purpose of this thesis is to improve a Photovoltaic (PV) power conversion system and achieve a new power converter with high efficiency and life-time improvement. The presentation of the work has been divided into three major parts. First, an overview of the photovoltaic system generalities will be presented in Chapter 2. The main elements and their characteristic of the photovoltaic system are remembered. In addition, a classification of different kind of photovoltaic system will be explained. Finally, the notions of efficiency of the global photovoltaic system and each elementary part are defined. These definitions are used to evaluate the photovoltaic power conversion structures and they help to determine the action areas in order to improve the efficiency characteristic of photovoltaic converters.

In the chapter 3, the state of art of on-grid PV systems is presented, analyzing from different types of general architectures as centralized topologies to more distributed topologies as the AC module. A special focus will be done in distributed topologies with DC optimizers that maximize the energy extraction and conversion of individual PV modules. The inter-connection between power converters and specially the parallel connection will be also studied.

Finally, the chapter 4 is dedicated to the presentation of a new structure based in paralleled converters which integrates controls laws to improve the efficiency and the life-time of power converters. Basing in losses analysis that shows the benefits and drawbacks of simple and multi-phase converters, an optimized architecture constituted by parallelized power converters, called Multi-Phase Adaptive Converter (MPAC) has been presented. Control laws which are patented allow the adaptation and rotation of phases depending on the power production in real time, reaching a more efficient converter. This control also improves the electric and thermal stress of components, guaranteeing a homogeneous aging. This control laws has lead to two patents about the management of adaptation points depending on the instantaneous power production and the meteorological effects [5]-[6]. Experimental tests have been done for global validation. Comparisons with a classical power conversion stage show the improvement in the global conversion efficiency which can be significant if we consider the total cycle of life of the PV systems.

The conclusion and possible future works associated to this thesis will be specified in the chapter 5.

CHAPTER 2

2 GENERALITIES: PHOTOVOLTAIC CONVERSION CHAIN

2.1 Introduction

Photovoltaic effect was presented for the first time by the French Physicist Alexandre-Edmond Becquerel in 1839 [7]. However, it is only in 1883 when Charles Fritts built the first photovoltaic cell (PV cell) producing electrical current that this discovery was recognized. Nevertheless this major advance in solar energy conversion did not immediately lead to innovations because the used materials were too expensive (a selenium substrate covered with an extremely thin layer of gold) and this type of PV cell had a very low efficiency. Only around 1% of the solar irradiance energy received at the surface of the sensor was converted in electricity.

The modern photovoltaic cell was first developed at Bell Laboratories in 1954 [8]. It was constituted by a diffused silicon PN junction and presented 4.5% of efficiency of converted solar power. In the same period, the interest for photovoltaic source highly increased linked to spatial applications which needed their own energy production source whatever the cost. Thanks to the use of photovoltaic systems in this area, cell efficiency was improved until 14% for the 1960.

In the beginning of 1970s, Dr. Elliot Berman designed a relatively cheap solar cell by using a poorer grade of silicon, which came for the silicon scrapings of microelectronic systems. In addition, the packaging of these cells was also done with cheaper materials [9], bringing the price down from $100 to $20 per watt. This huge cost savings opened up a large number of applications that were not considered before because of high costs and solar technology became practical for technologies other than satellites. Photovoltaic cells began powering navigation warning lights, horns on offshore oil rigs, lighthouses, railroad crossings, and many small domestic applications. This technology became present in households where connection to the traditional electricity grid was not affordable.

In 1980s, large standalone photovoltaic systems appeared. These systems are interesting because they can be considered as real electrical power generator sources. Large-scale, centralized solar-plants were favoured, in geographic sites where the construction of global electric-line systems was difficult, as distanced big cities and production plants in USA. Ambitious programs were initiated linked to new concepts like smart-grids. Later, PV systems were adapted to individual users or integrate buildings. Roofs quickly became good locations to PV sensors in domestic applications and their electrical power productions. In parallel, new photovoltaic cells technologies have been developed to increase their efficiencies and lifetime and reduce the manufactured cost. In 1984, the first amorphous silicon solar cell was introduced by ARCO [10] and in 1986, it was the first thin film photovoltaic module. New electrical structures of converters also appeared, which were more adapted to building integrate photovoltaic installations by specific electrical architectures and integrating particular control laws named MPPT. In these new types of power chains, new protections against hot-spot and reverse currents were integrated, providing more robustness and reliability to photovoltaic installations.

In the last 20 years, the world photovoltaic production has followed a constant and intense evolution. The price of photovoltaic installation drastically decreases thank to the impulsion of big photovoltaic projects carried out in Germany, Japan or USA and financial incitements proposed by the governments of different countries [11]. Nevertheless, although the efficiency of some photovoltaic cells has greatly increased, the integration of this

performing technology has not become feasibly on a large scale in terrestrial fields, and more particularly for individual homes. Indeed, except of spatial supplies which use the most efficient technology that currently exists, the efficiency of current PV cells used in PV farm or new building, is significantly low.

Nevertheless, costs of PV sources remain too high in comparison of fossil sources. One important potential innovative step to decrease global cost can be focused on the photovoltaic converter efficiency improvement. Indeed, a high level of losses can be appreciated on electrical matching of bad quality. Another important perspective with a high potential of innovation resides in keeping and guarantying high power conversion efficiency in the many different working conditions that must support a power installation as can be different sunlight capture levels and storage levels or to achieve a global high efficiency during the totality of its life-time. The work of this thesis was done in this global scientific problematic and was particularly focused on the efficiency improvement in all power conversion level stages between PV cells and loads.

In this chapter, an overview concerning the generalities of photovoltaic systems are remembered to introduce our work and to facilitate reader understanding the innovations presented in other chapters. In particular, the main elements composing a PV energy conversion chain have been defined, as well as some examples of classical control systems and protections modes that are today integrated in classical photovoltaic complete systems independently of the kind of the application. In addition, we remember classical evaluation methods used in PV systems. They are well-known in academic and industrial parts, and become the referent efficiencies criteria included in norms and technical data sheets. They are useful to better understand where must be done the priority improvements to increase the efficiency. Thus, the losses of the global system and their impact in the global efficiency are precised.

2.2 Photovoltaic generator

A photovoltaic generator (PVG) can be considered an energy source which directly generates power electricity by converting solar radiation into direct current electricity. Semiconductor materials able to create photovoltaic effect are used for this purpose. A PVG can produce electric power from milliwatts to several megawatts, depending on its size, composition and structure design. The smallest element of this type of generator is constituted by an elementary solar PV cell. Its technical size impacts its intrinsic performances. The interconnection of several solar cells gives PV modules or panels, which can be also connected together to create a high power global array with several PV strings. These different elements will be defined and detailed in the following part.

2.2.1 Photovoltaic cell

The basic element of a PV system is a solar cell or a PV cell which could be considered as a sensor of photon energy. Depending on the material used for their manufacturing, two different families can be distinguished: inorganic and organic PV cells. In the first family, the heart of each solar cell is a PN junction (quite similar of a PN junction diode structure used in electronics). Indeed, all semiconductor materials have the ability to absorb solar spectrum and convert a portion of the absorbed photons energy to carriers of electric current. Each material has different properties and can only convert a little part of the

solar spectrum depending on its physical properties but also on its atomic structures and sizes.

To generalize, a semiconductor material used to make a PV PN junction collects a percentage of energy carried by photons, transforms it in electrons creating currents collected via connectors and conducts them to a load before recombination. The generated electrical current is proportional to the irradiance received at the surface of the PV cell.

An example of a simple conventional solar cell structure done by crystalline silicon is depicted in fig. 2.1. [12]. Sunlight spectrum is incident from the top, on the front of the solar cell. A metallic grid forms one of the two electrical contacts of the diode and allows light to fall on the semiconductor PN junction between the grid lines and thus be absorbed and converter into electrical energy. An antireflective layer can be added between the grid lines to increase the amount of light transmitted to the semiconductor. Grid connections at the bottom of the PV cell can be done by metallic materials that have high electrical conduction property. It can be semi-transparent to increase active surface of the PV cell. The semiconductor diode is formed when n-type semiconductor and p-type semiconductor are brought together to form a metallurgical junction. This is typically achieved through diffusion or implantation of specific impurities (dopants) or via a deposition process. The other electrical contact of the diode is formed by a metallic layer on the back of the solar cell.

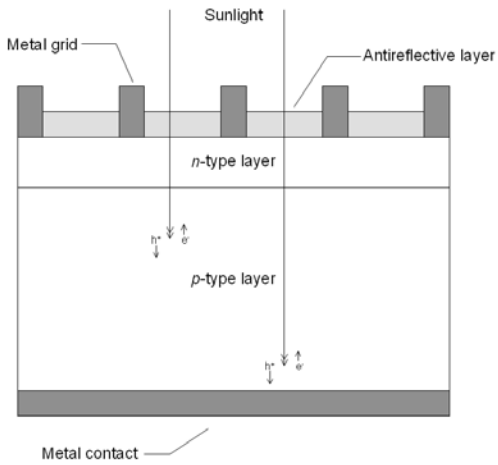

Fig. 2.1. A schematic of a simple conventional photovoltaic cell constituted by inorganic material. Establishment of electron-hole pairs [12].

The simplest model able to represent the behaviour of a photovoltaic cell is using an ideal current source I_{ph} in parallel with a diode (fig. 2.2). The R_s and R_{sh} resistances represent respectively the series and shunt resistances in the solar cells. The operating equation of current-voltage *I(V)* static characteristics, that can be also noted as $I = f(V)$, of a solar cell can be easily described by its electrical representation [7]:

$$I_{cell} = I_{ph} - I_D \tag{2.1}$$

$$I_{cell} = I_{ph} - I_o\left[e^{\frac{q(V_{cell}+R_s I)}{Ak_B T}} - 1\right] - \frac{V_{cell} + R_s I}{R_{sh}} \tag{2.2}$$

Where:

- I_{ph} *(A)* is the photocurrent,

- I_o *(A)* the saturation current,
- *A* the identity factor,
- *q (C)* the electronic charge,
- k_B *(JK^{-1})* Boltzmann's gas constant,
- *T(K)* the junction temperature,
- R_s *(Ω)* the series resistance,
- R_{sh} *(Ω)* the shunt resistance.

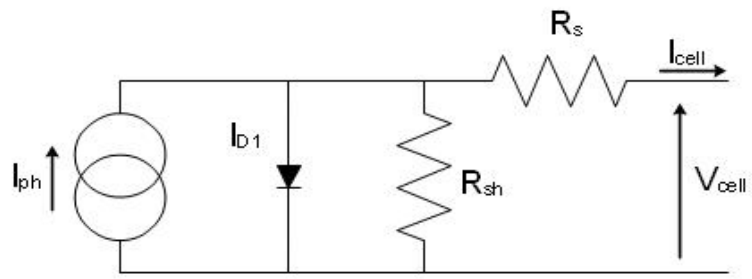

Fig. 2.2. The simplest electrical representation of a PV cell.

The equation (2.2) and its associated model have often been used in this work to represent the PV module behaviour in the global electrical PV chain model. Indeed, it represents main physical phenomena and can be easily implemented in the electrical simulation tools. The main limits of this model are the lack of the dynamic and heating physical phenomena of the PV cell. However, in a global system approach, this model can be considered sufficient to reproduce the behaviour of the PV cell and fit real conditions I_{cell} and V_{cell} as well as its interaction with other elements of the system.

The *I(V)* characteristics describe the electrical solar cell behaviours under the meteorological conditions in steady state cases (irradiance level and ambient temperature). To generalize, a solar cell graphs ($I = f(V)$ and $P = f(V)$), illustrated in fig. 2.3., have three significant points :

- the short-circuit current named I_{SC},
- the open-circuit voltage named V_{OC},
- the maximum power point called MPP.

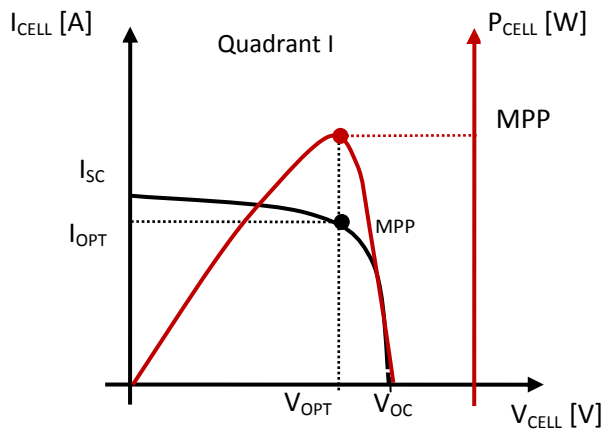

Fig. 2.3. Characteristic curves of a PV cell: $I = f(V)$ in black and $P = f(V)$ in red.

For V_{cell}=0 (short-circuit conditions), the produced current can be described with the following equation:

$$I_{SC} = I_{ph} - I_o\left[e^{\frac{q(V_{cell}+R_s I)}{Ak_B T}} - 1\right] - \frac{R_s I}{R_{sh}} \tag{2.3}$$

Nevertheless, the series resistance effect can be neglected in short-circuit conditions. In a first approximation, the short-circuit current can be considered equivalent to the photocurrent I_{ph}, which in this case, is proportional to the irradiance E_e (Wm^{-2}):

$$I_{SC} = I_{ph} = KE_e \tag{2.4}$$

At I_{cell} =0 (open-circuit conditions), all the light-generated current I_{ph} is flowing through the PV diode. Thus, the open-circuit voltage can be written as:

$$V_{OC} = \frac{Ak_B T}{q}\ln\frac{I_{ph}+I_{o1}}{I_{o1}} \approx \frac{Ak_B T}{q}\ln\frac{I_{ph}}{I_{o1}} \tag{2.5}$$

The last significant point of the *P(V)* curve form is the MPP which presents a maximum corresponding to the producible maximum power. This classical point is referred at the couple of electrical parameters named $V_{PV}=V_{opt}$ and $I_{PV}=I_{opt}$. As seen in fig. 2.3, this point defines an area, given by $P_{MPP}=V_{opt}*I_{opt}$, which is the largest rectangle for any point on the *I(V)* curve. For evaluate the quality of a cell, this rectangular can be compared with the one done by $I_{cc}*V_{oc}$ and we can introduce the definition of the PV form factor FF that is $P_{MPP}/(I_{cc}*V_{oc})$. More this factor is near than 1, more the PV cell can considered done with good trade-offs and near of its ideal characteristics.

2.2.2 Photovoltaic panel or module

Even using new generations of PVG with high efficiencies materials, current and voltage generations of one PV cell are very low to be used directly in domestic or industrial applications. For example, an elementary PV cell built in silicon provides several watts with less than one volt voltage level, which corresponds to the PN junction voltage drop of diodes.

In order to produce higher powers, the photovoltaic cells can be connected to create PV panels or modules. A series connection of cells increases the voltage of the generator, while the parallel connection increases its current (fig. 2.4.). Today, in classical modules/arrays, series and parallel interconnections of PV cells are used to obtain the needed PVG with the desired voltage and current characteristics.

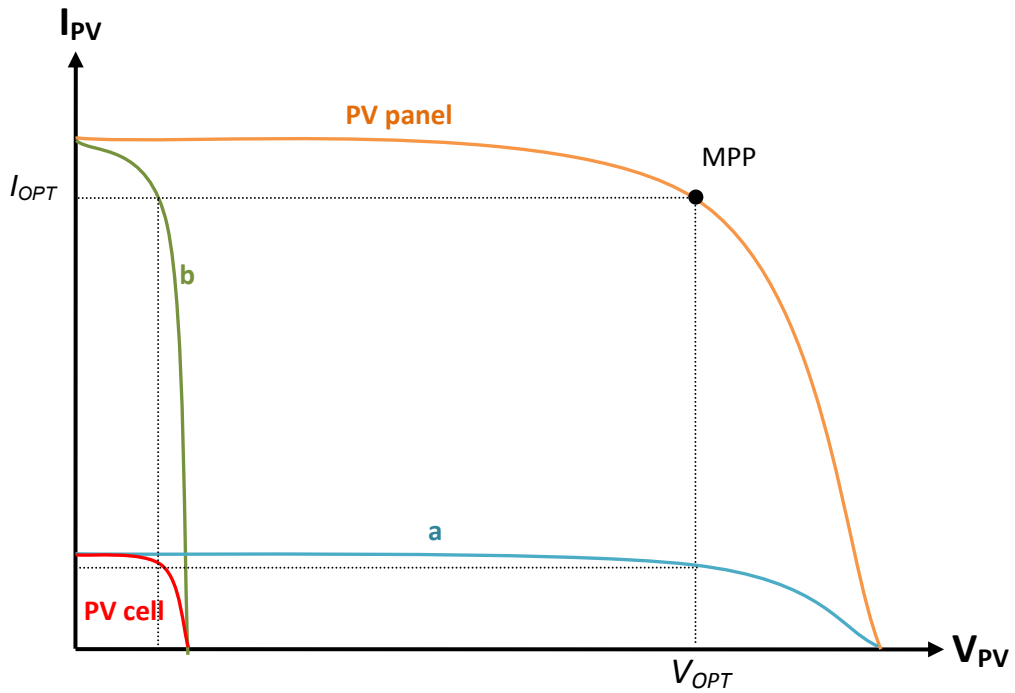

Fig. 2.4. The *I(V)* characteristics of a PV cells compared to one PV module. a) a *n* PV cells parallel connexion and b) a *p* PV cells series connexion.

As a PV cell, the characteristic of a PV module/array presents a Maximum Power Point (also named MPP) with associated current and voltage called respectively I_{OPT} and V_{OPT}. Nevertheless, the operating point of a PV module depends on the load connected to its output port. For instance, in the case of a battery connection, if a direct connection is done, the voltage of the battery will impose the working condition of the photovoltaic module.

Moreover, for high power PV applications and to achieve the desired voltage and current, modules are wired in series and parallel into what is called a PV Array. The flexibility of the modular PV system allows designers to create solar power systems that can get to a wide variety of electrical needs. Fig. 2.5. shows a PV cell, A PV module and a PV array.

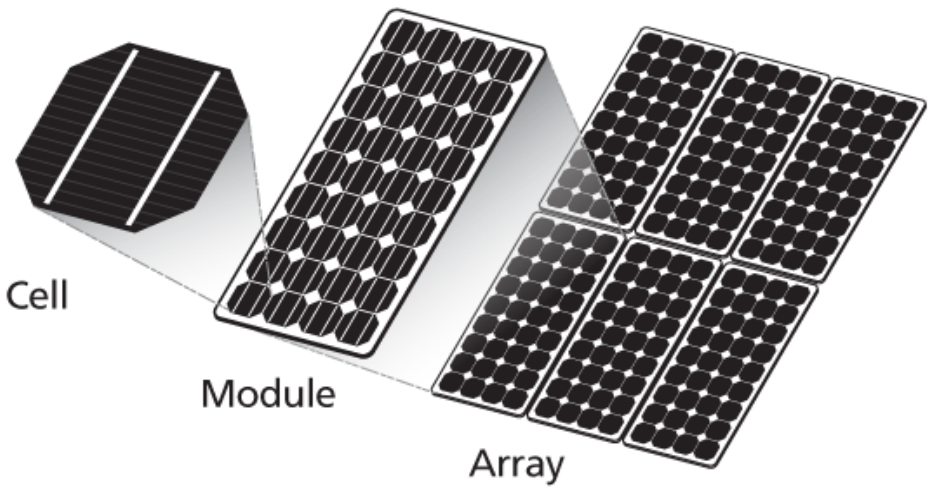

Fig. 2.5. A typical Photovoltaic Cell, module and array for first PV cells generation of micro-crystalline silicon material

2.2.3 PV cell or panel efficiency

The conversion efficiency of a PV cell represents the proportion of the photons energy that the PV cell can convert into electrical energy. Therefore, the maximum conversion efficiency of photons into electrical energy is named η_{PV} and it is defined by the following equation:

$$\eta_{PV} = \frac{P_{MAX}}{G.A_{eff}} \tag{2.6}$$

Where, P_{MAX} is the maximum energy potential available in the output of the PV panel; G (w/m²) the irradiance representing the photon power for unity of surface; and A_{eff} (m²) the effective area of the PV panel.

This efficiency depends on the material and technique used in the manufacturing of the photovoltaic cells. It is given by the manufacturers in data sheets of the PV panels. It is measured in specific standard conditions, i.e. 25°C of ambient temperature and under a normed irradiation of 1kW/m² which corresponds to 1,5AM[1].

2.2.4 Temperature and irradiance influences in the PV characteristics

External influences as irradiance and temperature have a direct impact in the photovoltaic energy production. Therefore the *I-V* characteristics of a PV cell are directly dependant on these factors.

Given for different values of solar irradiance, datasheets indicate the behaviour of *I(V)* and *P(V)* characteristics.

An example of these characteristics can be shown in fig. 2.6 : a PVG of a 125 W_P PW6 module of Photowatt manufacturer [13].

To simplify, the main effect of temperature can be seen in the value of V_{OC}. In effect, higher is the level of temperature, lower is the value of V_{OC}.

In the other part, the influence of the irradiation is more important in the I_{SC} current. Then, higher is the level of solar irradiation, higher is the I_{SC}, and in this way, higher will be the PV power.

[1] AM for Air Mass : refers to the length of the path through the atmosphere in relation to the shortest length if the sun was in the apex. 1.5AM correspond to irradiance received in the earth, in 0° altitude and in a solar zenith angle of *z*=48.2°.

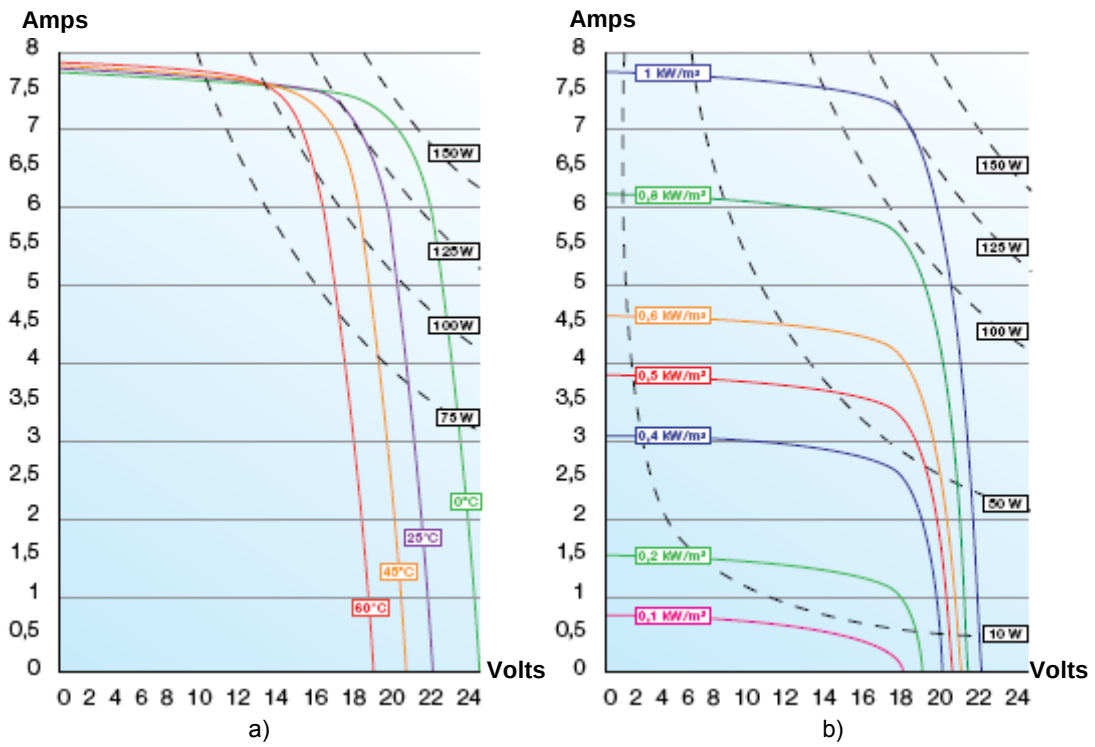

Fig. 2.6. *I(V)* characteristics of a 125W_P PW6 module of Photowatt manufacturer [13] for a) different temperature levels for a constant irradiance and b) different irradiance levels with constant temperature.

2.2.5 PV cell technologies

Nowadays, different techniques are used for the manufacturing of photovoltaic cells. Solar cells can be also fabricated from many different semiconductor materials. Nevertheless, the most commonly are made by silicon (Si): crystalline, polycrystalline, and amorphous. Other semiconductor materials such as GaAs, GaInP, Cu(InGa)Se2, and CdTe, to name a few of them are also used to make PV cells.

The fig. 2.7. shows a global vision of the efficiency evolution of these different technologies according to new improvements in the time, synthesized each year by NREL [14]. There is presented a detailed comparison of main families of photovoltaic technologies, as well as their efficiency progress in the time. We can notice in this graphic the progress of efficiency of each technology year after year.

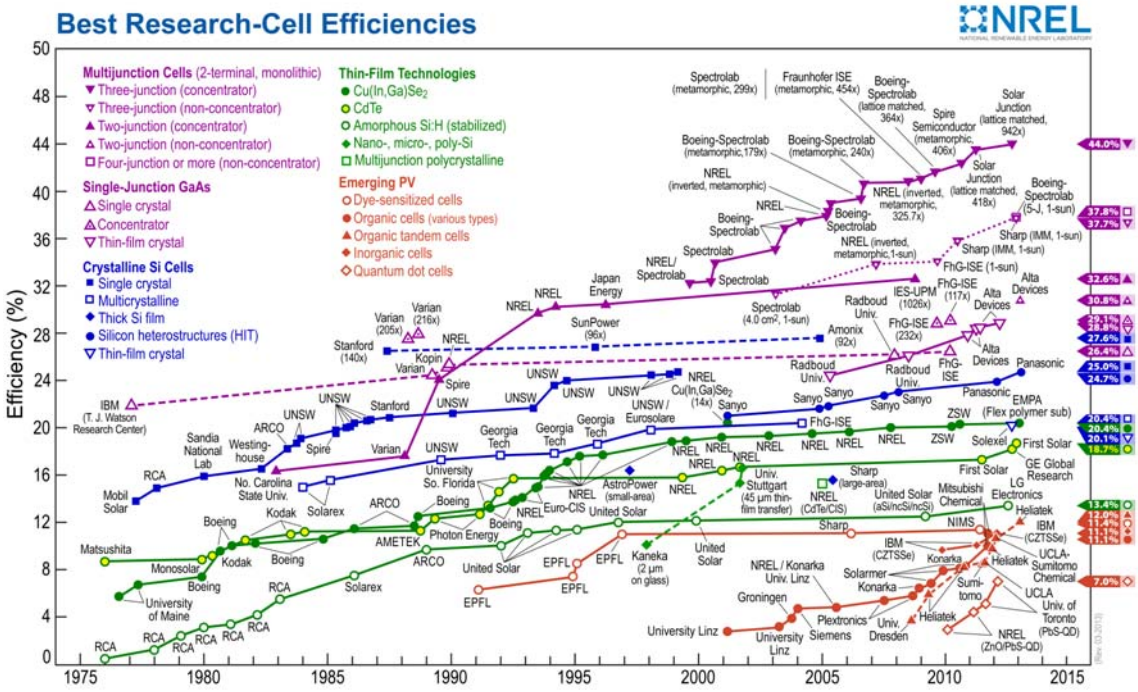

Fig. 2.7. Evolution of different photovoltaic technologies in the last decades [14].

The choice of each technology depends on different compromises between the energetic efficiency, associated bulk and price. Several large families of PV cells can be distinguished according to the used technology. We can signal the main ones.

- **Crystalline Si cells**

Crystalline silicon PV cells are the most common photovoltaic cells used today. They are also the oldest ones developed in a large way for domestic application since the sixties. This family has dominated PV technology from the beginning. It constitutes more than 85% of the PV market today. Although declination in favour of other technologies has been announced in the past numerous of times, these cells will presumably retain their leader role for a long time, at least in the next decade.

Crystalline silicon is the dominant family in the PV field because it can be easily linked to the evolution of microelectronics development. Another reason is the abundant resource of silicon in the world, making the cheapest cells. In this of photovoltaic cells family, two technologies can be distinguished:

1) **Monocrystalline silicon cell**: Monocrystalline silicon is an ordered crystal structure, with each atom ideally lying in a pre-ordained position. The framework of these PV cells presents an extreme crystalline perfection and very low quantity of impurities. For these reasons, it is the most efficient PV technology. The efficiency-record for laboratory PV cells is in 24.7%, record achieved in 1999 [15]. On a commercial scale, today SunPower fabricates the highest efficiency crystalline solar cells, arriving to manufacturing in large scale 24.2% efficiency solar cells near of the higher theoretical efficiency obtainable with this type of material [16]. However, the careful and slow processes required in the manufacturing become this photovoltaic cells the most expensive of silicon ones.

2) **Polycrystalline silicon**: These kinds of PV cells are less efficient than the mono-crystalline ones. However, drastic reduction on module manufacturing costs based on these types of materials can be done with equivalent life time [17]. Nevertheless, the purity of these cells is lower than the previous devices. The efficiency record of this kind of PV cells is 19.3% in 2010 [18] and commercial devices achieve efficiencies around 13%.

- **Thin films technologies :**

The term “thin film” makes reference from the method used to deposit a film, not directly referred to the thinness of the film itself. Thin-film cells are made from techniques of deposit materials in very thin and consecutive layers of atoms or molecules.

The main reasons on the development of these thin-films technologies are that the production of PV modules requires less energy and materials and then, they can be less expensive. Thin-films have the properties to be deposited over very large areas making more easily high A_{eff} than the previous silicon cells, and they can be recreated series–connected cells in a fast and inexpensive way to increase their PV voltage. Nowadays, both the efficiency and the long-terms stability of thin-film PV modules are improving [19],[22]. Simultaneously their manufacturing costs are constantly decreasing. Thin-film PV modules are particularly attractive for emerging applications such as green-field PV power plants and building-integrated PV.

These techniques can use silicon but also other materials with big absorption coefficient of the solar spectra. Although there are numerous materials able to be used to make thin-film PV cells, we do not list all of them because they are not the precise subject of this PhD. We can mention main materials used to create thin-films photovoltaic cell. For more details of this type of technology, it can be read [23]. We can signal the main well-known techniques used today in industrial arrays:

1) **Amorphous silicon**: In general, amorphous solids, such as common glass, are materials whose atoms are not arranged in any particular order. Thus, they do not form any crystalline structures and they contain large numbers of structural and bonding defects. Amorphous Si PV cells can be deposited at a low temperature on inexpensive substrates with a low-cost continuous or batch process. This manufacturing way is environmental friendly, it do not use heavy metals or rare elements and it requires low amount of silicon [24]. They have a lot of economic advantages over other materials that make them appealing for use in PV systems. Nevertheless, the efficiency of this kind of cells is low, with efficiencies around 7%. In addition, the expected lifetime of amorphous cells is shorter than the lifetime of crystalline cells. Today, amorphous silicon is common in solar-powered consumer devices that have low power requirements, such as wristwatches and calculators.

2) **Thin film cadmium telluride** (CdTe): In the past, these solar cells are the basis of a rapidly expanding technology with major commercial impact on solar energy productions. CdTe is unique among the IIB-VIA compounds, in that it exhibits the highest average atomic number, least negative formation enthalpy, lowest melting temperature, largest lattice parameter, and highest iconicity. Electronically, CdTe exhibits amphoteric semiconducting behaviour, making it possible both intrinsically and extrinsically to dope CdTe n and p-type. All these

factors complement its nearly ideal optical bandgap and absorption coefficient for terrestrial photovoltaic devices, making it a forgiving material to deposit and control in thin film form. The conversion efficiency of this PV cells is better than the amorphous silicon. The present generation of CdTe PV modules are typically 0.72m² in area and have achieved efficiencies above 10%, with peak power of the order of 75W. Nevertheless, the high toxicity of the Cadmium is a big drawback for the evolution of this technology.

3) **Copper indium Gallium diselenide** ($Cu(InGa)Se^2$) was considered promising for solar cells because of its favourable electronic and optical properties, including its direct bandgap with high absorption coefficient and inherent p-type conductivity. Cu(InGa)Se2 based solar cells have often been considered as being among the most promising of solar cell technologies for cost-effective power generation. Very high efficiencies have been demonstrated with Cu(InGa)Se2 at both cell and module levels. For example, a solar cell efficiency of 20.0% with 0.5cm² total area has been fabricated by the National Renewable Energy Laboratory (NREL) in 2008 [25]. Furthermore, several companies has demonstrated large-area, production-scale modules with efficiencies of 12-14% including confirmed 13.5% efficiency on a monolithically interconnected 3459cm² module [26] and pilot-scale modules with areas ~1000cm² and efficiencies >15%. Referring to [27] $Cu(InGa)Se^2$ solar cells and modules have shown excellent long-term stability in outdoor testing, in addition to their potential advantages for large-area terrestrial applications. One of the environmental issues related to the materials in $Cu(InGa)Se^2$ modules is the availability of less common elements like Indium and the Selenium.

- **Emerging PV cells:**

These cells use often organic materials, which have compatible properties with electronics field. For example, organic polymers or small organic molecular are used for their light absorption and charge transport properties. The main advantage of these technologies is that the “plastic” itself has low production cost in high quantities. Combined with the flexibility of organic molecules, they present a good option for new generations of photovoltaic applications. [28]

Recently the development of conjugated organic and polymeric semiconducting materials appears. This last technology is very promising for photovoltaic applications due to [29][30]:

– Its lightweight, low consumption of materials (i.e. films can be very thin), flexible shape, versatile materials synthesis and device fabrications and low cost for large scale industrial production.

– Its almost continuous tenability of materials’ energy levels and gaps via molecular design, synthesis, and processing.

– Its integrability into other products such as textiles (that can be used for fabricating items such as clothing and solar cell tents), flexible packaging systems, lightweight consumer goods, and future “all-plastic” optoelectronic devices that may be compatible with biological tissues.

Nevertheless, the main drawback of the organic cells resides in its low efficiency, low stability and its low strength and lifetime compared with other inorganic photovoltaic cells.

- **Multijunction cells:**

Tandem or more generally multi-junction solar cells are photovoltaic cells containing several junctions. Each junction is tuned to a different wavelength of light in order to get a bigger solar spectrum area light and increase the efficiency. The majority of multi-junction cells that have been produced to date use three layers, tuned to blue (on top), yellow and red (on the bottom). These cells require the use of semiconductors that can be tuned to specific frequencies, which has led to most of them being made of gallium arsenide (GaAs) compounds, often germanium for red, GaAs for yellow, and GaInP2 for blue [31]. Actually, producing a tandem cell is not an easy task, largely due to the thinness of the materials and the difficulties extracting the current between the layers. Thus, the manufacturing of this type of cells is very expensive and until today dedicated to spatial application.

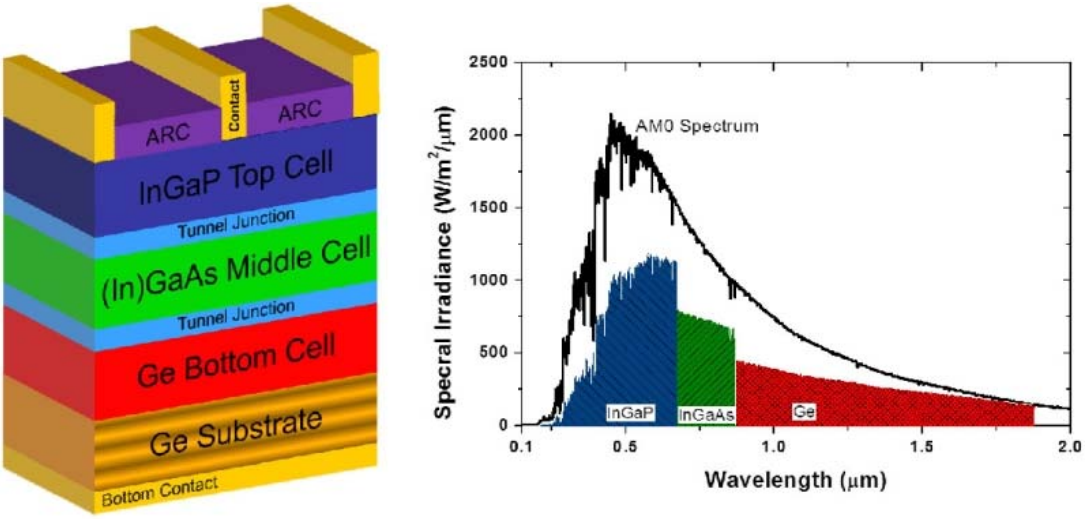

Fig. 2.8. Example of a multijunction solar cell and its spectral irradiance absorption [31]

The table. 2.1. sums up the best efficiency obtained for the commercial photovoltaic modules [32]:

Table. 2.1. Confirmed terrestrial module efficiencies under standard conditions.

Classification[a]	Effic.[b] (%)	Area[c] (cm^2)	V_{oc} (V)	I_{sc} (A)	FF[d] (%)	Test centre (and date)	Description
Si (crystalline)	22.9 ± 0.6	778 (da)	5.60	3.97	80.3	Sandia (9/96)[e]	UNSW/Gochermann [30]
Si (large crystalline)	21.4 ± 0.6	15780 (ap)	68.6	6.293	78.4	NREL (10/09)	SunPower [31]
Si (multicrystalline)	**17.3 ± 0.5**	**12753 (ap)**	**33.6**	**8.63**	**76.1**	**AIST (x/10)**	**Kyocera**
Si (thin-film polycrystalline)	8.2 ± 0.2	661 (ap)	25.0	0.320	68.0	Sandia (7/02)[e]	Pacific Solar (1–2 µm on glass) [32]
CIGS	**13.8 ± 0.5**	**9762 (ap)**	**26.34**	**7.167**	**71.2**	**NREL (4/10)**	**Miasole** [6]
CIGSS (Cd free)	13.5 ± 0.7	3459 (ap)	31.2	2.18	68.9	NREL (8/02)[e]	Showa Shell [33]
CdTe	10.9 ± 0.5	4874 (ap)	26.21	3.24	62.3	NREL (4/00)[e]	BP Solarex [34]
a-Si/a-SiGe/a-SiGe (tandem)[f]	10.4 ± 0.5[g]	905 (ap)	4.353	3.285	66.0	NREL (10/98)[e]	USSC [35]

2.2.6 Protections included in a photovoltaic generator

The PV cell association in good weather conditions does not present difficulties. But in certain cases of inhomogeneous irradiation, mismatch linked to aging or failure of one part of the array, it can cause destructives defaults in other PV cells in particular in shadowing conditions. Indeed, hotspots can appear and destroy a part of PV array. In order to avoid these destructive defaults and increase the global life-time of PV modules, it is necessary to provide the system with some active protections. These protections are normally carried out

by the use of simple electronic diodes in two different functions depending on where they are situated in the PV system. These functions are named respectively blocking diode (D_B) and by-pass diode (D_{BP}) (fig. 2.9).

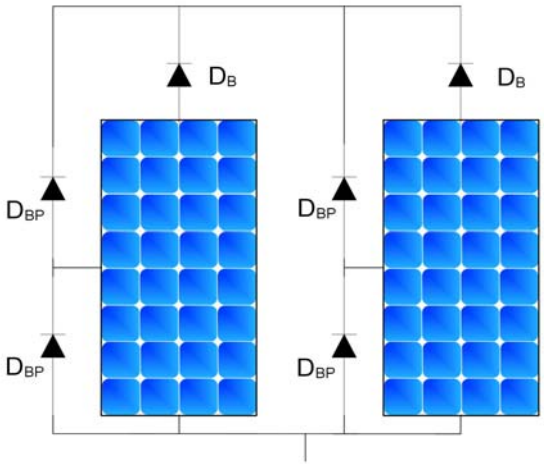

Fig. 2.9. The typical electric protections in a PV module: D_B, the blocking diode and D_{BP} the by-pass diodes

- **Blocking Diode:**

Each PV cell can either be an elementary power producer or a power consumer, depending on whether it is exposed to sunlight or not [7]. Electronic diodes D_B are inserted in series with each PV string and they are used for forbidden negative currents. Indeed, they avoid negative currents thought the PV module which produces less voltage than other at its ports due to shadowing or mismatching effects (fig. 2.10.). We can signal two typical situations where blocking diodes can help prevent this phenomenon:

1) **Blocking reverse flow of current form the battery through the module at night:**

In battery charging systems, the PV module voltage drops to zero at night. Without protections, the battery can easily completely discharge backwards through the PV module. This would not be harmful to the module, but would result in loss of precious energy from the battery bank. D_B diodes placed in the circuit between the PV module and the battery can block any leakage flow of current.

2) **Blocking reverse flow trough damaged modules from parallel strings during the day.**

Blocking diodes placed at the head of separate series wired strings in high voltage systems can perform yet another function during daylight conditions. If one string becomes severely shaded, or if there is a short circuit in one of the modules, the D_B prevents the other strings from loosing current backwards down the shaded or damaged string. The shaded or damaged string is temporally or definitively isolated from the others, and globally more current is sent on to the load. In this configuration, D_B are also called “isolation diodes”.

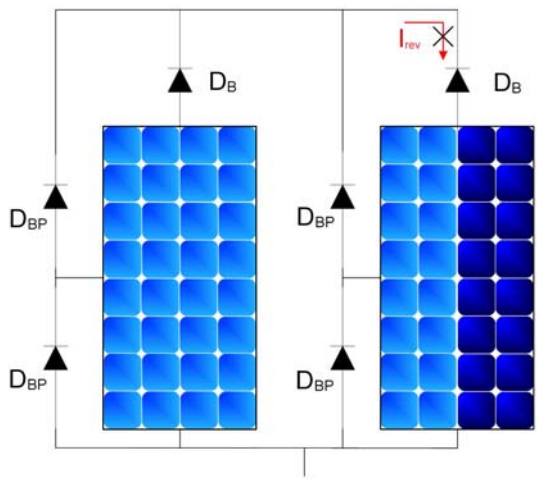

Fig. 2.10. Blocking diodes do not let leakage and reverse current to go into the PV module

- **By-pass Diode:**

When one part of a PV module is shadowed, the concerned PV cells will not be able to produce as much current as others. Since cells are connected in series, the PV cell which produced the lowest current imposes its current to other cells, being the lower of the produced current which is flowed through all cells. The differential of current of most lighted cells cannot be sent to the load. The unshadowed cells will force the shaded cells to pass this differential current through them. Thus, the shaded cells operate at higher currents than their short circuit currents and in a region of negative voltage (receptive region of operating). That causes a net voltage loss to the global PV module. In other words, the shadowed cells will dissipate power as heat. This phenomenon is named “hot spots”

The conduction of these diodes modifies the output characteristic of the generator. Indeed, it induces a step in *I(V)* characteristics of the PVG and due to a part of power production loss, two power maximum points appear in the PV *P(V)* characteristic (fig. 2.11).

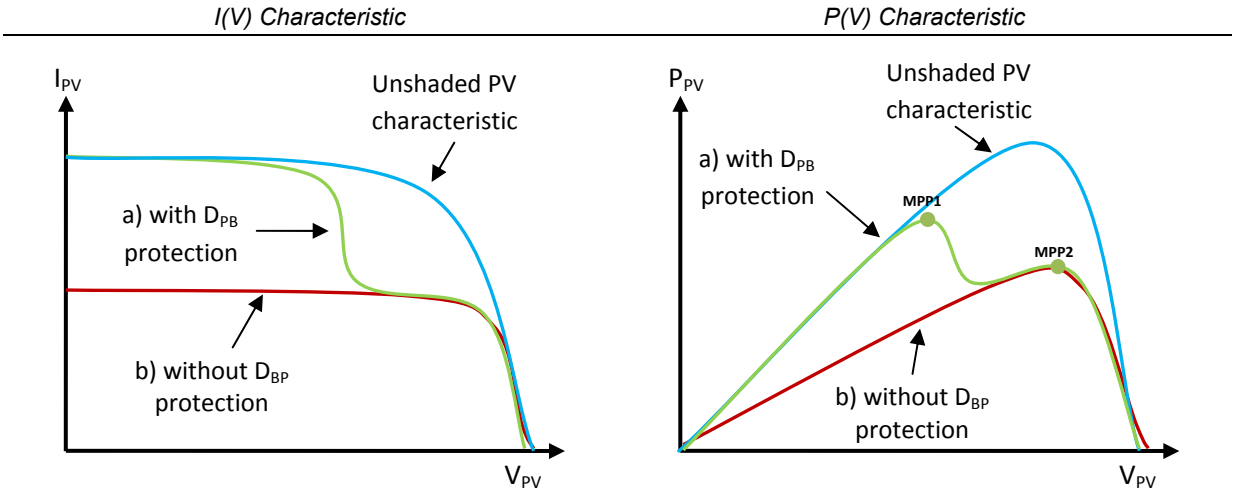

Fig. 2.11. Effect of a shadow on the *I(V)* and the *P(V)* characteristics of a PVG a) with its by-pass diodes protections b) without protections.

This phenomenon is avoided by the use of diodes in anti-parallel of a group of PV cells. In this configuration, they are named bypass diodes because they can allow a current

through them when a shadow occurs. When a cell in the series of a string is shaded and potentially consuming power, its voltage tries to become negative inducing a global reverse of the string voltage, then the by-pass diode passes into its on-state and allows a current through it. In this way, the only voltage drop is caused by the PV cell group protected by the active by-pass diode. Moreover, the hot spots are avoided and then, any definitive destruction occurs linked to this type of weather working conditions. Fig. 2.11. shows the place of a bypass diode and its operating mode.

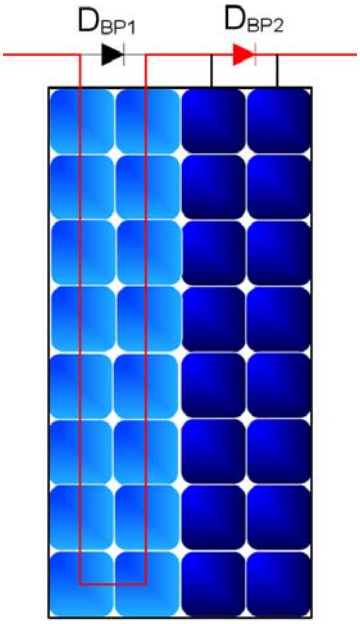

Fig. 2.12. By-pass diodes allowing the circulation of the current produced by the PV module in case of shadowing conditions.

These diodes are the minimum protections that present the photovoltaic systems. They are installed in exteriors junction box, adapted for possible maintenances in case of failure of these electronics components. Nevertheless, it is difficult to replace them when the PV modules are in roof installations, for access difficulties, or in big PV champ installation, because of the complexity on failure detections. In addition, this kind of protections are becoming obsolete, above all because of the extension of the use of power optimizers, which render useless these diodes, but make easier failure detection and therefore its eventual repairing.

2.3 Power Conditioning Units

The operating point of a PVG is determined by the intersection of its *I(V)*characteristic and the associated load *I(V)* characteristic. Typical characteristics of loads used with PVGs are presented fig. 2.13. The match with load characteristics needs the existence of one intersection point. As in one hand the *I(V)* characteristic of the PVG is dependent on irradiance and temperature and in another hand, *I(V)* characteristic load can also vary, in major time, it does not match with the maximum power point of the PV. For this reason, in PV system, power conditioning units (PCU) are used to provide a constant match between the specific characteristics of the PVG and the connected load. In general, these PCUs consist in power converters, which can be DC-DC converters for DC loads or DC-AC converters for AC ones.

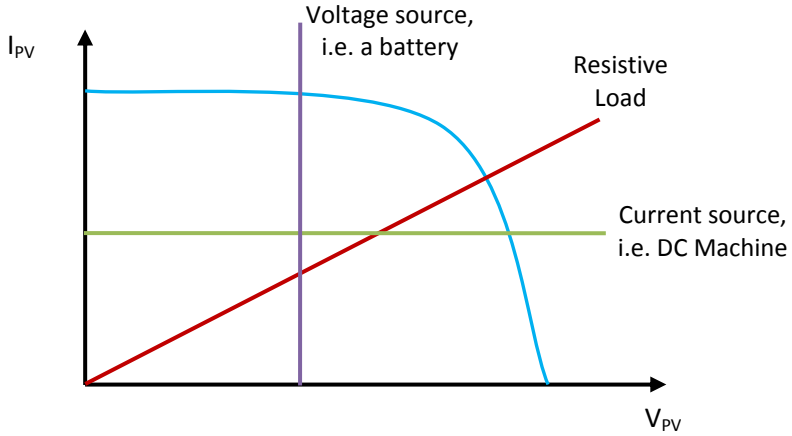

Fig. 2.13. *I(V)* characteristics of a PVG and the different kinds of loads that can be connected to it.

Moreover, whatever the type of converter used, a special circuit must provide an adequate control to the switches, in order to maintain the PVG voltage at its optimum value V_{OPT} and track at real time the maximum power point (MPP). This function is accomplished by dedicated control functions and algorithms called Maximum Power Point Tracking (MPPT). The identification of the MPP and eventually fixing the system's operating voltage at or near this point optimizes the energy production cost of the system.

The PCU also often integrates other functions as the security and protections task or islanding detection systems.

The fig. 2.14. shows a typical schema block of an elementary power conversion chain, constituted by a PVG including its electrical protection, a PCU, composed by the switching power converter and its MPPT control, and the load.

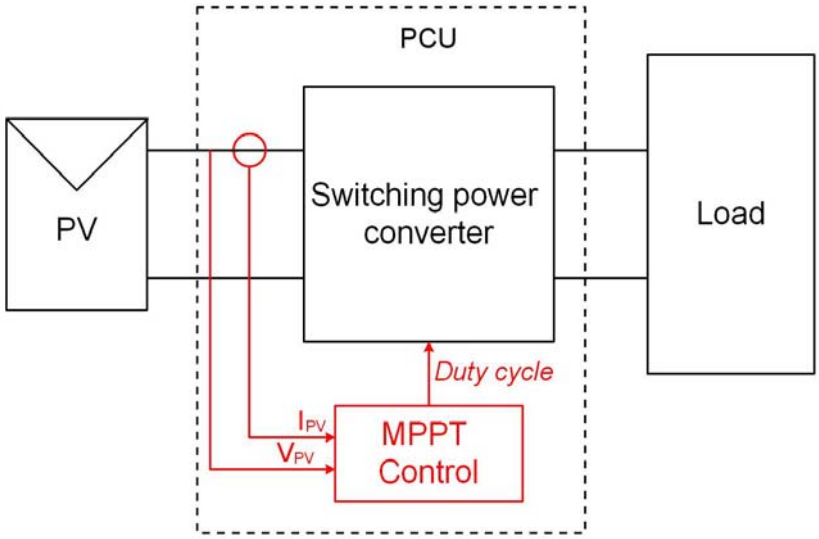

Fig. 2.14. Simplest electrical scheme block of a typical power conversion chain.

2.3.1 Classification of photovoltaic systems

Nowadays, the grid-connected systems and stand-alone system for isolated loads supply are the two principle applications of PVGs. Photovoltaic systems can be designed to

provide DC and/or AC power service. They can operate interconnected themselves with of the utility grid or be independent. They can be also connected with other energy sources and energy storage systems.

2.3.1.1 On grid applications

Grid-connected or utility-interactive PV systems are designed to operate in a complex environment, interconnected with others electrical sources and loads to the electric utility grid. The interface component necessary to make a good grid-connection is an inverter. Indeed, the input DC power produced by the PV array is converted by static components into an output AC power, compatible with the grid voltage and its power quality requirements. In addition, others functions can be assured by the inverter like the function of islanding which consists in automatically stopping the power supply when the utility grid is not energized.

Although an inverter is an essential element of an on-grid PV system, other elements and the architecture can vary. Fig. 2.15. represents the one of the simplest example of a grid connected installations. The PV DC current is converted into AC current by the inverter. The inverter is connected though a meter box to the grid and the AC loads. The meter box is a bidirectional device. It allows the current transfer from the PVG to the grid and loads but also, in the contrary sense, that is, it permit the power supply of loads from the grid utility. The PV power production is used either to supply on-site electrical loads, or to feed it back to the grid when the PV system output is greater than the on-site load demand. At night and during other periods when the electrical loads are greater than the PV system power production, the balance of power required by the loads is received from the electric utility. A safety feature is required in all grid-connected PV systems, which ensures that the PV system does not continue to operate and feed back onto the utility grid when the grid is down for service or repair.

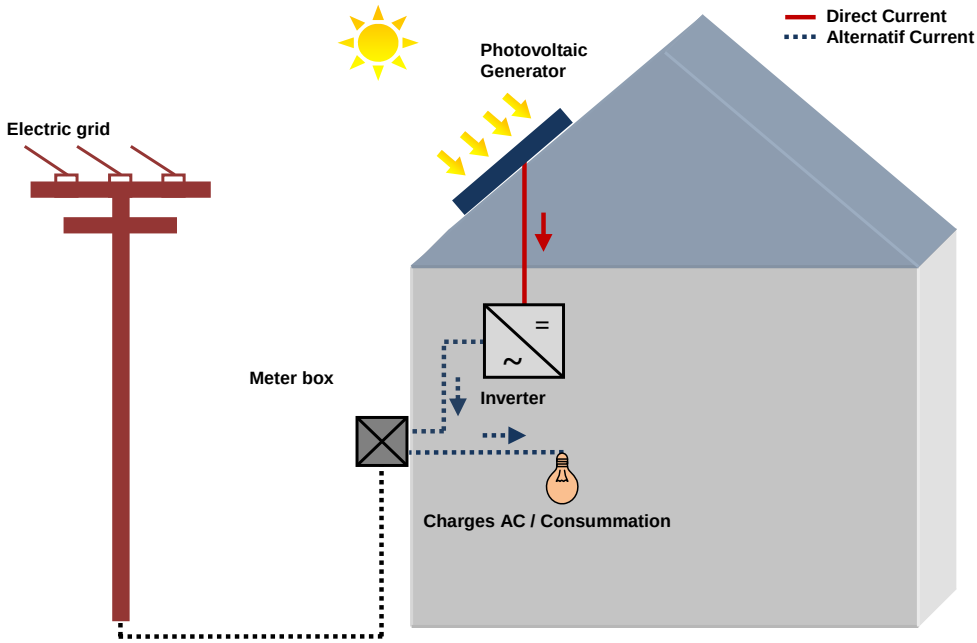

Fig. 2.15. Grid connected photovoltaic system

In the previous on-grid PV system configuration, the PV electricity production is first used to supply on-site loads, and the surplus of electricity is sold to the electrical companies.

However, in other types of grid connections, the total amount of produced PV electricity is sold. In these cases, the on-site loads are feed by the public electric grid. This type of configuration has been widely used, above all because of the economical incentive presents in many countries [13]. In fact, almost these helps has been limited, the governments had guaranteed a specific sold price for many years, which was normally higher than the buying price of public grid electricity. In this configuration, the PV system has two box meters, in this case, both of them unidirectional: one to sell PV electricity toward the grid and the other to buy electricity from the grid.

The use of a battery as storage systems in residential grid connected systems is forbidden in the European countries as France and Spain. In contrary other countries as USA and Australia allow it. The presence of a battery involves the connection of a charge controller in the output of the inverter which manages the charge/discharge cycles of the battery. The surplus of the PV energy production is stored in batteries. Only in case that the batteries are full the energy is injected in the grid. In the same way, the system is feed by the public grid only in the case that the PV electricity production and the storage systems have not enough power to feed all the loads. Moreover, systems with a battery bank can provide power in case of electricity grid failure. Fig. 2.16 shows an example of an on-grid system with battery storage devices.

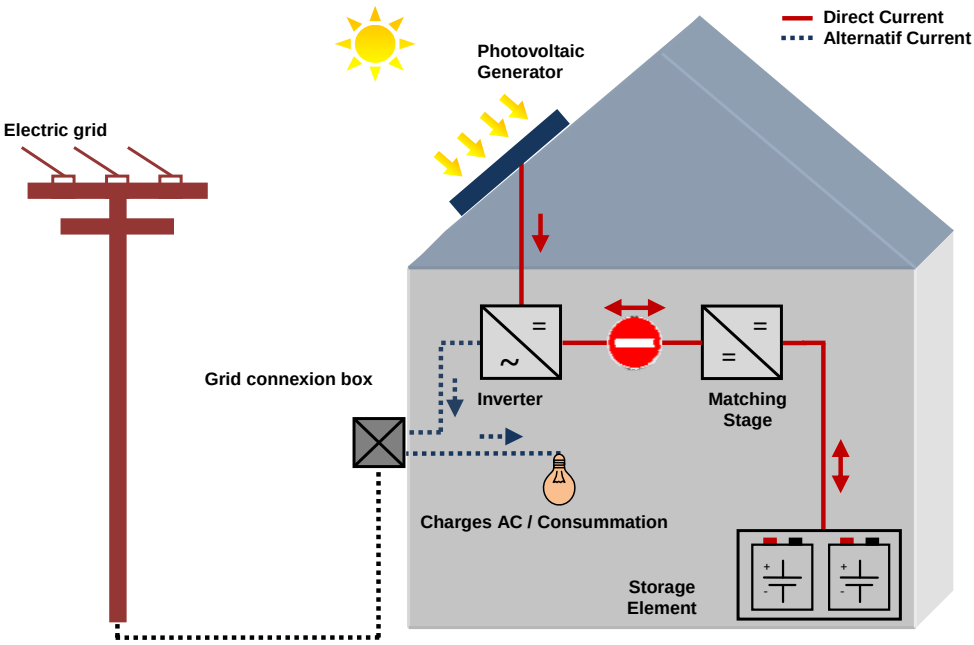

Fig. 2.16. Grid connected photovoltaic system with storage system.

2.3.1.2 Stand-alone systems

Stand-alone PV systems are designed to operate independently of the electric utility grid. They are generally designed and sized to supply some specific DC and/or AC electrical loads. In some cases, these types of loads can be supplied in addition by others sources coupled by a PV array, like wind or thermal ones. In this case the global system is called a PV hybrid system.

In many stand-alone PV systems, batteries are needed for energy storage to assure a global flexibility in the use of energy when its production is not possible. Fig. 2.17. shows an

example of diagram for a typical stand-alone PV system powering DC and AC loads. This kind of installation needs a DC-DC converter as a first matching stage between PV arrays, DC loads and a Battery Management System (BMS). Normally, this converter is a bidirectional converter and must assure as well as possible the MPPT control, the charge/discharge of the battery and the power supply of loads. Sometimes, an inverter is connected to the battery as a second stage in order to supply AC loads.

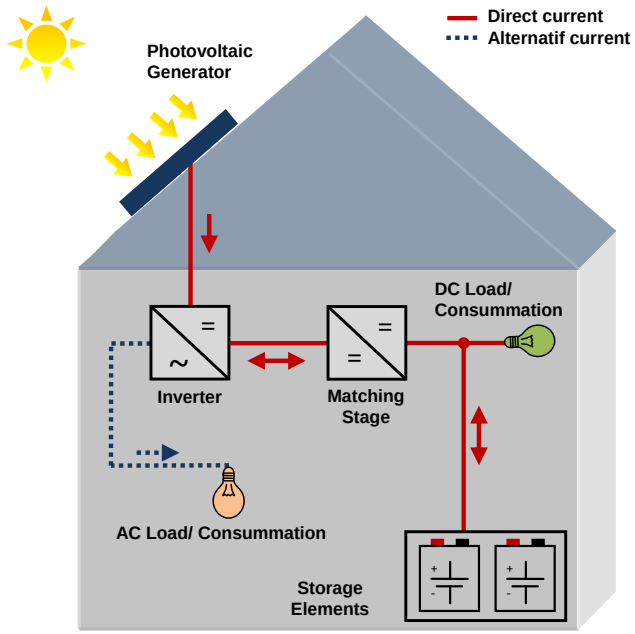

Fig. 2.17. Example of Isolated or off-grid photovoltaic system for domestic applications

Therefore, the matching stage and its internal electrical structure depend on applications for which it has been chosen or designed as well as the types of loads. In the next chapter, the matching stage and its different power conversion structures will be analysed in more details.

2.3.2 Maximum Power Point Control Tracking

The main goal of a MPPT control is to automatically find at each time the V_{OPT} and I_{OPT} of a PV array and then to allow it to operate at its P_{MPP} under given temperature and irradiance. Best MPPT control algorithms have to be fast, stable, robust, and efficient. They should respond quickly to changes in atmospheric conditions (i.e. temperature and irradiation) and be robust to disturbances or malfunctions and ageing. Moreover, an MPPT has to be efficient over a large power range.

MPPT methods, commonly used in widespread applications, are currently reported in the literature [34]-[35]. Most techniques respond to changes in both irradiance and temperature, but some are specifically more useful if temperature is approximately constant [36]. Most techniques would automatically respond to changes in the array due to aging [37], though some are open-loop and would require periodic fine tuning [38][39].

The number and the quality of sensors required to implement the MPPT control also affects the method. In most of the control methods, two sensors are required to measure respectively the voltage and the current of a PV array at each time and from which can be

calculated with high precision or evaluated the PV power array. Both, the current and voltage measurements are an important parts in the MPPT controls, since they affects in the accuracy and the efficiency of the controls. The place of each sensor can be done at the input and/or output ports of the power converter stage associated with the PVG. It varies depending on precision and cost required or also on topologies of converters used.

For cost and simplest algorithms reasons, some MPPT use only one sensor like in [53]-[54] a voltage sensor or in [55] a current one. Most of the time, it is easier and more reliable to measure voltage than current. With these types of systems, the evaluation of the PV power cannot be as high level than the previous ones. However, for cost, robustness and simple solutions reasons, they are widely used in industrial products.

Comparison among the techniques and their implementation has been discussed in dedicated papers [34]. Depending on used control methods, MPPT can be mainly categorized into following families:

- **MPPT based on measure of the fractional-open-circuit-voltage**

This method is derived from the observation that, usually, the MPP voltage, V_{OPT}, is a fraction of the open-circuit one, V_{OC} [56]-[57]. For one PV array at given temperature and irradiance, the proportionality relation between both values is quite constant:

$$V_{OPT} \approx k_1 V_{OC} \tag{2.7}$$

For more precisions, since k_1 is dependent on the characteristics of the PV array being used and its ageing, some MPPT usually has to be determine in advance V_{OPT} and V_{OC} for the specific PV array at different irradiance and temperature levels. k_1 has been reported to be between 0.71 and 0.78 for silicon crystalline PV arrays.

When k_1 is known, V_{OPT} can be computed using (2.7) after measuring V_{OC} periodically. This measurement is carried out by disconnecting the PV panels from the load for a short time. One of the drawbacks of this method is the temporally losses of power occurred during these momentary disconnections. Moreover, the component and the circuit that guarantee the correct and accurate disconnection of the PV array must be take into account. This circuit adds cost and losses to the system.

Moreover, since equation (2.7) is only an approximation, the PV array technically never operates at its MPP, with the loss of power inherent of this imprecision. However, for some low cost and low power applications, this can be sufficient. Indeed; it is a very easy and cheap to implement as it does not required DSP or microcontroller control.

- **MPPT based on the fractional-short-circuit-current measure**

This method is based on the observation that, under varying atmospheric conditions, the current of the MPP, I_{OPT}, is relatively proportional to its short-circuit current, I_{SC} [56],[58]. Like in the previous method, we can define k_2 as:

$$I_{OPT} \approx k_2 I_{SC} \tag{2.8}$$

Where k_2 is a proportionality constant. Just like in the fractional V_{OC} technique, k_2 has to be determined according the PV array that is used. The constant k_2 is normally found to be between 0.78 and 0.92.

To use this method, an additional switch is needed to periodically short circuit the PV source. During this temporal short-circuit, I_{SC} can be measured via a current sensor. This increases the number of components and cost.

- **The incremental conductance MPPT method**

The incremental conductance (IncCond) method described for example in [41]-[43][45] is based on the fact that the slope of the *P(V)* curve is zero at the MPP, positive on its left, and negative on its right, as given by:

$$\begin{cases} \dfrac{dP}{dV} = 0, \text{ at MPP} \\ \dfrac{dP}{dV} > 0, \text{ left of MPP,} \\ \dfrac{dP}{dV} < 0, \text{ right of MPP} \end{cases} \tag{2.9}$$

Is the step between each MPP evaluation is relatively small, we can deduce:

$$\frac{dP}{dV} = \frac{d(IV)}{dV} = I + V\frac{dI}{dV} \cong I + V\frac{\Delta I}{\Delta V} \tag{2.10}$$

It can be rewritten as

$$\begin{cases} \dfrac{\Delta I}{\Delta V} = -\dfrac{I}{V}, \text{ at MPP} \\ \dfrac{\Delta I}{\Delta V} > -\dfrac{I}{V}, \text{ left of MPP,} \\ \dfrac{\Delta I}{\Delta V} < -\dfrac{I}{V}, \text{ right of MPP} \end{cases} \tag{2.11}$$

The MPP can thus be tracked by comparing the instantaneous conductance (I/V) to its incremental ($\Delta I/\Delta V$) as shown in the flowchart in fig. 2.18. V_{ref} is the reference voltage at which the PV array is forced to operate. At the MPP, V_{ref} is equal to V_{OPT}. Once the MPP is reached, the operating PV array is maintained at this point until a change in ΔI is noted, indicating a change in irradiance or temperature and therefore in MPP. Then, V_{ref} is modified to track the new MPP.

The increments size determines the rapidity of the MPPT. Fast tracking can be achieved with important increments but the system might not operate exactly at the MPP and instead oscillates around it. A compromise should be found to this type of control.

Like in case of P&O method, measurements of the instantaneous PV array voltage and current require two sensors are required.

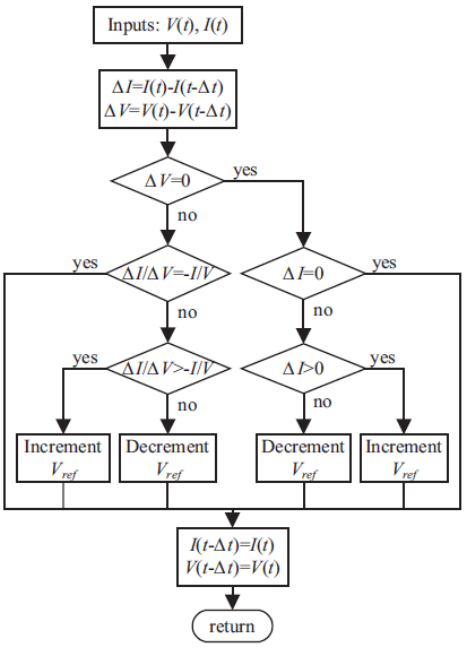

Fig. 2.18. The algorithm of the Incremental Conductance MPPT method [42]

- **Hill-Climbing/Perturb and Observe MPPT control families**

Hill-climbing [44]-[48] and Perturb and Observe [48][54] (P&O) methods are different ways to implement the same fundamental method. In one hand, Hill-climbing involves a perturbation in the duty ratio or the power converter and in another hand, P&O uses a perturbation in the operating voltage of the PV array. It can be notice that perturbing the duty ratio of power converter perturbs the PV array current too and consequently perturbs the PV array voltage.

The P&O MPPT method is based in the following criterion [49]: if the operating voltage of the PV array is perturbed in a given direction, and this perturbations involves an increase of the PV power, this means that the operating point has moved toward the MPP, and therefore, the operating voltage must be further perturbed in the same direction. Otherwise, if the PV array power decreases, the operating point has moved away from the MPP and therefore, the direction of the operating voltage perturbation must be reversed. The operation is constantly carried out until the MPP is reached, and them, at steady state, the operating point oscillates around the MPP. The fig. 2.19 from [50] shows the chart diagram of the P&O MPPT method algorithm. This family of MPPT control was chosen by the LAAS in the past to develop control algorithms which still today present high performances in steady state and in transient. We used some of them in our converter prototype to recover MPP, in association with new control algorithms.

The oscillations around the MPP represent one of the drawbacks of P&O MPPT technique, since they give rise to the waste of some amount of available energy. Several improvements of the P&O algorithm have been proposed in order to reduce the number of oscillations around the MPP in steady state, but they slow down the speed of response of the algorithm against changes in atmospheric conditions and decrease the efficiency of the algorithm during cloudy days [50].

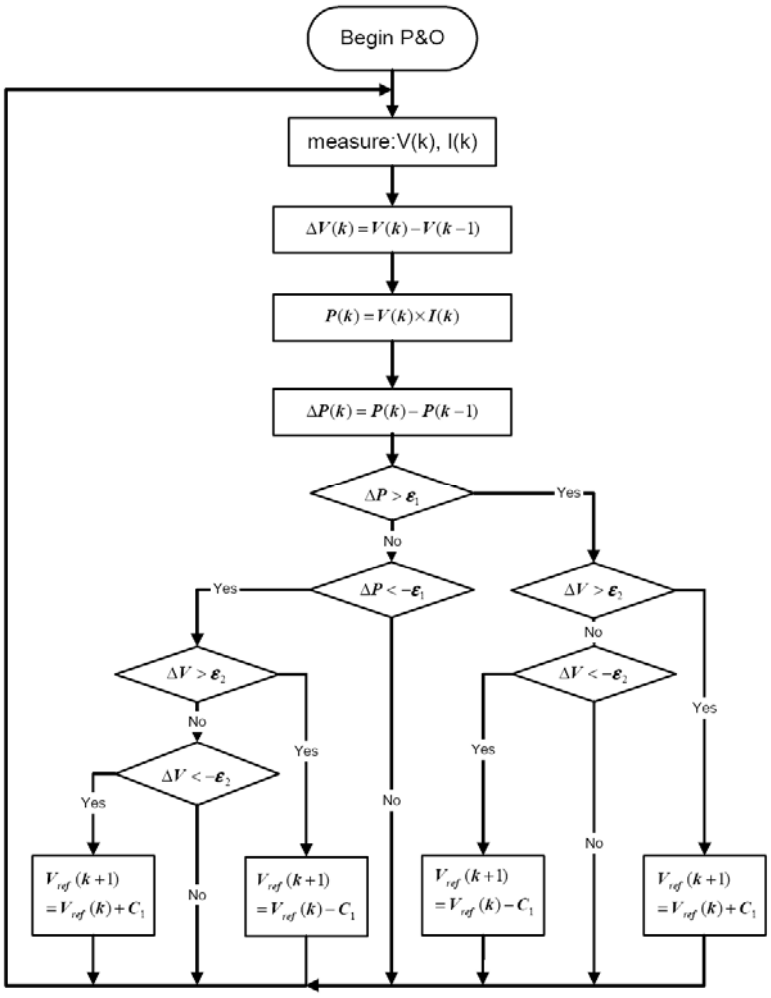

Fig. 2.19. Algorithm of the P&O MPPT method [50].

- **MPPT based on Fuzzy logic control:**

This control deals with uncertainty in engineering by attaching degrees of certainty to the answer to a logical question. This type of control incorporates a simple, rule-based *IF X AND Y THEN Z* approach to a solving control problem rather than attempting to model a system mathematically. It generally consists of three stages: fuzzification, rule base table lookup, and defuzzification. Microcontrollers have made using fuzzy logic control [59][64] popular for MPPT over last decade.

During fuzzification, numerical input variables are converted into linguistic variables based on a membership function similar to fig. 2.20. In this case, five fuzzy levels are used: NB (Negative Big), NS (Negative Small), ZE (Zero), PS (Positive Small), and PB (Positive Big). Other references [61][62] uses seven fuzzy levels, probably for more accuracy systems. The *a* et *b* variables are based on the range of values of the numerical variable.

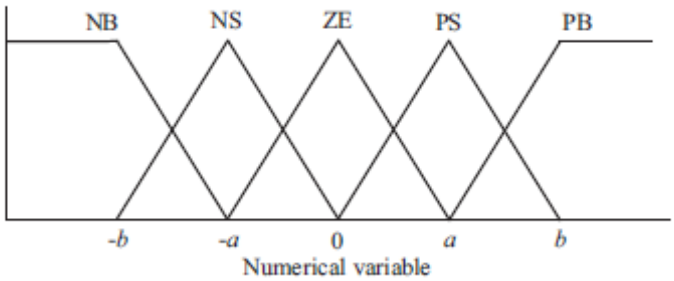

Fig. 2.20. Membership function for inputs and output of fuzzy logic controller

The inputs to a MPPT fuzzy logic controller are usually an error E and a change in error ΔE. The user has the flexibility of chossing how to compute E and ΔE. Since dP/dV vanishes at the MPP, [63] uses the approximation:

$$E(n) = \frac{P(n) - P(n-1)}{V(n) - V(n-1)} \tag{2.12}$$

and

$$\Delta E(n) = E(n) - E(n-1) \tag{2.13}$$

Once E and ΔE are calculated and converted to linguistic variables, the rule base table such as table. 2.2. [64], is looked up to define the fuzzy controller output variable value, which is typically a change in the duty ratio ΔD.

The linguistic variables of the table are based on the power converter that is used and also on the knowledge of the user about the system. In the defuzzification stage, the fuzzy logic controller output is converter form a linguistic variable to a numeric variable using a membership function as in fig. 2.20. In this way, an analogical signal is provided to the power converter control to track the MPP.

Table. 2.2. Fuzzy rule base table [64]

E \ ΔE	NB	NS	ZE	PS	PB
NB	ZE	ZE	NB	NB	NB
NS	ZE	ZE	NS	NS	NS
ZE	NS	ZE	ZE	ZE	PS
PS	PS	PS	PS	ZE	ZE
PB	PB	PB	PB	ZE	ZE

This control has the advantage to be robust and relatively simple to design as it does not require the knowledge of the exact model. Moreover, its performance under varying atmospheric conditions has been shown.

However, it requires the complete knowledge of the operation of the PV system by the designer in choosing the right error computation and coming up with rule base table. Indeed, the effectiveness of the control depends a lot on this knowledge.

- **MPPT using Neural Network:**

Neural Network is made up by simple processing units, the neurons, which are connected in a network by synaptic strengths, where the acquired knowledge is stored. Neural Networks commonly have three layers: input, hidden, and output layers (fig. 2.21). The number of nodes in each layer varies and is user-dependent.

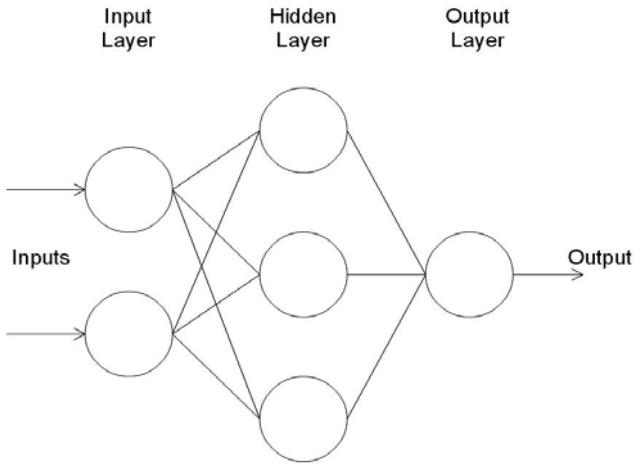

Fig. 2.21. Example of a neural networks

In PV dedicated Neural Networks MPPT controls, the input variables can be PV array parameters like V_{OC} and I_{SC}, atmospheric data like irradiance and temperature, or any combination of these [38]-[39]. The output is usually one or several reference signals like a duty cycle signal used to drive the power converter to operate at or close to the MPP. The efficiency of the MPPT control depends on the algorithm used by the hidden layer and how well neural networks have been trained. The training process can involve tests in the PV array over month or years to record patterns between the inputs and outputs of the neural networks. After, they are normally implemented in microcontroller devices to carry out the control.

Since most of PV arrays have different characteristics, each neural network has to be specifically designed to each of them. Moreover, the aging of PV modules involves characteristics changes with time. That implies the necessity of training neural networks to keep MPPT accuracy.

2.3.3 MPPT efficiency

As describe in previous part, numerous methods to track MPP exist. It is difficult to know exactly their performances and then to choose the more appropriate for each particular application. In addition, some ones are less efficient than others in fastness, fitness, robustness, type of PV module, geographic sites, etc. But datasheets of converters including these types of algorithms do not often give details. The most used type of evaluation of the MPPT control is the MPPT efficiency η_{MPPT}. The MPPT efficiency is defined as the ratio

between the average electrical power, P_{in}, produced by the PV array within a defined measuring period and its maximum power P_{MAX} able to be produced in the same period and in the same conditions test.

$$\eta_{MPPT} = \frac{P_{in}}{P_{MAX}} \tag{2.14}$$

The difficulty of this indicator is to guaranty the accuracy of values obtained. Indeed, in major cases, it is very difficult to know exactly in simultaneous times and with sufficient precisions P_{in} and P_{MAX}. Even, in some systems, P_{MAX} cannot be known in time.

Nowadays, the efficiencies of MPPT controls given in datasheets are high, the best of them exceed 99% but not enough details on measures are given to know the exactitude of this data. Nevertheless, this efficiency is important criteria of choice to determine the best used method for one application.

2.3.4 shows a resume of major characteristic of PV array MPPT techniques available [34].

Table. 2.3. Comparison of major characteristics of PV array MPPT techniques [34].

MPPT Technique	PV Array Dependent?	True MPPT?	Analog or Digital?	Periodic Tuning?	Convergence Speed	Implementation Complexity	Sensed Parameters
Hill-climbing/P&O	No	Yes	Both	No	Varies	Low	Voltage, Current
IncCond	No	Yes	Digital	No	Varies	Medium	Voltage, Current
Fractional V_{OC}	Yes	No	Both	Yes	Medium	Low	Voltage
Fractional I_{SC}	Yes	No	Both	Yes	Medium	Medium	Current
Fuzzy Logic Control	Yes	Yes	Digital	Yes	Fast	High	Varies
Neural Network	Yes	Yes	Digital	Yes	Fast	High	Varies
RCC	No	Yes	Analog	No	Fast	Low	Voltage, Current
Current Sweep	Yes	Yes	Digital	Yes	Slow	High	Voltage, Current
DC Link Capacitor Droop Control	No	No	Both	No	Medium	Low	Voltage
Load I or V Maximization	No	No	Analog	No	Fast	Low	Voltage, Current
dP/dV or dP/dI Feedback Control	No	Yes	Digital	No	Fast	Medium	Voltage, Current
Array Reconfiguration	Yes	No	Digital	Yes	Slow	High	Voltage, Current
Linear Current Control	Yes	No	Digital	Yes	Fast	Medium	Irradiance
I_{MPP} & V_{MPP} Computation	Yes	Yes	Digital	Yes	N/A	Medium	Irradiance, Temperature
State-based MPPT	Yes	Yes	Both	Yes	Fast	High	Voltage, Current
OCC MPPT	Yes	No	Both	Yes	Fast	Medium	Current
BFV	Yes	No	Both	Yes	N/A	Low	None
LRCM	Yes	No	Digital	No	N/A	High	Voltage, Current
Slide Control	No	Yes	Digital	No	Fast	Medium	Voltage, Current

2.3.4 Power static converter used for matching stage

The task of a power static converter is to process and control the flow of one or more electrical source to one or more loads by matching its voltages and currents in a form that is both optimal for source and load.

A static converter is a meshed of electrical components that acts as a linking, adapting or transforming stage between at least two electrical sources: one must be considered like a generator and the other one, like a load.

An ideal static converter controls the flow of power between its input to its output with 100% efficiency. Power converter design aims to achieve ideal efficiencies. A static power converter is composed by:

- Non-linear elements, mainly semiconductors switches used in switched mode
- Passive elements like capacitors, inductances and transformers. These reactive components are used for intermediate energy storage but also for voltage and current filtering. They generally represent an important part of the size, weight, and cost of the equipment and can reduce its global lifetime [65].

In photovoltaic field, a static converter processes PV DC current and voltage into DC or AC ones. The power converter can be designed with different topologies and with one or several intermediate conversion stages. This topology will mainly depends on the type of the load (DC or AC), the level of the input and the output voltage and the power of the PVG. In the chapter 3, the types of photovoltaic power converter structures will be analyzed with more details and for different types of installations.

The electrical characteristic and control of the power converter structure has a special importance for the maximal exploitation of a photovoltaic system. No matter the structure of the system, a good control system and an efficient power converter are need to an optimal power transfer to the load. The power conversion system takes bigger importance in sources as the PVG. In fact, these systems need an important initial investment and any minimum loss in energy production can involve significant losses in the retour of investment. For the same reason, the reliability and life-time of the structure are also important. This way, it is important to achieve high efficiency and big reliability and life-time photovoltaic power conversion systems.

2.4 Definition of efficiencies in photovoltaic chains

The main aim of all new converter topology for photovoltaic systems is the improvement of efficiency. To evaluate a photovoltaic conversion chain, there is the need to have the same criteria to compare structures. The most significant efficiencies used in this context are named: the global or the total efficiencies and the European efficiency.

The term efficiency applied in electrical field is defined as the ratio of the effective or useful output power to the total input power received by any system. In a photovoltaic system, the efficiency of the system can be defined as the ratio of the energy supplied to the load to the total energy of the sunlight received at the surface of the PV generator.

Nevertheless, the PV chain is composed by many elements and each of them has its own power energy efficiency. The improvement of each performance to achieve a better efficiency even of few percentages, in each part of the PV chain is the scientific approach we adopt in order to achieve an optimum PV system. Before detailed our method and expose some of obtained results, we need to define all efficiencies we used in our work. In following lines, the definition of total efficiency and the “weighted efficiencies” specifics to photovoltaic applications are detailed.

2.4.1 Notion of total efficiency

In order to evaluate the performance of all the photovoltaic system, the total efficiency is defined. The total efficiency takes into account all the structures presented within the photovoltaic conversion chain: the PVG, the power conversion structure and its associated MPPT control. It is defined by the multiplication of efficiencies of all parts or in other words. It will help us to know exactly the percentage of the power deliverable by the sun, transformed in the PVG and transferred by the matching stage between PVG to a load. We can sum up this notion trough different ratios as :

$$\eta_{TOTAL} = \frac{P_{MAX}}{G.A} . \frac{P_{in}}{P_{MAX}} . \frac{P_{out}}{P_{in}} \tag{2.15}$$

$$\eta_{TOTAL} = \eta_{PV} . \eta_{MPPT} . \eta_{CONV} \tag{2.16}$$

Where η_{PV} is the standard used for PV panel efficiency, η_{MPPT} the MPPT efficiency and the η_{CONV} the converter efficiency.

In this PhD, we had essentially focused our works to the conversion chain, and for this reason, only η_{MPPT} and η_{CONV} will be considered in this chapter. Therefore, the efficiency named $\eta_{PV_{chain}}$ will be used. This efficiency takes into account both efficiencies that integrate the power adaptation stage: the MPPT efficiency and the power converter one. It will be defined with the following equation:

$$\eta_{PVchain} = \frac{P_{in}}{P_{MAX}} . \frac{P_{out}}{P_{in}} = \eta_{MPPT} . \eta_{CONV} = \frac{P_{out}}{P_{MAX}} \tag{2.17}$$

We can notice that these efficiencies depend on time and used temporal measures to calculate their ratio. We can introduce the notion of instantaneous efficiencies that are based on several electrical measures in small time intervals, smaller than the switching period of the converter. We can qualify them of instantaneous efficiencies and in particular on power ones.

In order to evaluate correctly the quality of the photovoltaic conversion chain, it is important to study the transfer of energy toward the load in a large range of time, for example an hour, a day, a month, a year. In this way, we will more interested by the global energy produced by a PV generator and the totality of the energy transferred to the load in a day. From these values, the average daily efficiency can be defined. This efficiency will be noted $\overline{\eta}_{CONV}$ and it will be defined as:

$$\overline{\eta}_{CONV} = \frac{\text{Transferred energy}}{\text{Produced energy}} \tag{2.18}$$

Thus, if we know the maximal power that the PV generator can produce in each moment, we can calculate/evaluate the maximal potential energy that it can supply during a day. From these previous instantaneous values, the average MPPT daily efficiency, named, $\overline{\eta}_{MPPT}$, can be calculated :

$$\overline{\eta}_{MPPT} = \frac{\text{PV Produced energy}}{\text{Maximale energy}} \tag{2.19}$$

The total average daily efficiency of the photovoltaic conversion chain will be calculated with the following equation:

$$\overline{\eta}_{PV_{Chain}} = \overline{\eta}_{MPPT} \cdot \overline{\eta}_{CONV} \tag{2.20}$$

The measure of the energetic efficiency of the average daily efficiency will allow comparing in most precise way the different conversion stages. This way of evaluation is more pertinent than by the use of instantaneous efficiencies since these ones are linked to a particular moment and conditioned by the measuring conditions. Moreover, in a photovoltaic system, the energy that is transferred to the load is the element to take into account.

2.4.2 Power converter efficiency

The efficiency of a power converter is defined as the ratio between its input power and its output power. This way, higher is the efficiency, the transferred and usable power to the load will be bigger. In the same time, as output power corresponds to the input power minus the loss that the inverter involves, the efficiency is directly associated to the loss of the power converter, and bigger are the losses of the converter, lower is the efficiency of this converter.

$$\eta_{CONV} = \frac{P_{out}}{P_{in}} = \frac{P_{in} - P_{Loss}}{P_{in}} \tag{2.21}$$

Where P_{out} represents the average power in the output terminal of the power converter and P_{in} the input average power for one period.

Classical efficiency versus input power characteristic of a power converter is shown in fig. 2.22. There is a unique maximum efficiency point that normally fit with the nominal power of the converter, which normally occurs in quite low power. For higher power levels than this nominal power point, the power losses increase considerably and the efficiency falls down. The achievement of flat efficiency power converters within the efficiency keeps high even in higher power levels is the subject of many works and studies. Indeed, there is a great amount of losses due to this phenomenon and improvements in this power range will allow better exploitation of power conversion systems.

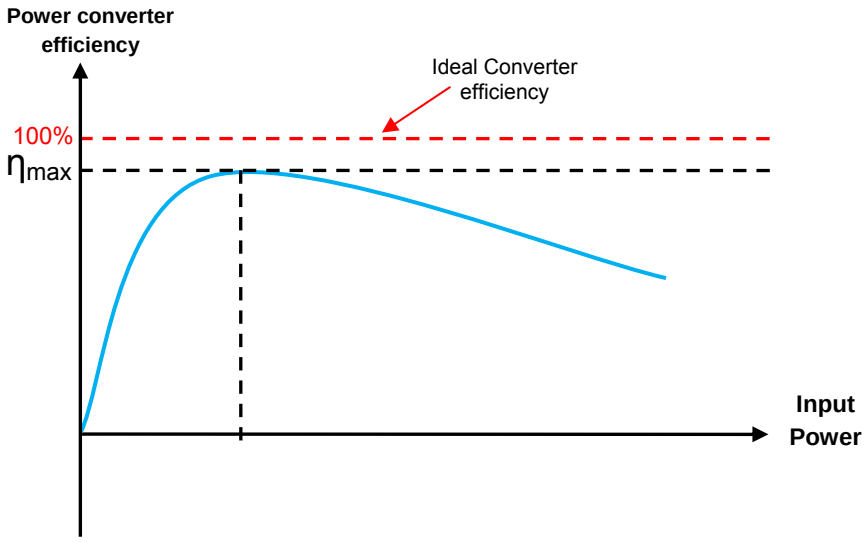

Fig. 2.22. Typical efficiency characteristic of a power converter in relation with increasing input power.

In power electronics domain, the sizing of a power converter, either for a DC-DC type or DC-AC type, is based in strict rules that take into account the maximal constraints that each element must suffer (current, voltage, switching frequency, operating temperature…). The conversion stage is correctly sized if the electrical conversion efficiency is maximal for the rated power, that is, for the most used power range. This allows minimizing the conversion loss in the time of functioning of the converter.

PV sources differ with other input conditions and therefore, their input power varies highly with external parameters such as weather, time, temperature etc. Due to this variation, converters cannot be designed for a unique nominal power but for an important range of variation. Consequently, it is very difficult to allow a maximum and optimal power transfer between source and load for all working conditions. Other efficiencies are introduced by inverters designers to have objective criteria of comparison.

2.4.3 CEC and EURO weighted efficiencies

The converter efficiency is linked to the working power. In a PV system, the operating point and the power level of the converter are directly imposed by the solar array. The PVG energy production is not constant and changes depending on irradiation and temperature. In summary, better is the irradiation, greater is the energy production and in contrary, higher is the temperature, minor is the energy production. These changes are directly dependant on the season of the year, the hour of the day and the weather. The photovoltaic energy production is not the same in winter and summer or in presence of a sunny or a cloudy day. The fig. 2.23. shows some examples of these phenomenon by measures which had been carried out in the laboratory installation for different type de PV modules and in different condition days. In the top, the difference between sunny and cloudy days can be seen by means of the measures made with a PV multi-crystalline module of 85 W_P in two days of September 2008. The presence of clouds prevents to irradiation to arrive to the PV array and the energy production drops. The bottom of this figure represents the behaviour of a amorphous silicon PV array of 1,5 W_P during different seasons of the year 2008. These diverse curves show the difference in maximal puissance production and daytime length according to season.

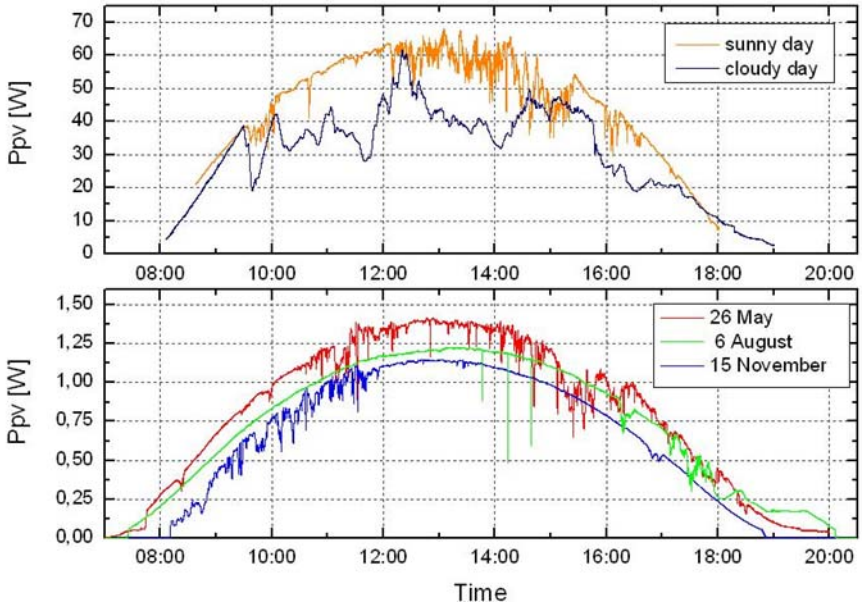

Fig. 2.23. Representation of PV power productions profiles of 85 W_P PV module during a sunny and cloudy day (top) and the production of 1.5 W_P PV module during different seasons (bottom).

In order to evaluate the efficiency of a power converter in these real operating conditions the notions of CEC efficiency and EURO efficiency has been introduced [66]-[67]. They take in consideration the statistical lighting conditions, and therefore, the energy productions in a given geographical place along a year. The CEC efficiency is used for south USA installations, where the insulation is high. The EURO efficiency is used for European photovoltaic installations, which support lower irradiation levels. The formulas of these efficiencies are respectively defined in the equations (2.22) and (2.23):

$$\eta_{Euro} = 0.03*\eta_{5\%} + 0.06*\eta_{10\%} + 0.13*\eta_{20\%} + 0.1*\eta_{30\%} + 0.48*\eta_{50\%} + 0.2*\eta_{100\%} \quad (2.22)$$

$$\eta_{CEC} = 0.04*\eta_{10\%} + 0.05*\eta_{20\%} + 0.12*\eta_{30\%} + 0.21*\eta_{50\%} + 0.53*\eta_{75\%} + 0.05*\eta_{100\%} \quad (2.23)$$

Where the index of $\eta_{x\%}$ represents the x% of the photovoltaic delivered rated power and the coefficients correspond to the statistic average working time of each operation point. For a better comprehension, this efficiency can be represented by a histogram (fig. 2.24.) where it is easier to see the statistical repartition of the operating for each power in Europe. For example, the power converter will work in 50% of its rated power in 48% of time. To summary, these definitions demonstrates that photovoltaic generators work in average between 30% and 100% of its rated power 80% of its operating time in European region and 90% in south USA installations.

If we juxtapose the efficiency characteristic evolution of a classical Boost, we notice that this converter is not well adapted for photovoltaic applications. Its conversion efficiency decreases when the PV power increases and the point of maximum efficiency do not fit in with the power wherein the converter works the most part of the timer.

Thus, in the aim to improve the daily efficiency and to make that the converter works in the point of maximal efficiency most of the time, displacement of the efficiency curve must be envisaged for that (fig. 2.24).This way, a flat efficiency characteristic, which presents a high efficiency in all the functioning power range, is desirable for this kind of applications.

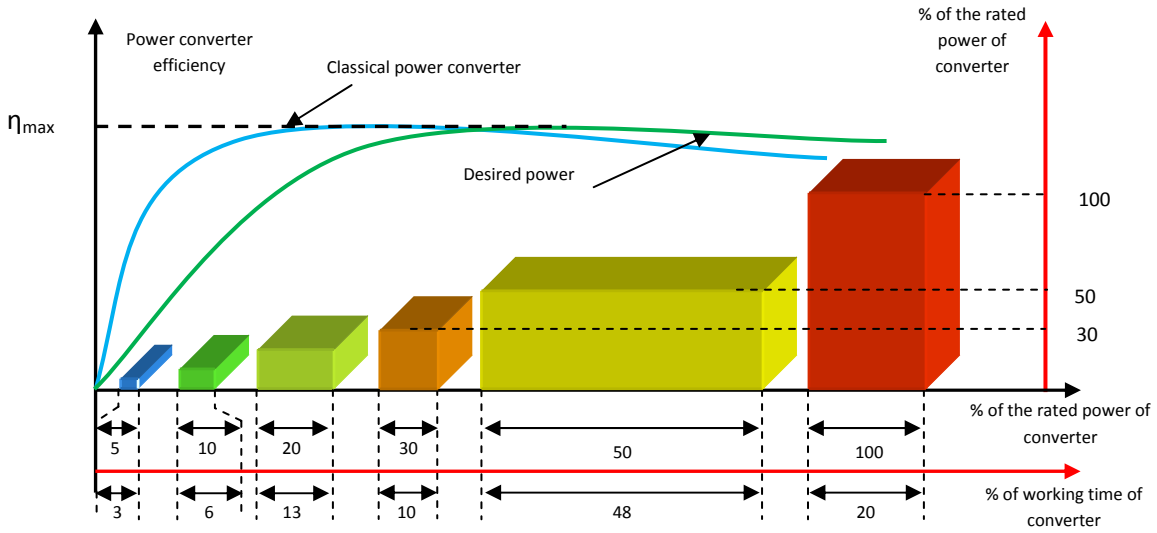

Fig. 2.24. Representation of the European efficiency expression as well as the efficiency characteristic evolution of a classical Boost.

These efficiencies allow a more realistic comparison between converters, either DC-DC converter or DC-AC inverters. For this reason, it is being used increasingly and more and more photovoltaic converter manufacturers like SMA or FRONIUS [68]-[69] provide this data to consumer in addition of the traditionally given maximal efficiency data. It is becoming a reference when photovoltaic dedicated converters are compared either in commercial domain or in scientific research areas [70]-[74].

2.4.1 Synthesis

The measure of the energetic efficiency of the average daily efficiency will allow better comparing in photovoltaic field than instantaneous efficiencies. This manner of evaluation is more pertinent than by the use of instantaneous efficiencies since these ones are linked to a particular moment and conditioned by the measuring conditions. Moreover, in a photovoltaic system, the energy that is transferred to the load is the element to take into account.

The conversion efficiency of a power conversion stage depends on the input voltage level, the temperature, etc., and it represents an instantaneous efficiency of the transferred power measured in given conditions.

The efficiency of a conversion stage which includes the power converter and its associated power optimization controls can be also defined in an instantaneous moment. However, the measuring conditions are even more difficult to reproduce for different test and to guarantee the same test results which allow their comparison. Thus, the instantaneous power and efficiency notions do not allow carrying out precise comparative tests to know the evolution of improvement in the structure. In the same manner, it does not allow the comparison of different structures dedicated to PVG and functioning in different ways.

For comparison of different structures and their evolution, the notion of average efficiency is the most appropriated. In addition, it is easier to compare the energetic gain

obtained in a day if we measure the total energy transferred to the load, instead to look to power efficiencies which varies permanently.

2.5 Conclusion

Generalities about the photovoltaic conversion system have been introduced in this chapter. Each of the elements of a PV installation has been defined and explained: from the PV generator, to power converter passing though its protections, characteristics and its control.

First, the PV energy generation device has been introduced. The PV cell is the essential element of the PV system. Being the energy production of this cell very low, the interconnection of PV cells allows bigger PVGs called modules and arrays. The PV cells have suffered a large evolution along last decades. Traditional techniques as the crystalline silicon solar cell have improved in efficiency and new promising techniques have came out.

The major characteristic of this photovoltaic energy source is its non lineal energy production characteristic, which depends, in one hand, on the atmospheric conditions and on the other hand in the connected load. Because of this non linearity in the power production, the importance of a PCU has pointed out. The PCU normally consist on a power converter and its associated MPPT control. Different methods of MPPT controls have been explained, pointing out the advantages and drawback of them. The efficiency concept in the MPPT control has been also defined which is considered as the major evaluation method of this type of control. Finally, the total efficiency of a photovoltaic power conversion system and the efficiency of power converter have been defined. The weighted CEC and EURO efficiencies has been also defined which remark the importance of high efficiency in a large range of input powers for photovoltaic power converters.

Much effort has been carried out in the improvement of photovoltaic cell efficiency. These improvements are normally hard, slow and need lot of economical investment. Nevertheless, the other part of the photovoltaic system can be also widely improved, normally with lower economical investments. In fact, the power conversion efficiency and control efficiency are as important as the PVG efficiency, as the benefits of PV cell efficiency improvements are lost if their electrical energy is not efficiently transferred to the load. This way, research in either the MPPT control or the power conversion structure efficiency and very useful and can involve important benefits in the total efficiency of the photovoltaic installations.

CHAPTER 3

3 EVOLUTION OF PHOTOVOLTAIC CONVERSION CHAINS

3.1 Introduction

At the beginning of the spatial PV supplies in 1960s, PV arrays had designed to working around a 12V in the aim to be connected to lead acid batteries via DC electrical buses. The matching stage was composed of DC-DC isolated converters. More recently, PV arrays are equipped with simple algorithms to recover the PPM. In terrestrial field, PV arrays have firstly used for isolated applications as solar water pumps or storage batteries charging systems. Since this period, the output PV voltage around the 12V (or a multiple of this voltage) was instituted as an absolute verity even for grid connected applications. In addition, during a long time, the trade-off energy produced/cost effective did not allow a power converter for matching electrical characteristics of the PV source to a load essentially because of its cost and its short working lifetime until failure.

In parallel, bad working of electrical utility or absence of it in a large part of the country makes thinking in new solutions and about in 1970, in USA, the problematic of first smart-grids was proposed. Thus, PV energy began to interest some governments and industries in the way to replace fossil energy sources to produce electricity in new grids. Theses ones were constituted to transport AC electricity, making evident the need of inverters to convert DC electricity of PVG on AC current and voltage and adapt the difference in voltage levels. Since this time, the either passive or active electronic components used in power converters had evolved to more performing and efficient elements. In the same goal, the photovoltaic conversion system has also become more efficient, robust and performing inducing important changes in topologies and structures.

The objective of this section is to show the way that photovoltaic converter topologies has made from centralized converter to distributed power system. In this chapter, different photovoltaic converter topologies are analyzed, pointing out the advantages and drawbacks for each of them. Moreover, we will focused in the DC optimizer structures, analyzing their electrical structure solution that are present in the scientific literature. We analysed for each of them their advantages and disadvantages. We finish with the studies of existing solutions to improve efficiencies and life-time of SC.

3.2 On-grid photovoltaic systems particularities

Before starting our analysis, we remember that PV systems are structured into several operational configurations. Each configuration has a basic power electronic interface, also called Power Conditioning Unit (PCU) or a power stage, which interconnects the PV source to the utility grid or directly the load. In this way, the photovoltaic conversion chain is composed by the PVG, the PCU and a load. Depending on the application, the PCU structure varies. In the case that the load is a DC load, as a battery or DC machine, the power converter structure is a DC-DC converter. For AC loads or grid connections PV systems, the power converter is a DC-AC inverter. In both structures, control laws are associated to power conversion structure, which includes MPPT control and adapted sensors and securities for a correct functioning and the adaptation to the load or output characteristics.

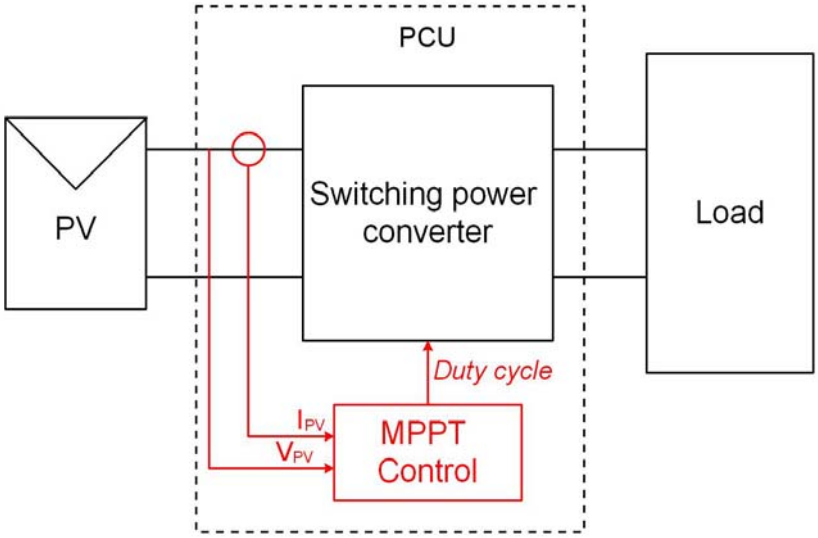

Fig. 3. 1. PV conversion chain

3.2.1 Properties of a grid connection

Today, although the stand-alone PV installation progress constantly in the world and in particular in insulate sites, the most part of PV installations are designed to the electrical grid connection. According to 2009 report of IEA-PVPS on installed PV power [75], the cumulative grid-connected PV capacity of IEA countries is 95.9%, in comparison of the only 4.1% that is installed in stand-alone PV systems. Fig. 3. 2. shows the growth in PV capacity from 1992 to 2009 for off-grid and grid connected PV installations. In this way, as well the PV system as the output signal must be adequate to local laws and standards requirements of the public grid, in terms of frequency, maximum voltage, harmonics, …

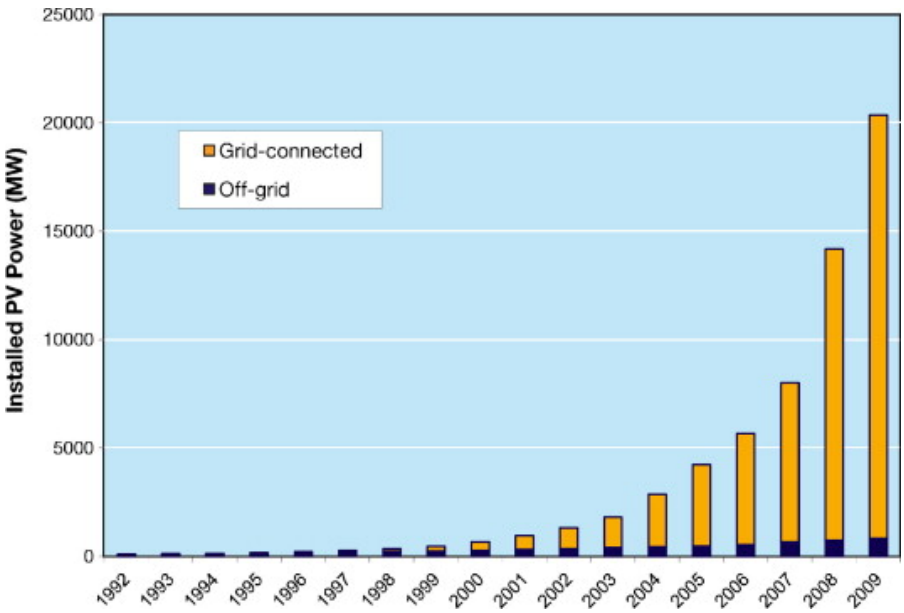

Fig. 3. 2. Cumulative installed capacity between 1992 and 2009 in the IEA-PVPS reporting countries

These standard deals with issues like power quality, detection of islanding operation, grounding, etc. This standard may vary between each country, and in this way, the requirements for each PV installation will change depending where are going to be installed.

Our purpose is not to analyze all standard that regulates the PV installations around the world. Nevertheless, we are interested in the important issues that a grid utility connection necessitates in term of characteristics and standard requirements, in order to specify the principal characteristic of a PV on-grid system. This analysis will be concentrated above all in French and European legislation because it is probably the place where this work will be carried out.

The grid utility supplies an AC voltage waveform, with sinusoidal form. The nominal voltage for European grids is 230V ±10% [76], that is, the output nominal voltage of the all power system designed to a grid connection must be between 207V and 253V. Moreover, the inverter must operate without problems when harmonics according to the table 3.1. are present in the grid [77].

Table 3.1. Values of individual harmonic voltages at the supply-terminals for orders up to 25. The THD of supply voltage, including all harmonics up to the order 40, shall be less than 8% [77].

Odd harmonics, non multiple of 3		Odd harmonics, multiple of 3		Even harmonics	
Order [h]	Voltage [%]	Order [h]	Voltage [%]	Order [h]	Voltage [%]
1	100	3	5,0	2	2,0
5	6,0	9	1,5	4	1,0
7	5,0	15	0,3	6	0,5
11	3,5	21	0,2	8	0,5
13	3,0	>21	0,2	10	0,5
17	2,0			12	0,2
19	1,5			>12	0,2
23	1,5				
25	1,5				
>25	0,2 + 12,5/h				

The nominal frequency for European grids is also regulated by EN 50160 standard [76], and it is fixed to 50 Hz ± 0,5 Hz.

The current harmonics are regulated by the EN61000-3-2-1 standard [78] in the most of countries, including European countries. The limits imposed by this standard are showed in the table 3.2. However, other countries as Japan and United States demand a current Total Harmonic Distortion (THC) below 5% and any harmonics below 2% of the fundamental current.

Table 3.2. EN 61000-3-2-A harmonic current limits [77].

Odd harmonics		Even harmonics	
Order [h]	Current [A]	Order [h]	Current [A]
1	16,0	2	1,08
3	2,30	4	0,43
5	1,14	6	0,3
7	0,77	>8	1,84 / h
9	0,40		
11	0,33		
13	0,21		
>13	2,25 / h		

Another issue to take into account in grid-tied photovoltaic installation is the grounding of the system and the equipment and its effect in the need of an electric isolation. Equipment ground is required in all countries. System ground is required in some countries for systems with voltages over 50 V (PV module open circuit voltage) [77]. Equipments ground involves that all metallic surfaces be grounded. Systems ground involves the negative (positive) terminal of the PV array(s) being connected to the ground.

Finally, the inverters are also provided of protection for islanding situations. Islanding is the continued operation of the inverter when the grid has been removed by purpose, by accident or by damage. That is, the grid has been removed from the inverter, which then only supplies local loads. The inverter must be able to detect it and take appropriated protections to protect people and equipments [77].

These protections can be carried out through active or passive detection circuits. The passive ones do not have any influence on the power quality, as they just monitor grid parameters. This method is used in the detection of under- and over- voltage and frequency; voltage phase jump; voltage harmonics and Rate-Of-Change-Of-Frequency. The active schemes introduce a disturbance into the grid and therefore, the power quality may be affected [79].

3.2.2 A static power converter concept

In a photovoltaic system, a Power Conditioning Unit (PCU) is necessary, not only to adapt the photovoltaic power production to specific load characteristic, but also to extract the maximum power from the PV generator. The PCU consists normally of switched-mode power converters with associated control laws.

The task of a power static converter is to process and control the flow of one or more electrical sources to one or more loads by matching its voltages and currents in a form that is optimal for both, source and load. In general, they contain power and control input ports, and a power output port. The input and output power ports can be DC or AC types. Nevertheless along this thesis, only DC input power ones will be take into account as the PVG is a DC source. DC-DC power converters, shown in fig. 3. 3.a, are used for DC loads as batteries and DC machines. DC-AC converters, in fig. 3. 3.b, are the power converters for grid connection and isolated AC loads.

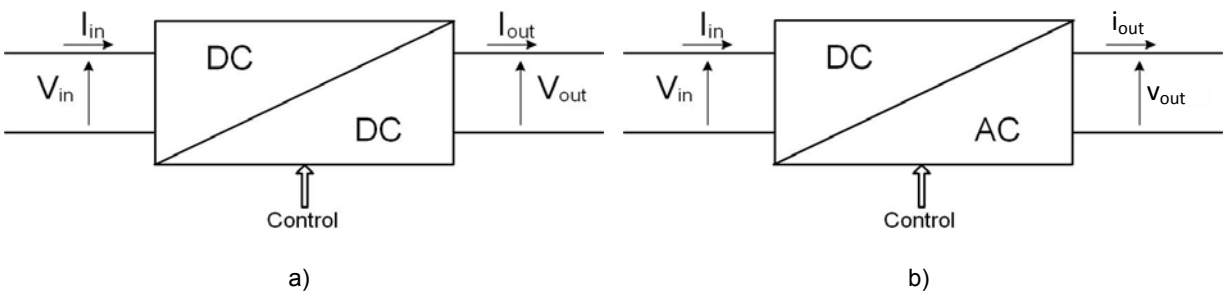

Fig. 3. 3. Schema blocks of a) DC-DC converter and b) DC-AC inverter

A static converter is a meshed of electrical components that acts as a linking, adapting or transforming stage between at least two electrical sources. One is the input generator and the other one, the load. The structure is composed by:

- Non-linear elements, mainly semiconductors switches used in switched mode
- Passive elements like capacitors, inductances and transformers. These reactive components are used for intermediate energy storage but also for voltage and current filtering. They generally represent an important part of the size, weight, and cost of the equipment and can reduce its global lifetime [80].

In the fig. 3. 4., the main elements of a power converter are represented :

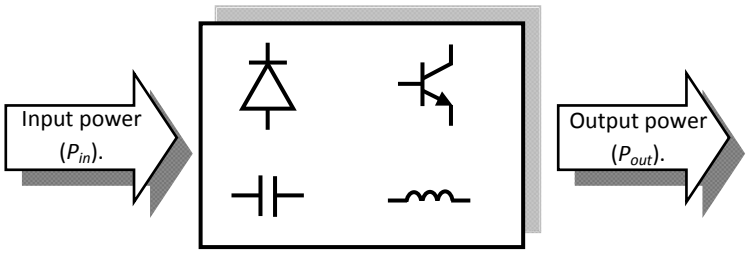

Fig. 3. 4. Schematised energy transfer though a power converter.

An ideal static converter controls the flow of power between its input to its output with 100% efficiency and it is recreates all the input power in the output port. This is the fundamental power conservation law applicable to all static converters.

$$P_{IN} = P_{OUT} \tag{3.1}$$

Process and transfer of the electrical power is made by semiconductor switches, in particular the time during they are at their on-state. For a simple structure with only one active component, the variable of adjustment is named duty cycle (that is, the ratio of on/off time named α). A relation between the input and output voltage/current defines this adjustment, given by equations (3.2) and (3.3), is valid for continuous conduction modes:

$$\alpha = f(V_{IN}, V_{OUT}) \tag{3.2}$$

$$\alpha = f(I_{IN}, I_{OUT}) \tag{3.3}$$

In on-grid PV installations, at least one inverter is necessary to guarantee the grid connection. The mains functions of an inverter is to create correct sinusoidal output electric signal, respecting, all the requirement of the public electric net in frequency and THD issues.

Apart from to respect the main legislation and standard, photovoltaic inverters have other constraints: low lifetime and reliability, high cost and low efficiency.

Grid-tied photovoltaic installations must compete with other better positioned and cheaper electricity producers as nuclear energy, thermo-electrical and hydroelectric plants. In this way, it is important to reduce the price of all the photovoltaic installation, including the cost of the power stage. The electricity power generator cost is measured by €/W or $/W. That is by, how much € or $ have been need to be invested for each produced W.

Moreover, the system must be as efficient as possible. The initial cost will be recover by selling the produced electricity and once the cost price is returned, the PV instalator can made benefits. As sold electricity is the electricity amount that is inserted into the grid, the system efficiency, including inverter efficiency is in direct relation with the efficiency. Thus, smaller are losses, higher is the systems efficiency and more energy can be injected into the grid, increasing the benefits.

Another constraint for PV installation is the lifecycle cost, which is directly linked with inverter reliability. In fact, inverters generally must be replaced every 5-10 years, whereas modules have a life of 25 years or more. In this way, investment in new inverters is required 3-5 times over the life of a PV system, which increases considerably the lifecycle cost of PV installations.

To resume, a photovoltaic power converter must adapt the photovoltaic energy production to public electric utility constraints, respecting the legislation and standards. But also in the same importance level, the inverter must be efficient, reliable and affordable in order to respond to industrial constraints and be competitive with other more economical and reliable traditional energy production systems.

3.2.3 Main structures of power inverters used for matching PV stages

The inverters can be classified by different families : the number of power processing stages and the use or not of a transformer categorize the power inverter.

3.2.3.1 Number of power processing stages

The power conditioning units in the photovoltaic system connected to the public grid can be composed by one, two or more power converters connected in cascade (fig. 3. 5.) Normally, they are not more than two converters, which can be also denominated stages. A higher number of stages involve more cost and less efficiency, but in addition, they offer the possibility of a better signal adaptation.

The inverter in fig. 3. 5.a is a single-stage inverter. This unique stage must handle itself all the tasks as the MPPT, grid current control, and in some cases, the voltage amplification.

Fig. 3. 5.b shows a dual-stage inverter. The first stage is a DC-DC converter, in which normally the MPPT control is performed as well as the voltage amplification if it is needed. The second stage is an inverter. Its main function is to modulate a sine-wave output signal and control the grid current insertion.

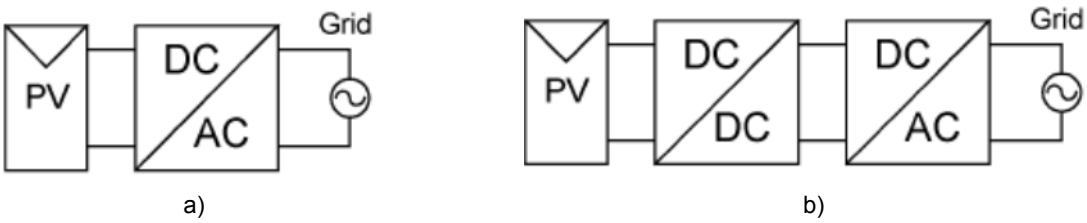

Fig. 3. 5. Two types of PV inverter depending in number of processing stages: a) single-stage inverter and b) dual-stage inverter

3.2.3.2 Power inverters with Transformer

The eventual presence and the type of transformer can be also used as criteria to classify the structures of power processing systems.

The use of a transformer is sometime a paradox in PV inverters. In some countries, as stated previously, the system grounding is not required if the PV maximum output voltage is less than 50V. Nevertheless, it is hard to achieve high-efficiency voltage amplification without transformer. In the other hand, for higher PV voltage levels, there is not needed for voltage amplifications and therefore, the transformer is not required for this function.

Two types of transformers are used: line-frequency transformer and high-frequency transformer. A line-frequency transformer are voluminous and heavy and in this way their increase the size, weight and the cost of the power stage. For this reason, nowadays, the high-frequency transformers are widely used since they have smaller size and weight due to a higher working frequency.

The bigger drawback of transformer is their low power transfer efficiency, which penalize considerably the Photovoltaic total efficiency.

3.2.3.3 The H-bridge inverter

The H-bridge inverter is one of the most common and simplest used inverter structures. Its name, H-bridge, is derived from the typical graphical representation of such circuit that is shown in fig. 3. 6. for a PV grid applications. It is built with four switches, and it main function is to inverse the input DC signal into an AC output signal. Closing S_1 and S_4 switches and opening S_2 and S_3 switches, a positive voltage is applied into the output port. The contrary operation, that is, closing S_2 and S_3 switches and opening S_1 and S_4 switches, a reverse voltage is applied in the output port. The switched of the same switching cell (S_1-S_2 and S_3-S_4) can never be closed at the same time, as this could cause a short circuit of the input source. The H-bridge inverter with a DC source, as it is the case of a PVG, generates a square wave voltage across the output port. For this reason, filters are needed in order to create a sinusoidal waveform output, agreed with grid-connection law and standards requirements.

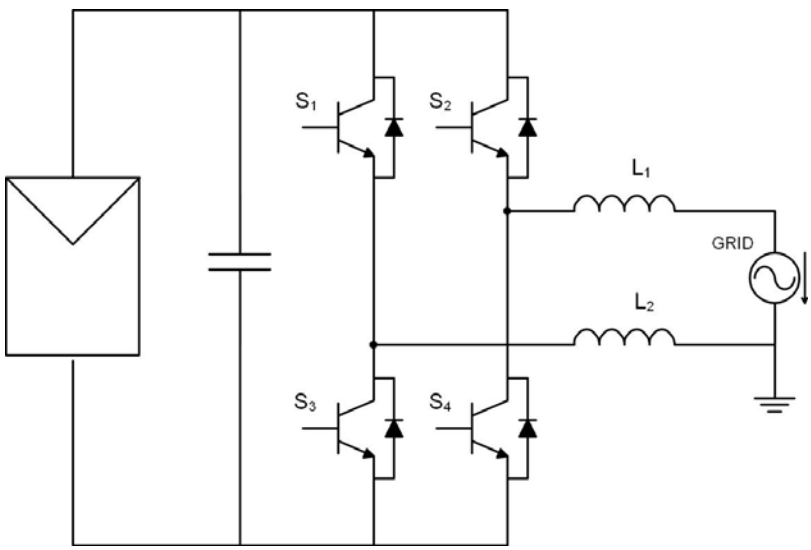

Fig. 3. 6. Electric schema of the H-bridge inverter.

The H-Bridge converter is traditionally used in centralized architecture PV systems [81]. The first centralized converters used this structure. The main reason was that this inverter is simple, does not have lot of components and it is easily controllable in order to achieve a correct waveforms that can be connected directly to the grid. Nevertheless, it presents other disadvantages, principally due to the special characteristic of PV sources.

One of the most important characteristic of this converter is the function that it can accomplish : the adaptation of the current and the voltage signals. In fact, it cannot be achieved any voltage step-up transformation operation, and in this way, a minimum voltage level must be guaranteed in the input port in order to get to the grid-connection voltage level.

The other difficulty presented by this kind of structure in photovoltaic applications is the MPPT control. Indeed, the system does not let any degree of freedom. This structure does not allow a real MPPT control because only one independent value can be controlled (one duty cycle) and it must guarantee a minimum voltage level in the input port to a correct grid-connection output signal.

For this reason, the advantage of being one of the simplest DC-AC converters is also one of its biggest drawbacks for its utilisation in PV systems. In fact, the H-bridge inverter is a structure that gives a unique degree of freedom, making difficult to accomplish in the same time, the inversion of current, and the MPPT control operation.

In this way, the most of the time, the photovoltaic grid-connected connected system use two-stage inverters. The first stage is normally a DC-DC converter in charge to match electrical characterises and with the help of the MPPT control extracts the maximum of PV energy. The second stage consists on the DC-AC converter that regulates the output current to achieve a sinusoidal waveform, in phase with the utility electrical grid.

The structure uses normally MPPT control and can assure a correct match with the grid utility. The first structure consists normally in a boost or buck converter. The second stage is normally an H-bridge converter. Being the DC-DC converters who is charged of the voltage amplification and the MPPT control, this tasks are avoid in the inverter and in this way, its control is only dedicated to a correct sinusoidal and grid in phase output signal creation.

3.3 Power architectures of PV systems

The architecture of the power converter is important in a PV system. This structure determines the main characteristics of the photovoltaic installation, as the amount the PV modules need for the PV system and its type of connection. The effect of the partial shadowing or mismatch between PV modules in the energy production will also depends on the type of the architecture. Nevertheless, the price and cost of the PV also depends on the choice of the architecture. In resume, the choice will involve a bigger or smaller energy production and efficiency as well as an importance difference in the cost. For this reason, it is important to know different types of architecture in order to choose the correct PV architecture for each PV installation.

The main architectures of the nowadays PV system will be analyzed, following their evolution and looking for the future tendency. Finally, the electric structures of DC optimizers will be analyzed as introduction to the work carried out in this thesis.

3.3.1 Main grid-tied photovoltaic systems

Historically, the first grid connected photovoltaic installations where built using the centralized topology (fig. 3. 7.) [82]. This structure connects a large number of PV modules to the grid through only a high power inverter. In this type of installation, the photovoltaic modules are first connected in series building strings, in order to reach high voltage levels (normally 400V). The interest is to avoid a voltage amplification stage in the power inverter, and simplify the power conversion structure in this way. The strings are connected in parallel to increase the input current, and therefore the power. These installations could have from several kW to some MW peak of power.

These structures are characterized by its high robustness and reliability and they have been widely used in spatial applications, to supply electricity to isolated villages or house and in big photovoltaic farms for electrical generation plants.

The biggest drawback of this type of topology resides in the MPPT centralisation. As only one power-processing unit is charge to process all the PV modules, and therefore, there is a unique MPPT control, the mismatch losses between the PV modules and partial shadowing have a huge effect in the power system efficiency.

Another drawback for this kind of installations is the halt of all the energy production in case of the breakdown of the power inverter, as all the PV power is passed though the alone inverter.

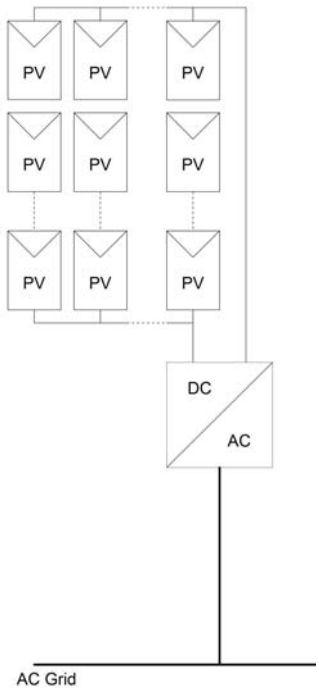

Fig. 3. 7. Photovoltaic system based in centralized architecture

The centralised inverters are being considering the past of earth photovoltaic system applications. Although they are still used in big photovoltaic farms, other PV structures begin to be used in order to exploit the PV energy in more distributed way and harvest bigger efficiency. First, the string and multi-string topologies have took the place of centralized inverters, which divide the PV arrays into strings. Later, a bigger division is taking place, and

the PV group is directly divided in individual PV modules connected to a unique power converter.

3.3.1.1 String level energy management solution

A string is a group of PV panels connected in series. In the multi-string [83] and string architectures [84] (fig. 3. 8.a and fig. 3. 8.b), the PV array is divided into PV strings. In multi-string topology, each string is connected to a DC-DC converter. The outputs of the DC-DC converters are connected to the centralized grid-tied inverter. The difference for the string topology is that each string is directly connected to the grid by an inverter. In both topologies, each string benefits of the MPPT control and the maximum power point tracking is carried out in more distributed way than the centralized architecture. Thus, a partial shadowing in one of the string does not affect to the energy production of other strings and the PV power production is improved.

As each converter is connected to fewer panels than in centralized architecture, the initial investment can be smaller, being the user who determines the size of the installation depending in the number of installed inverters. So on, for particular and domestic users, the investment is easier. Nevertheless, the problem of the decrease of efficiency due to mismatch losses between PV panels is not really solved with these topologies, as a partial shadow in a PV panel follow affecting to all the PV string.

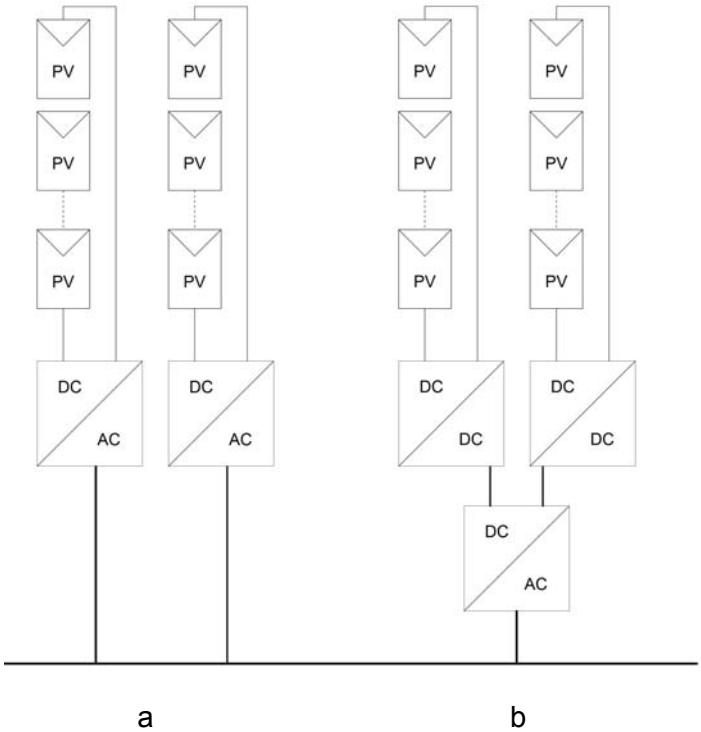

Fig. 3. 8. String level energy management photovoltaic architectures: a) string topology and b) multi-string topology.

3.3.1.2 Module Level Power Management (MLPM) photovoltaic solutions

The latest PV system topologies tend towards the distribution of the power processing system. In order to increase the efficiency of PV systems, Module Level Power Management

(MLPM) solutions are fast growing. It is expected to be almost the 40% of the residential PV installations for 2014 [85].

The MLPM systems consist on micro-inverters and DC power optimizers, which manages the energy of PV modules individually. The fig. 3. 9. shows the micro inverter, optimiser and total MLPM system installation forecast for until 2014 [86].

Micro-inverters convert direct PV current (DC) from a single PV module to alternating current (AC), whereas optimizers use DC-to-DC converter technology to take full advantage of the power harvest from the PV systems.

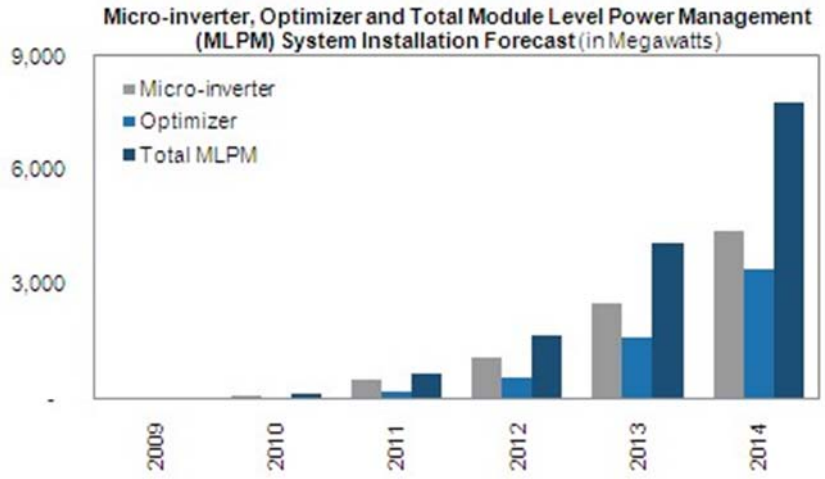

Fig. 3. 9. Micro-inverter, DC-optimizer and MLPM PV system installation forecast [86]

Micro-inverters consist on AC-DC power structures that manage the power of a unique PV module and integrating module dedicated MPPT control (fig. 3. 10.a.). They are designed to be connected to an electrical network. Therefore, they include in their structure the voltage amplification, the MPPT control and the inversion and the adaptation to grid connection. They are also been known as AC module structures.

This kind of structure presents many advantages. The most important is the distribution of the MPPT control in each PV panel, avoiding the problems due to the mismatching of them. In this way, the system can extract the maximum power of the PV panel. Moreover, these kinds of installations ask for a small initial investment, as we can install the PV modules one by one. As well as the facility of enlarging of the PV installation, due to the parallel operation capability in the AC side.

However, this system has also disadvantages. As the system is designed to connect the PV panel to the grid, the needed voltage amplification is important. This amplification can means a reduction of the overall efficiency. In addition, this amplification can involve complex electronic circuits and therefore, the increase of the price of the watt. Nevertheless, these systems are intended to be mass-produced, with low manufacturing cost and low retail prices. Additionally, they can become “plug and play” devices, easy to use, even by people with any knowledge of electrical installations. Taking into account these last effects, this kind of system could become interesting to domestic users.

As the AC modules are the DC-AC converters dedicated to one PV module, the DC optimizers are the DC-DC converters dedicated unique PV module and though to be integrated in multiple inputs distributed system. In this way, the output of these converters is a DC bus that is in the same time the input of a grid connected inverter. The goal of the DC optimizer is to extract the maximum power possible from the PVG, placing the MPPT in a distributed way.

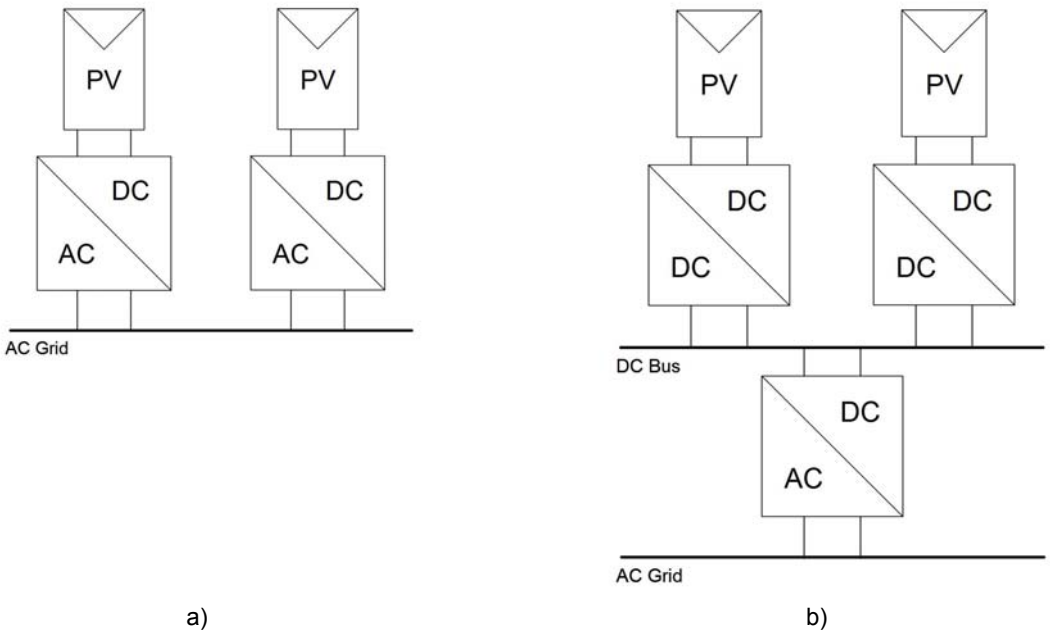

Fig. 3. 10. Distributed PV architectures: a) AC module and b) DC optimizer connected to DC bus and Grid-tied inverter

3.3.2 DC-DC structures in PV systems

The DC-DC converters in photovoltaic systems are traditionally used for battery charging PV applications. They did historically used in stand-alone photovoltaic installations. In stand-alone PV systems, the PV energy has to be stored in order to guarantee the energy when the sun is not present. In this way, battery-charging systems from the PVG are used.

In grid connected system, the use of the battery has been avoid and as all the energy was directly used or inserted in the electric grid, the traditional domestic photovoltaic structure has avoid the DC-DC power structure.

Nevertheless, the transition from centralized structures to other distributed architecture has helped to the apparition of new structures where the DC-DC power converter is includes as in multi-string structures or DC optimizers.

The use of DC optimizers to extract the maximum photovoltaic energy is more widely used. These structures are placed next to the PV module, and they extract the maximum energy from the PV module in a distributed way. According to photovoltaic use forecast studies [85], in the future, the use of this kind of architecture will increase considerably, taking an important part of the total residential photovoltaic installations.

In resume, the DC-DC structures can be distinguished by the presence or not of a battery in the system, which will determine the structure of the global system. The fig. 3. 11. shows two mains examples of a distributed PV system with a DC-DC power converter.

The first one is characterized with a battery as intermediate state (fig. 3. 11.a). As normally the voltage of a battery is about 24V or 48V, the conversion structure must be a step-up converter. The other structure is characterized by a 400V DC bus output (fig. 3. 11.b). New smart-grid and micro-grid systems are hydride systems with several different power sources, as the photovoltaic, fuel-cell or wind generators. In some of this smart-grid, the power sources are all connected to a 400V DC bus, which is the input of a grid-tied inverter. In this way, the DC module structure connected to this DC bus must have a great voltage transformation level, keeping high conversion efficiency.

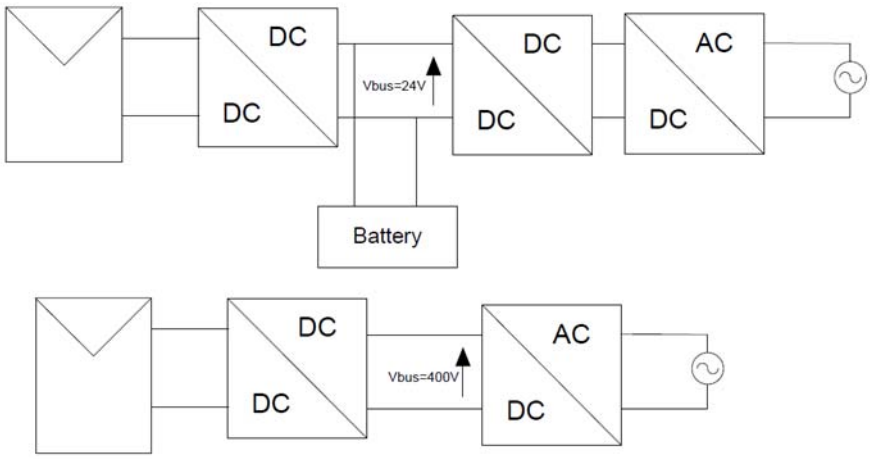

Fig. 3. 11. Two example of DC-DC structures in a distributed PV system

The first architecture uses an intermediate battery to stock energy for the moments that there is not photovoltaic energy production. This kind of installation cannot benefit of advantages in electricity sold, and therefore few people use this system. Nevertheless, in stand-alone systems, a battery is necessary to guarantee a constant energy supply and this type of installation must be into account. Moreover, the micro-grid system concept, saw as a future distribution system, forecasts the presence of batteries. For this kind of systems, authors in [87] point out the interest of using battery level DC bus instead of charging battery by means of step-down converter in systems of higher voltage bus.

3.3.2.1 Study of classical DC-DC boost converter

The simplest step-up DC-DC converter structure is the boost converter. The electrical schema of the boost converter is reminded in the fig. 3. 12. The boost converter is one of the simplest DC-DC converters. It is a switched mode converter able to produce a dc output voltage that is greater in magnitude than the dc input voltage. It does not have galvanic isolation. Its simplicity, low number of components, the facility for control and high efficiency make this structure adequate for photovoltaic systems.

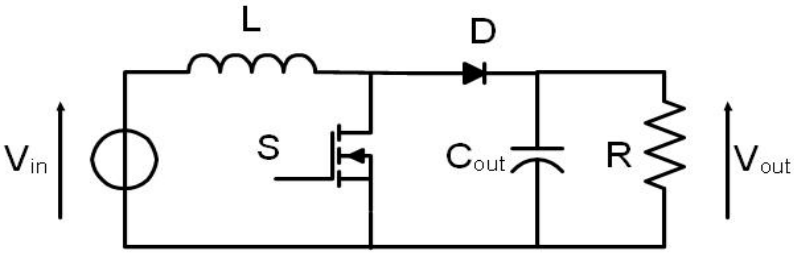

Fig. 3. 12. Electric structure of the boost power converter

For practical realization of the switch cell, a MOSFET and a diode are needed, as shown in fig. 3. 12. An inductor is used as internal storage energy element. The inductor acts as a load when it is being charged and it absorbs energy. When it is being discharged, it acts as an energy source.

The basic principle of a Boost converter consists of two distinct states (ON and OFF) as shown in fig. 3. 13. and the energy transfer through the loads is carried out in three steps. In first step, the inductor is charged as the S_1 switch is turn on. In a second step, the inductor is discharged through the switch S_2 to the load and C capacitor. In last step, the C capacitor is discharged to the load, maintaining a constant voltage level in the load, and at the same time, the inductor is charging, as the S_1 switch is an ON state.

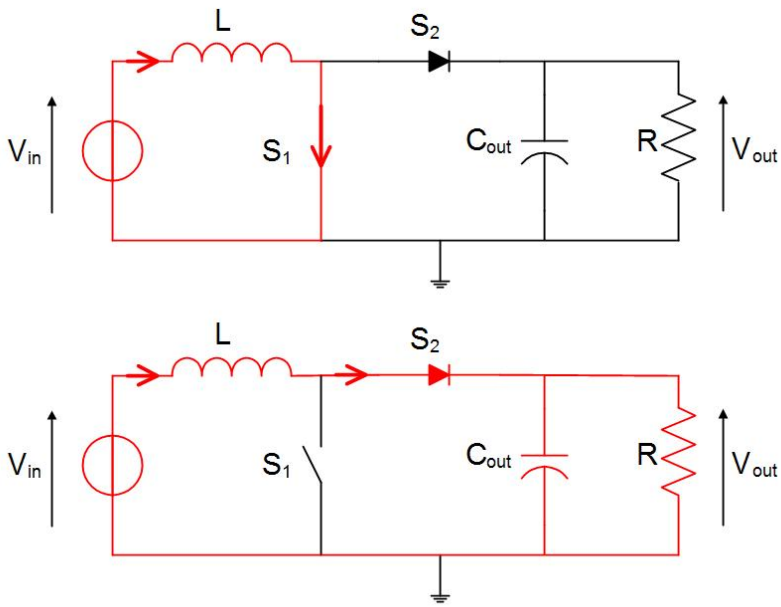

Fig. 3. 13. ON and OFF state of a boost converter

For a continuous operating mode, the ratio between the input and output voltage is defined by the following equation.

$$\frac{V_{out}}{V_{in}} = \frac{1}{1-\alpha} \tag{3.1}$$

Then:

$$\alpha = 1 - \frac{V_{in}}{V_{out}} \tag{3.4}$$

In theory, the voltage gain of the boost converter can be infinite when the duty cycle is close to one. However, the switch turn-off period becomes short when the duty-cycle increases and the current ripples of the power device are large with high-step-up conversion. That increases the power device conduction losses and turn-off the current. Moreover, the voltage stress of the switch and the diode is equal of the output voltage, which is large in high-output-voltage applications. The cost of the switches with high voltage stress is rather higher that of the switches with low voltage stress. The switching and reverse-recovery losses are significant due to the hard-switching operation. Furthermore, the power level is limited by the single-phase single-switch solution.

This converter is still adequate for battery charging DC-DC photovoltaic applications or for systems with low voltage bus in which high-step-up voltage amplification is not needed. Nevertheless, for more complex structures, which ask for a high-voltage-step-up operation, is not utilisable.

3.3.2.1.1 Losses in a boost converter

As we have detailed in the previous section, the efficiency of a power converter can be defined as the ratio between the output power and the input power and the output power will be determined by the losses of the system in the power transfer:

$$\eta_{PV} = \frac{P_{out}}{P_{in}} = \frac{P_{in} - P_{Losses}}{P_{in}} \tag{3.5}$$

More than one technique can be used to determine the losses and therefore the efficiency of a power converter. One of the techniques uses equivalent circuit models of power structures by representing the converters as a transformer with α as duty cycle. Another method analyses the losses of components one by one and determines the total losses by the addition of all of them.

The converter can be represented as a DC transformer. In [89], this model of representation is used to get a model for losses evaluation. As the DC converter can be represented with a transformer model (fig. 3. 14.a.), in the same way, it can be simplified by referring all the elements to the secondary side (fig. 3. 14.b). This model can be extended by the equivalent circuit elements. Non idealities, such as sources power losses, can be modelled by adding resistors as appropriate. After, using basic circuit development techniques, the drop of voltage and therefore, the losses of each component can be calculated.

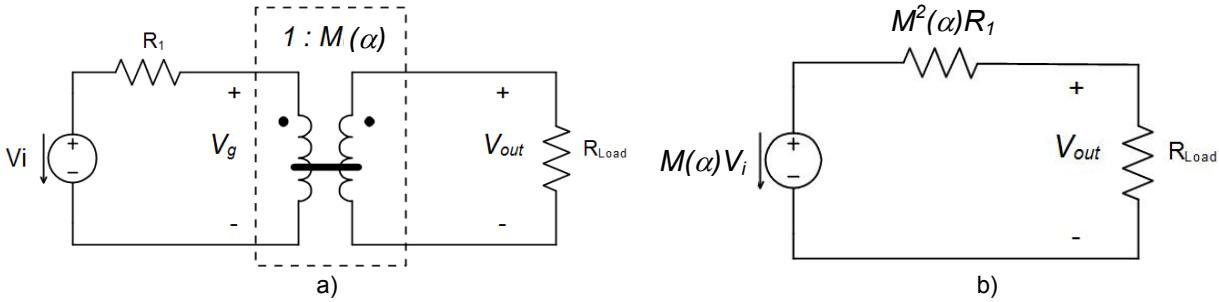

Fig. 3. 14. Representation of a boost DC-DC converter by a DC transformer (a) and its equivalent circuit in primary side (b).

The boost converter example will be used to implement this technique and evaluate its efficiency.

First, the inductor copper losses can be taken into consideration. The practical inductor presents two types of power losses: a) copper losses, originating in the resistance of the wire, and b) core losses, due to hysteresis and eddy current losses in the magnetic core. The model that describes these losses is presented in the fig. 3. 15.

Fig. 3. 15. Equivalent model of inductor representing copper losses by series resistor RL

The conduction losses of semiconductor can be also modelled. The forward voltage of a MOSFET can be modelled with reasonable accuracy as an on-resistance R_{DSon}. In the case of a diode, a voltage source plus on-resistance yields presents a good model. The fig. 3. 16. shows the equivalent model of boost converter in on and off states.

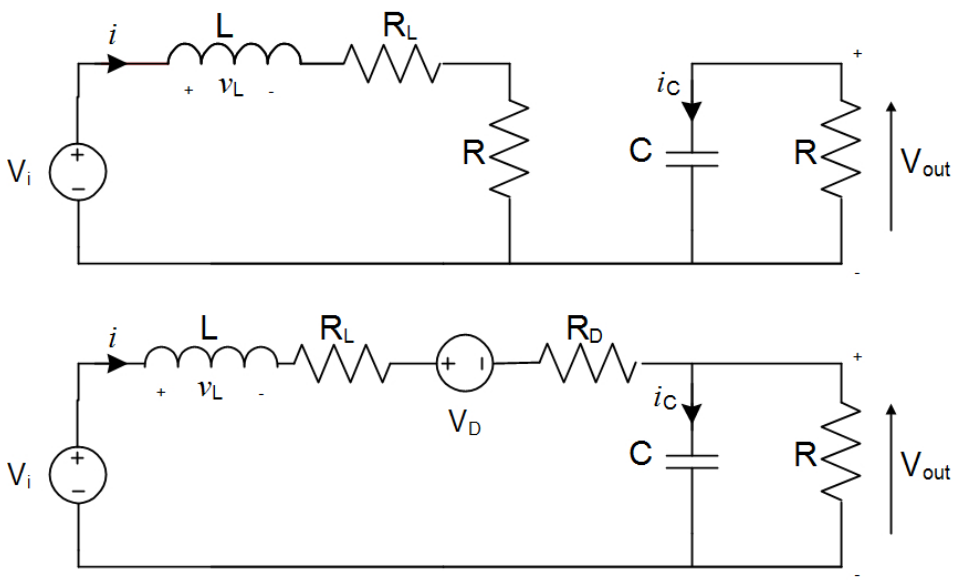

Fig. 3. 16. Boost converter circuit: when MOSFET conducts (on state), et when diode conducts (off state)

This circuit can be represented as an idea transformer model. The fig. 3. 17. shows the equivalent circuit model of boost converter including the ideal transformer, inductor winding

resistance, and MOSFET and diode conduction losses. The term α corresponds to the duty cycle of the converter, that is, to on-state, and the term α' corresponds to off state.

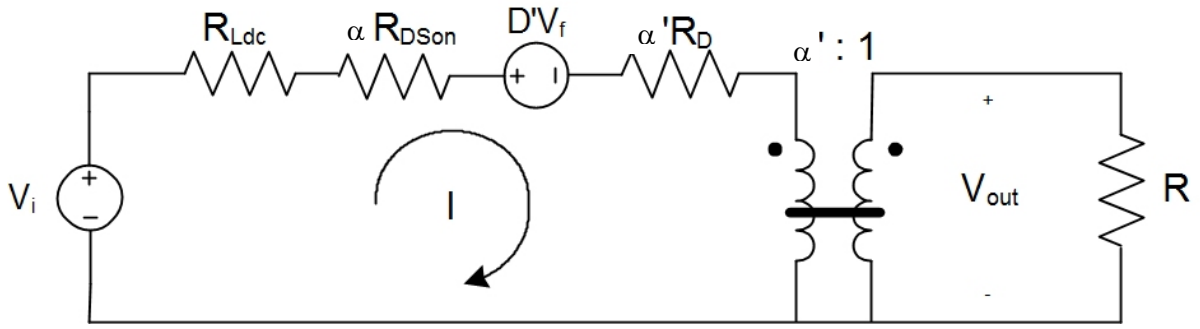

Fig. 3. 17. Equivalent circuit model of boost convert including an ideal transformer, diodes and MOSFET losses.

Once the equivalent circuit model is inserted into the boost converter, the circuit can be analysed in the same manner than the circuit used for the ideal lossless converter, using the principle of inductor volt-second balance, capacitor charge balance and small-ripple approximation.

Following these techniques [89], the efficiency of a boost converter can be sum up in the following equation:

$$\eta_{boost} = \alpha' \frac{V_o}{V_i} = \frac{\left(1 - \frac{\alpha' V_f}{V_o}\right)}{\left(1 + \frac{R_{Ldc} + \alpha R_{DS(on)} + \alpha' R_D}{\alpha'^2 R}\right)} \tag{3.6}$$

Where,

- α : Duty cycle of power converter
- α' : Off state duty cycle of power converter
- V_o : Output voltage of the DC-DC converter
- V_i : Supply voltage or the photovoltaic voltage
- V_f : Voltage Drop of the diode
- R : Output Load Resistance
- R_D : Condution resistance of the Diode
- $R_{DS(on)}$: On resistance of the MOSFET
- R_{Ldc} : DC resistance of the inductor

Nevertheless, this model does not take into consideration the switching losses, which must be integrated in more evolved model.

Another method to estimate losses is to take the power structure as a group of interconnected components. Looking one by one, these components and their losses, all losses can be estimated. This last method was taken for this study because of its simplicity.

The losses of this structure are focused in the switching element composed by the MOSFET and the diode, and in the intermediate storage element that is the inductor. Moreover, the energy supply for drivers and control elements must be taking into account, as it also produces losses [90].

The inductor is a passive component and therefore, it only supports conductions losses. Nevertheless, two kinds of conduction losses are presented in the inductor: the losses caused by the DC resistance (P_{Ldc}) and the losses caused by the AC resistance (P_{Lac}) [91].

As the inductors are not ideal component, they have resistance inherent in the metal conductor. This resistance can be modelled as a resistor in series with the inductor and it is composed by the AC resistance and the DC resistance. In fact, the current though the inductor is composed by the DC or low frequency component and the AC component, as it is appreciated in the fig. 3. 18. In order to predict the inductor losses correctly, this must be separated into the two components.

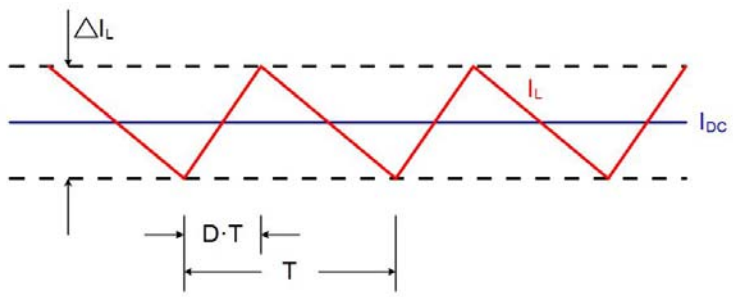

Fig. 3. 18. AC Current through an inductor in a typical DC-DC converter

To calculate low frequency or DC losses, we use the low frequency resistance, which is quoted DCR in inductors data sheets. The current is the RMS value of the current and the ripple values through the inductor. In this cases where the ripple value is small, this value can be taken as the input DC current, that is, PV current.

$$P_{Ldc} = R_{Ldc} \cdot i_m^{\ 2} \rightarrow P_{Ldc} = R_{Ldc} \cdot I_{PV}^{\ 2} \tag{3.7}$$

Where,

- R_{Ldc} : On resistance of the Mosfet
- i_m: Current through the inductor, that is the same that the input current of the dc-dc converter, that is, the PV current. In following reference it will be directly call IPV

High frequency losses are evaluated using the AC resistance, quoted ESR and the RMS value of the ripple current only. Inductor AC conduction losses are defined as:

$$P_{Lac} = R_{Lac} \cdot i_{Lac}^{2} \tag{3.8}$$

Where

$$i_{Lac} = \frac{1}{2\sqrt{3}} \cdot \Delta I_L \text{ and } \Delta I_L = \frac{V_o - V_i}{L} \cdot \frac{V_i}{V_o} \cdot \frac{1}{f}$$

$$P_{Lac} = R_{Ldc} \cdot \left(\frac{1}{2\sqrt{3}} \cdot \Delta I_L \right)^2 \tag{3.9}$$

$$P_{Lac} = \frac{R_{Ldc}}{12} \cdot \left(\frac{V_o - V_i}{L} \cdot \frac{V_i}{V_o} \cdot \frac{1}{f} \right)^2 \tag{3.10}$$

Where,

- i_{Lac} : AC Currant through the inductor
- V_i: Supply voltage or the photovoltaic voltage
- V_o : Output voltage of the DC-DC converter
- L : Inductance
- f : Switching frequency

The diode and the MOSFET are active components and they compose the switching cell. They support both switching losses and conductions losses.

The MOSFET device can be represented as it is shown in fig. 3. 19.a, with three parasites capacitors. As in the switching operation these capacitors must be charged, this involves losses. The more important losses are created by the charging of the junction capacitance (P_{Qds}). Moreover, in the switching of the MOSFET gate charge must be charged, which is traduced as additional losses (P_{Qg}). As last losses lied with the MOSFET switching operation, there are the losses called switching losses, which takes into account the effect that the turn off and turn on of the switch is not instantaneous. As can be appreciated in fig. 3. 19.b., power losses peaks take place meanwhile the turning off and the turning on (P_{sw}).

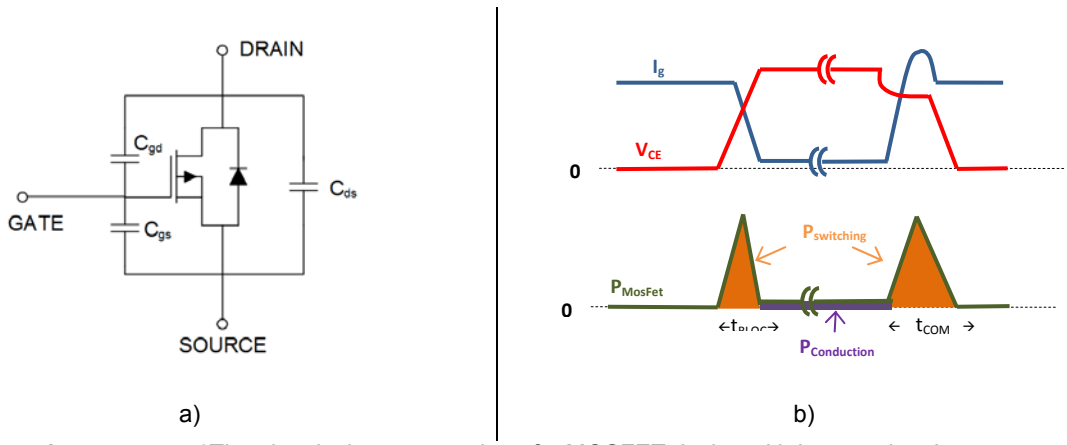

Fig. 3. 19. a)The electrical representation of a MOSFET device with its parasite elements; and b) switching losses evaluation,

Finally, the internal resistance $R_{DS(on)}$ produce losses in the MOSFET (P_{ON}). These losses depend on on the current through it and on the time fraction that the MOSFET conduct current (ON state)

Gate charge losses:

$$P_{Qg} = Q_g \cdot V_g \cdot f \tag{3.11}$$

Where,

- Q_g : Gate charge of the Mosfet
- V_g : Gate drive voltage of the Mosfet
- f : Switching frequency

Junction capacitance Mosfet losses:

$$P_{Q_{DS}} = \frac{1}{2} \cdot C_{DS_H} \cdot V_i^2 \cdot f \tag{3.12}$$

Where,

- C_{DS} : Junction capacitance of the Mosfet

Switching losses:

$$P_{sw} = \frac{1}{2} \cdot V_o \cdot f \cdot \left(\left(t_f + t_r \right) \cdot I_{PV} + \frac{\left(t_r - t_f \right)}{2} \cdot \Delta I_L \right) \tag{3.13}$$

Where,

- t_r : Rise time at switching on
- t_f : Fall time at switching off

Conduction losses:

$$P_{ON} = \frac{V_o - V_i}{V_o} \cdot R_{ds(on)} \cdot \left(i_{PV}{}^2 + \frac{\Delta I_L^2}{12} \right) \tag{3.14}$$

Where,

- $R_{DS(on)}$: On resistance of the Mosfet

The last element that produces losses is the diode. It produces conduction and switching losses. Nevertheless, the switching losses are very low, and therefore they will be considered negligible. Thus, we will only consider conductions losses, which are represented with the following equation:

$$P_D = \frac{V_i}{V_o} \cdot V_f \cdot I_{PV} \tag{3.15}$$

Where,

- V_f : Voltage drop of the diode

The power consumption of the control IC and drivers is also a loss for the system:

$$P_{CTRL} = V_s \cdot I_{CC} \tag{3.16}$$

Where,

- V_s : Voltage supply for the IC control and drivers
- I_{CC} : Supply current of IC control and drivers

Total losses are the sum of all individual losses:

$$P_{Loss_T} = P_{Ldc} + P_{Lac} + P_{Qg} + P_{Qds} + P_{sw} + P_{On} + P_D + P_{CTRL} \tag{3.17}$$

Considering that the photovoltaic voltage change is negligible, as well as the battery voltage change and operating switching frequency is fixed, some losses are quadratic function of I_{PV} (P_{Ldc}, P_{On}), other losses are linear function of I_{PV} (P_{sw}, P_D) and they are another losses that keep constant for any I_{PV} value ($P_{Lac}, P_{Qg}, P_{Qds}, P_{CTRL}$). The above formula (3.17) can be simplified as:

$$P_{Loss_T} = a \cdot i_{PV}^2 + b \cdot i_{PV} + c \tag{3.18}$$

Where,

$a \propto P_{Ldc} + P_{On}$;

$b \propto P_{sw} + P_{D_{on}}$;

and $c \propto P_{Lac} + P_{Qg} + P_{Qds} + P_{CTRL}$.

This losses equation can be integrated in the efficiency equation (3.5). Fig. 3. 20. represents the simulation of the efficiency of a boost converter for a fixed temperature and input and output voltages. The simulation parameters are given in table 3.3. and table 3.4. The phenomena of the increasing and decreasing efficiencies can be explained by the losses equation. In low power, when the input power is near to null production, the constant loss has major importance. As these losses are kept constant for all the power levels, but the input power is lower, the efficiency is low. As the power level is increasing, the effect of constant losses is decreasing, and the other losses affects proportionally in relation of the input power until the maximum efficiency point is reached. The decrease in the efficiency is caused by

the losses that are dependant of the squared current ant it parabolic effect. In this way, for higher power level, the efficiency is lower.

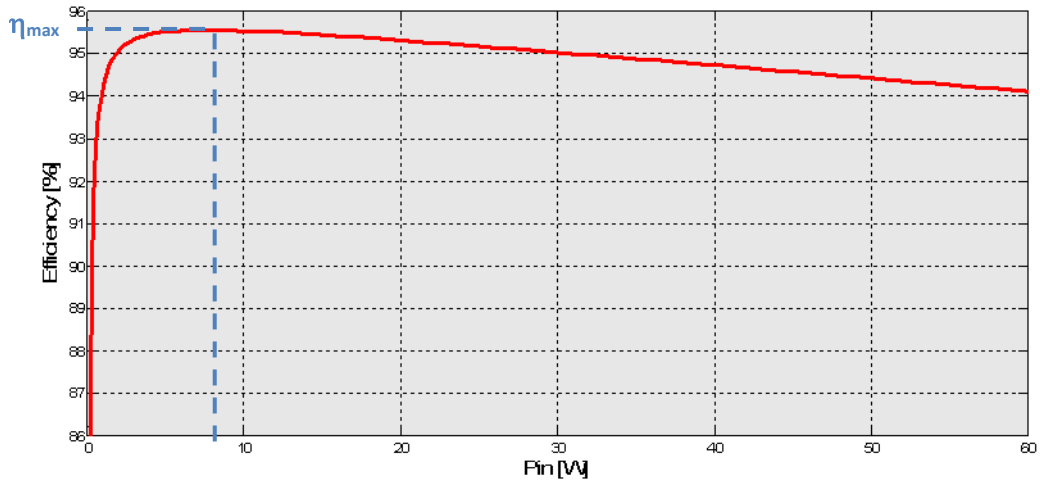

Fig. 3. 20. Efficiency simulation of a boost converter

Table 3.3. Simulation parameter for efficiency calculus:

Vin	14.5V
Vout	24V
Frequency	320000Hz

Table 3.4. Components parameter for the efficiency simulation

Inductance L	33 10^{-3} F	tr	35 10^{-9} s
RLac	0.5 Ω	tf	27 10^{-9} s
Qg	5.3 10-^{9} C	tdoff	7.9 10^{-9} s
Vg	5 V	tdon	19 10^{-9} s
Cds	75 10^{-12} C	Vf	0.59 V
Ron	0.075 Ω	Icc	0.5 10^{-3} A

3.3.2.2 Other DC-DC converter structures used in DC optimizers

As the boost converter presents a limited voltage conversion gain for efficiency high-voltage-step-up operation, other structures must be envisaged. There are many researches in this field, looking for efficient high step-up DC-DC converters.

Taking as base the boost structure, authors in [92] and [93] present the three level boost (fig. 3. 21.) which can double the voltage gain in comparison of the classical boost converter. In addition, this structure halves the power voltage stress compared to a classical boost. Low voltage stress and high-performance MOSFETs with low $R_{DS(on)}$ can be used to reduce circuit cost and the conduction losses. Besides, the structure presents improvements in switching losses and EME noise due to the low voltage stress. However, as the power devices operate in hard-switching condition, the reverse-recovery problem of the output diode is severe. Some solutions are possible in order to get the soft-switching performance using converters as the active zero voltage transition three voltage converter [94] or the passive lossless soft-switching three-level boost converter [95].

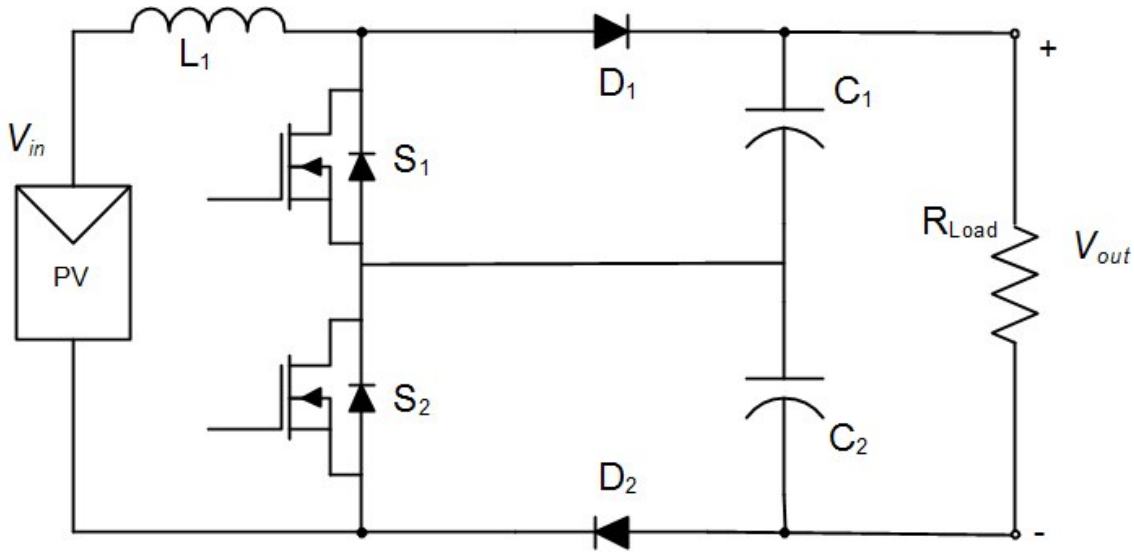

Fig. 3. 21. Three level boost DC-DC conversion structure

However, sometimes, the voltage conversion of the three level converter is not high enough to achieve desired power levels. An option to solve this problem is the cascaded structure where two boosts are connected in cascade (fig. 3. 22.) to double the voltage conversion gain. In addition to extend the voltage gain, the current ripple can be further reduced.

The voltage stress of the first stage is low. It can operate in high frequency in order to improve power density. The second stage can work in low frequency to reduce switching losses. Although this converter can achieve high voltage conversion gain, the main disadvantage of this structure is that it needs two sets of power devices, magnetic cores and control circuits. So on, it becomes in an expensive and more complex system. Another issue of this converter is the stability and the control system must be designed carefully.

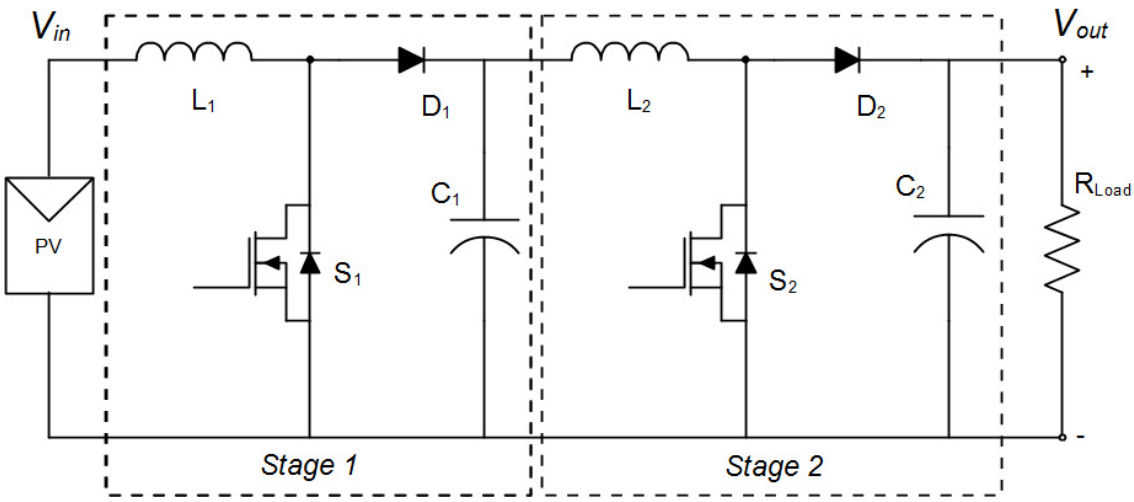

Fig. 3. 22. Two cascade boost power structure

Cascaded boost converters have considerable amount of components, which involves cost, complexity and losses. To reduce the number of components, the two active switches of the cascaded boost converter can be integrated into one switch to reduce the circuit complexity [96]-[99]. This new structure is called quadratic converter (fig. 3. 23.). It is a simpler structure, only one power device must be controlled and the instability issue is avoiding in comparison with the cascaded boost converter. However, this converter presents high EMI levels, due to the hard switching and the absence of the auxiliary commutation. Many researches have been carried out in order to improve this problem. Examples of this research are the soft switching quadratic boost converter [100] or the transformless single switch quadratic boost converter [101].

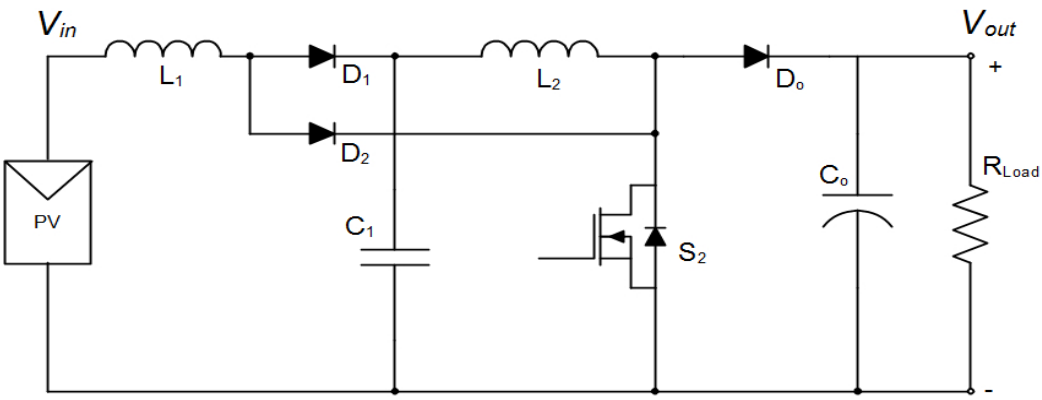

Fig. 3. 23. Quadratic boost structure

In non-isolated converters, the utilisation of coupled inductor is an utilised technique to achieve big voltage conversion gains. The second winding of the coupled inductor works as a voltage source. This one is in series with the power branch and the voltage gain is extended by the turns ratio design of the coupled inductor. Authors in [102] present a high-step-up converter with coupled inductor. An auxiliary circuit has been added in order to achieve the soft-switching performance and reduce the switching loss. This auxiliary circuit provides ZVS and ZCS turn-on conditions for the switch and as the turn-on period of these auxiliary switches is short, the additional losses are reduced. The disadvantage of this topology resides in its complexity and high cost, due to high number of switching cells.

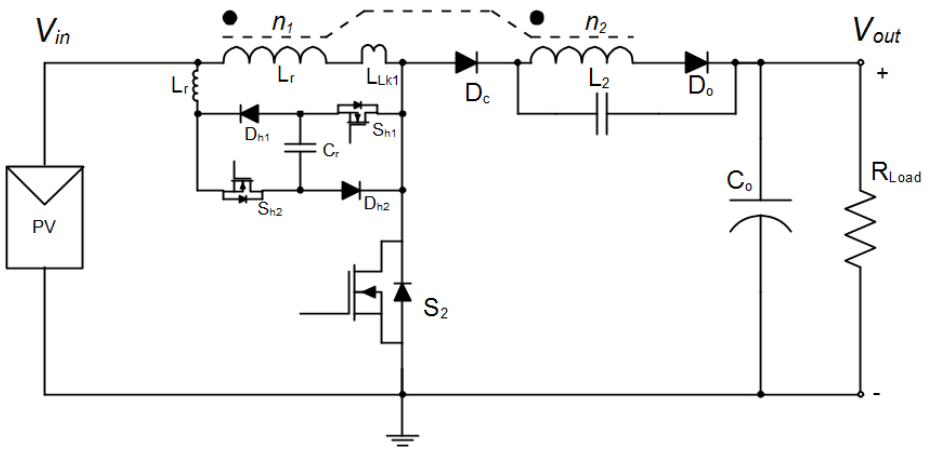

Fig. 3. 24. Coupled-inductor DC-DC power converter

The capacitor can be used as another voltage source to achieve a high-step-up conversion. The literature presents many switched-capacitor DC-DC converters with large conversion ratio [103]-[105]. An *N*-stage High-step-up converter with switches capacitors is shown in the fig. 3. 25.a. [104]. Each switched-capacitor cell is composed of a capacitor, a diode, and two switches. Each capacitor can be taken as a voltage source, which is switched and recombined by the switch devices. The current path is provided by the diode when the switch turns off. High-step-up and wide-range conversion is possible by employing *N* stages of the switched-capacitors cells.

However, this structure presents a large number of active switching devices. In order to reduce the number of the power MOSFETs and gate drivers, an *N*-stage high-step-up-switched-capacitor resonant converter is proposed in [105]. The circuit is shown in fig. 3. 25.b. In this case, the switched-capacitor cell is composed by two diodes and two capacitors. The lack of active switches in the switched-capacitor cells simplifies considerably the circuit structure.

Nevertheless, both structures have many components, which involve a high cost and complexity. Thus, the control of these structures is delicate and request complex control systems to guarantee the stability. The voltage drop and therefore the power losses in all the switching components cannot be neglected. Therefore, although they present very transformation rapport, the low efficiency of the structure constitute a big drawback for its utilisation in PV systems.

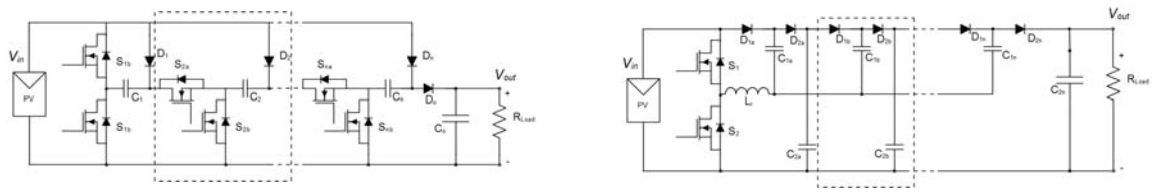

a) b)

Fig. 3. 25. Two structure of N-stage high-step-up converters with switched capacitors.

A different technique to achieve high conversion ratios is the use of multilevel converters. The general multilevel concept is based in the same principle and use the capacitor as a voltage source. The fig. 3. 26. shows an example of the high-step-up converter with a general multilevel cell [106]. Each basic cell is made up of a clamp capacitor and two switches that operate in complementary mode. This kind of structures can obtain a

high voltage gain by the parallel or series structure of the basic cells. High-efficiency, high power density and bidirectional performances are achieved for the converter.

In this kind of structures, there is no need of magnetic components such as the inductor or the transformer. However, a large number of power devices are necessary to get high voltage gain, which increases circuit complexity and cost. In addition, the output voltage regulation capability is poor in a wide load variation because the output voltage must be a fraction or a multiply of the input voltage.

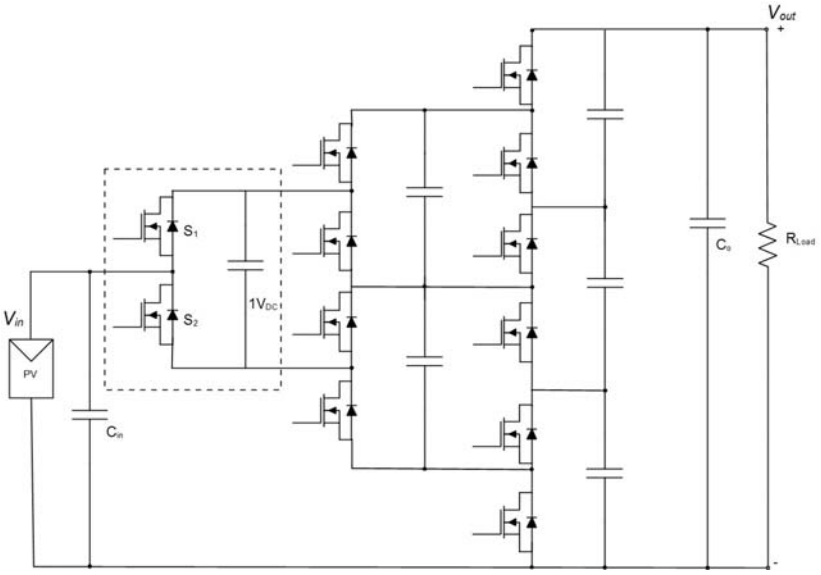

Fig. 3. 26. Electric structure of a high-step-power converter with multilevel cells.

Another technique to achieve high step-up converter is to use a transformer. Apart from adding galvanic isolation, a transformer allows to have big voltage conversion gain using the core-winding ratio. Nevertheless, the core loss adds an important and non-negligible amount of loss to the structure, and they are often not used for this reason in this kind of DC optimizers. When a galvanic isolation is needed, it is normally integrated in the inverter.

However, the transformer can be also integrated in the DC-DC converter as authors in [107] do. They present a new resonant DC-DC converter topology with galvanic isolation for DC module applications. (fig. 3. 25.). The structure consists in a half bridge LLC resonant converter. Its soft switching feature, for the MOSFET in primary side and for the diodes in the secondary side, characterizes this converter. Moreover, it can achieve a compact design with high efficiency. The authors have added an additional half-wave-rectifier (HWR) to conventional LLC resonant converter.

The HWR is formed by two diodes, a MOSFET and a capacitor and it is added in the secondary side of the transformer. A diode and the MOSFET form a unidirectional switch that disables the HWR. In normal condition, the HWR is disabled and the power conversion will be made though the LLC resonant converter. In the case of the photovoltaic power is smaller than the power rate and the photovoltaic voltage smaller than nominal voltage the HWR is enabled. In this case, the both output of HWR and converter are added and support together the 400V DC bus.

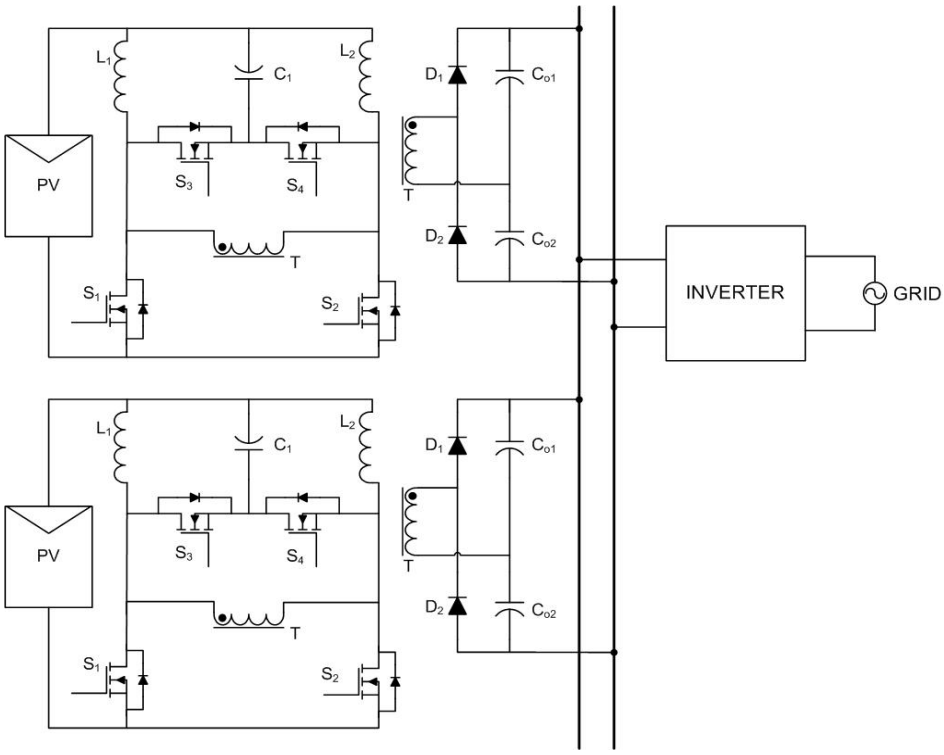

Fig. 3. 27. Electric structure of a resonant DC-DC converter with galvanic isolation for DC module applications

Many other researches are carried out in series output connexion of PV DC-DC converters. The series output connexion of converters allows higher voltage level in the V_{Bus}, without the need of high conversion ration converter. Nevertheless, these structures can be considered as inter-connections between converters, and therefore, they will be analyzed in the following section.

3.3.3 Synthesis

The literature presents many structures that try to achieve high voltage gains with high efficiency. Nevertheless, to reach both objectives is a complicated task. Indeed, most type of structure achieve either one or the other goal, but difficulty both of them. The table 3.5. summary the characteristics of the mentioned DC-DC converter structures.

Table 3.5. Review of presented DC-DC converter structures:

Structure	Number of component		Simplicity of the structure	Control complexity	Cost	Efficiency
	Active D-S	Passive C-L				
Boost converter (Fig. 3. 12.)	1-1	1-1	++++	-	+	++
Three level boost (Fig. 3. 21.)	2-2	2-1	+++	+	++	+
Cascaded boost (Fig. 3. 22.)	2-2	2-2	+++	+++	++	+
Quadratic boost (Fig. 3. 23.)	3-1	2-2	+++	+	++	+

Coupled Inductor DC-DC (Fig. 3. 24.)	4-3	3-3	++	+++	+++	-
N-stage high step-up converter (Fig. 3. 25.a.)	1-2/cell +2-2	1C/cell +1C	-	++++	++++	--
N-stage high step-up converter (Fig. 3. 25.b.)	2D/cell +2S	2C/cell +1C	-	++++	++++	--
Multilevel converter (Fig. 3. 26.)	2S/cell	1C/cell +2C	-	++++	++++	--
Resonant DC-DC converter (Fig. 3. 27.)	2-4	3-2 +transfor.	+	++++	+++	+

Most structures mentioned previously achieve high voltage gains, nevertheless, they presents important drawback in terms of complexity of cost. In effect, these structures are composed by numerous of components.

3.4 Association of power converters

The inter-connection between several power converters is a well-known used technique to design new and more advantageous power conversion structures. Interconnecting simple converter structures allows improving characteristics that with only one converter will not be possible. The connection of these converters can consist on cascaded converter design with the equivalent of internal electrical bus. It can also concern parallel and series inter-connections of Static Converters (SC). Fig. 3. 28. shows the schema block of cascaded, series and paralleled connected power transfer structures.

By interconnecting different structures, new tasks that only with one converter cannot be achieved are reached. For instance, the series and parallel connection of converter involve a major power transfer capability. The series connections increase the voltage. The parallel connections are used to increase the current. The cascade converters are used to assure several different functions in the structure. For instance, it allows increasing the degrees of control of the converter, making possible a voltage step-up function in addition to DC-AC transformation; or it increases the transformation ratio. Moreover, due to an intermediate bus, the addition of storage stages is possible.

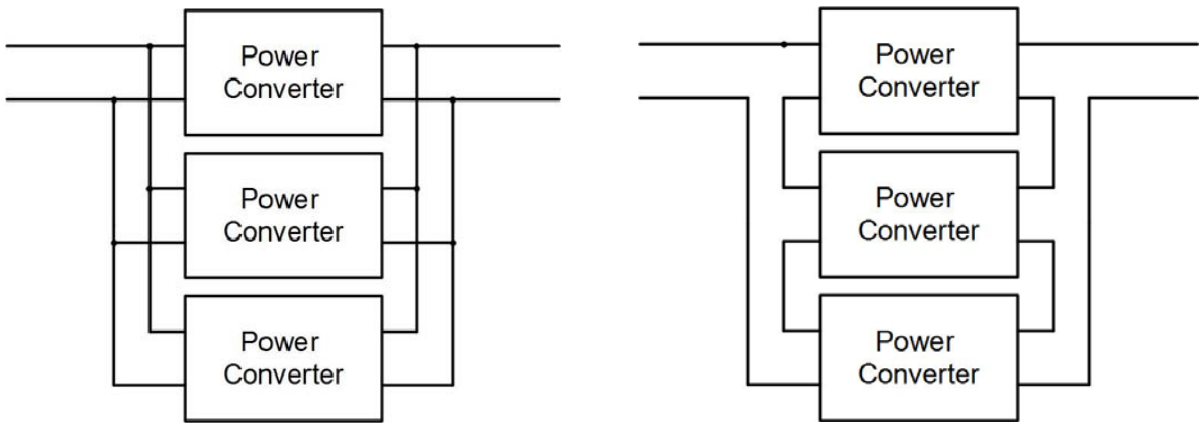

a) b)

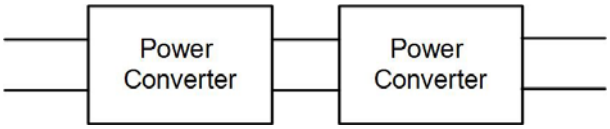

c)

Fig. 3. 28. Three type of power converter connections: a) Paralleled connection, b) Series connection, and c) Cascaded connection.

The three different associations of power converters are widely used techniques today in various applications. For instance, in embedded fields as computers and satellites, we can note complex distributed architectures with more than three stages in cascade and a lot of SC in parallel to achieve more robust architectures through the concept of redundancy. In railway systems, there are new series topologies linked to parallel ones which achieve high voltage levels and supplies locomotive motors. Today, interconnecting power converters allow resolving lot of electrical problems. New optimized structures with new or even improved characteristics can be achieved with new techniques of inter-connections. In latest studies to improve performances, the specific behaviours of sources and loads are taken into consideration to design new conversion stages, and not only the electrical characteristics that must support the structure to avoid failures. Many type of association can be envisaged, nevertheless, because in our work, we are focused only on PV applications, only the parallel, the series and cascaded association were analysed and their main principles will remember below.

3.4.1 Cascaded power converters

Two power converters can be cascaded when the output port of the first power converter is directly connected to the input of the second one, creating a new structure. The cascaded converters can be both of same characteristic and structure or totally different structures depending on applications.

In new photovoltaic systems, a typical structure of cascaded converters can be composed by a simple DC-DC structure with its MPPT control and another simple DC-AC structure which allow the grid connection, for instance, by cascading a boost, a buck or a buck-boost converter with an H-bridge inverter [111]. In this example, the structure can achieve the amplification or reduction of the PV voltage at first stage and an inversion of the voltage through the second one. Fig. 3. 29. shows an example of cascaded converters with a boost converter and H-bridge inverter.

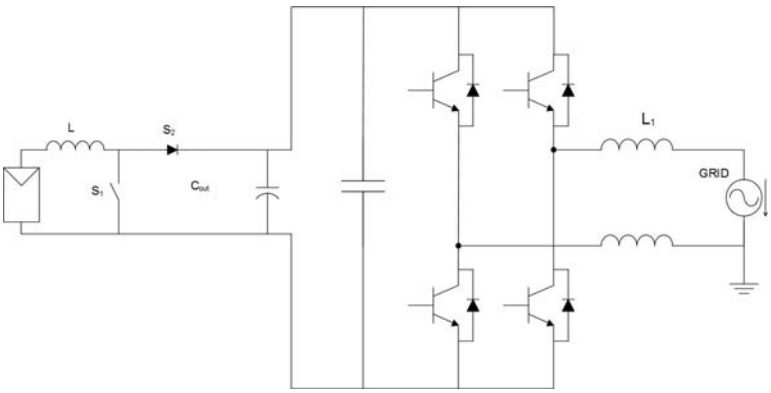

Fig. 3. 29. Example of cascaded converters with a boost converter and H-bridge inverter.

In photovoltaic systems, today, this is a widely used technique to improve the performances of classically used alone H-bridge inverters as shown in examples of the previous sections. In fact, due to highly variable characteristics of PVG, the input voltage level is not always guarantee in the input of the inverter, in particular with presence of shadows in irradiance and by-pass diodes to protect PVG from these phenomena. In grid-tied applications, the specifications in the output port are induced by the high constraints of the grid. Nevertheless, this kind of structure guaranties a perfect adapting of the voltage level to its inversion and thus, the output signal quality which is imposed for electrical grid connection permissions is assured.

Another problem that can be solved by cascaded converters is the high step-up voltage amplifications without transformers. The simplest step-up existing converter is the boost converter. In theory, as we said previously, the voltage gain of the boost converter can be infinite when the duty cycle is close to one. However, in real realization, this is not the case and the voltage gain is limited.

An example of commonly used cascaded boost converters has been presented as a power optimizer in section 3.3.2. as well as its simplified quadratic boost structures (fig. 3. 22. and fig. 3. 23). In fact, the association of same characteristics DC-DC converters is used to achieve higher voltage ratio characteristic and by connecting two boost converters in cascade a double voltage conversion gain can be achieved as have been explained in the previous section. Moreover, apart from extend the voltage ratio, the current ripple can be further reduced with this kind of structure. Nevertheless, the need of two sets of power devices, magnetic cores and control circuits become these structures in an expensive and complex circuit.

3.4.2 Series connection

Many researches are carried out in series output connexion of PV DC-DC converters (fig. 3. 30.). The main goal of this kind of connection is to avoid the problem of high-step-up voltage transformation as the cases exposed in the previous part. In series connected ports, the voltages are added. Thus, higher voltage can be achieved in the output port, and therefore, this output port can be directly connected to a grid-tied inverter, assuring an adequate voltage level for its inversion and grid connection. Nevertheless, as all the output must have the same current level, the system often presents a big instability and its control a high complexity to resolve it, representing the biggest drawback of this kind of connection.

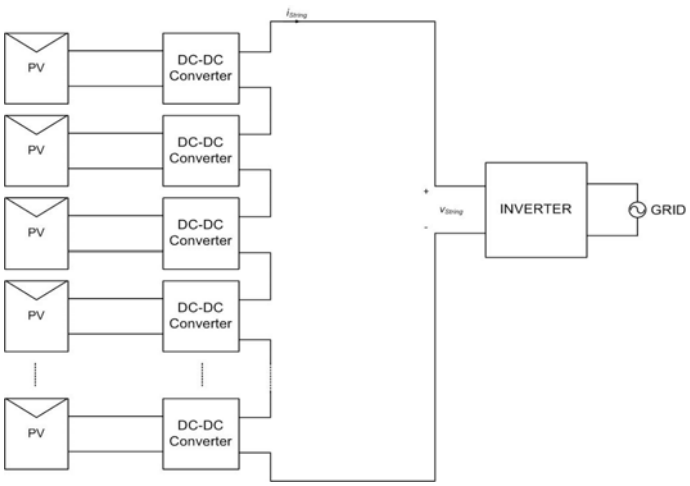

Fig. 3. 30. The schema block of DC-DC series connected converters for PV application

In order to adapt the output voltage according to working condition (shadowing, mismatching...) of each PV generator, this kind of structures normally use converters that can operate in step-up and step-down mode. The Buck-Boost, the FSBB and the CÚK are some of the used structures.

Authors in [108] present a module integrated converter for series connected photovoltaic application using a Four-Switch Buck-Boost (FSBB) converter (fig. 3. 31.). The power structure decouples each solar panel form the rest of the string, making the module insensitive to changes in the string and allowing it to operate at the optimum PV power. A high efficiency conversion is achieved by the minimisation of indirect power at the nominal operating point, which is achieved by the use of a converter having a buck-boost characteristic, designed to have a voltage conversion ratio of unity at the nominal operating point. With a multi-switch realization, this converter has three possible operation modes: buck, boost and pass-through. Working in one of this operating modes will depends in the global I_{string} and the maximum power point of each PV module of the moment. A MPPT control will guarantee that the solar panel work in the MPP. An additional control will switch the operating mode to buck, boost or through-pass mode.

Buck operation is realized when $I_{PV}<I_{string}$, since others modules operates in higher power due to mismatching conditions or shadowing effects. In this case, the switch N_4 is permanently on, while N_2 is permanently off. Devices N_1 and N_3 will allow to the converter to work in buck mode.

The converter enters in boost mode when $I_{PV}<I_{string}$ due to other modules in the string operating at a lower power. In this operation mode, N_2 is always turned-on and N_4 turned-off. Switches N_2 and N_4 operate with duty cycles D and $1-D$ respectively and allow the boost operation mode.

Finally, the structure works in through-pass mode when operating conditions of the string are nominal and balanced, and therefore, $I_{PV}\approx I_{string}$. During this mode, the PV panel is operating at its MPP and no additional control is needed. In this case, the input is directly connected to the output via the switch device N_3 and N_4. In this way, the effect does not affect to other systems parts. The structures as well to increase as decrease the voltage level. In this way, the output current can be also been controlled in the way to be the same

for all the series connected power conversion structures. Nevertheless, the disadvantage of this structure is evident in its low instability and in its complex control.

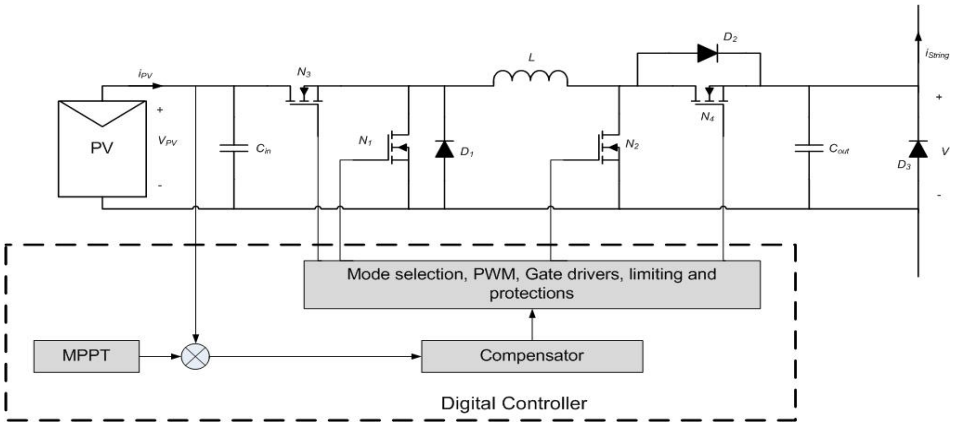

Fig. 3. 31. Electric structure of the FSBB with its associated control

Although the study of series connected PV converters is increasing, the parallel connexion is still used today and many authors present innovative advances to find the best structure to this kind of structures. The main characteristics of these structures must be the high step-up keeping high conversion efficiency and low price.

3.4.3 Parallel connection

The parallelization of power converters is one of the simplest forms of connecting power structures. For this reason, it is a one of the most used interconnection techniques. Apart from the simplicity of control, the parallel connected power converters add robustness, redundancy and power capability of the systems. Moreover, it can add availability from fault tolerant with N+1 modules and ease of maintainability with redundancy implementation. [112]

Because the input and output ports of the converters are connected in parallel, it is also called PIPO connection (Parallel input-Parallel output). Fig. 3. 32. represents the schema block of this type of connection.

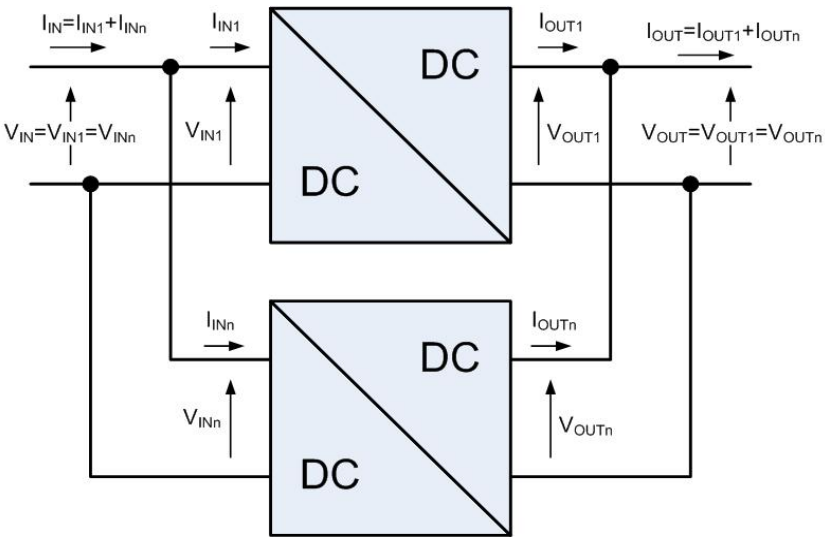

Fig. 3. 32. Schema block of the PIPO structure

The main characteristic of this kind of structures is the distribution of current among the converters or phases. The input and output voltage of all the phases is the same as they are connected in parallel, in contrary, the current is divided between the phases. This division can be identical or not and it will depend on the current control strategy that is used as well as in the little mismatches that exist between different phases [113]-[114].

The major advantage of these structures is the reduction of the thermal and electric stress in the components. As the charge is divided, a bigger power charge can be transferred without an increase in the power component stress. In this way, the system gains in robustness and in reliability.

This kind of configuration is mostly used in high current and low voltage applications, for example in microprocessor alimentation. However, it can be also used in high power applications (high voltage and high current), as it is used in electric motor alimentation present in high speed trains.

It is also used in the system of low voltage levels but high current levels. The power supplier for microprocessors is an example of the use of the parallelisation of power converters, as it is the case of Point of Load (POL) or Voltage Regulator Modules (VRM) [115][117]. Uninterruptable power supplies (UPS) use also often this kind of structures. [118]-[119]

The parallel connection of converters allows the connection of almost all the converters structures. Either DC-DC converters or inverters can be connected in parallel. Nevertheless, a successful selection of the paralleling scheme requires a firm understanding of merits and limitations of different paralleling schemes. The paralleling scheme must be selected by taking the complexity, cost, modularity, and reliability into consideration. Various interactions among converters modules must be incorporated into the control design and system integration to ensure stability, reliability and good dynamic performance.

The parallel operation of power converters was first introduced in the inverter uninterruptible power systems (UPS) [119] for purpose of increasing output power capacity and system reliability. Various system topologies and their associated control schemes have been reported. Assuming that all inverter modules are identical, it was shown that simplicity in the system control, system protection and maintainability depend greatly on the system configuration [120]-[121].

Recently, there has been an increasing interest in the paralleled DC-DC converters modules, for reasons of increasing system reliability, facilitating system maintenance, allowing for future expansion and reducing system design cost [122]-[126]. Indeed, paralleling mode increases the power processing capability and improves the reliability because stresses are better distributed and fault tolerance is guaranteed. A uniform stresses is achieved when the input current is shared appropriately among the converters. Moreover, the paralleled converters have been utilized for energy efficiency improvement. In the photovoltaic field, the efficiency improvement is also carried out by paralleled converters. However, many advantages in paralleling converters are linked to its control systems.

In PV field, many industrial PV inverters include a master-slave concept for connecting 3, 4 or more inverters [127]. Solarmax manufacturer used this structure in some of its industrial inverters (Fig. 3. 33.). With the master-slave concept both master and slave

devices are connected in parallel on the DC side with the master controlling how many slaves are operating depending on the amount of solar energy available. At low radiation levels, this enables higher system efficiencies compared to the case where all inverter are permanently operating [128]

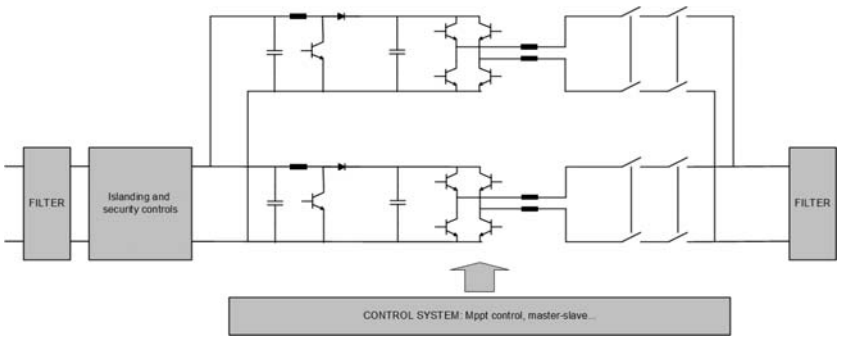

Fig. 3. 33. The structure of SolarMax 4200C and 6000C inverters using Master-Slave control.

The IG plus PV inverters of Fronius manufacturer use this kind of control by means of the MIX (Master Inverter eXchange) system concept [129]-[130]. The MIX architecture includes *m* parallel-connected inverters. The power conversion system is connected to a single PV generator with a fixed nominal power formed by all the available PV modules. The system is commercialized for PV power productions levels from 3.5kW to 12kW and it normally uses three paralleled inverter configurations.

One of the inverters assumes the role of the master and the other ones are the slaves. The system is reconfigured depending on the DC power value present at the PV generator output, modifying the number of active inverters connected to the PVG at any time. The fig. 3. 34. shows the three possible configurations available in such system. In this way, the inverter achieves three equal efficiency peaks, which enables a more constant efficiency over a wider input voltage range (fig. 3. 35.).

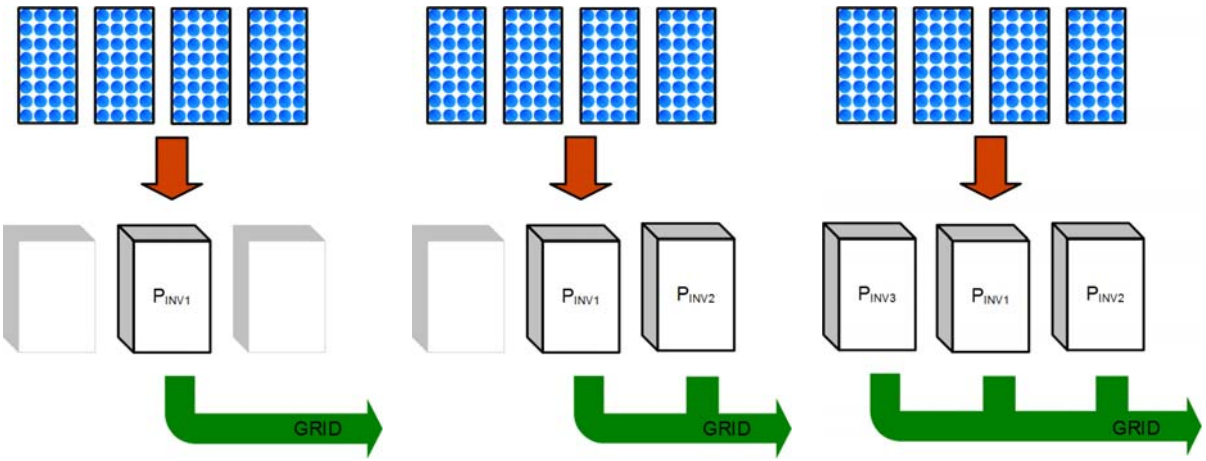

a)*n=1* b)*n=2* c)*n=3*

Fig. 3. 34. The three possible configuration of MIX system for three paralleled inverters PV system.

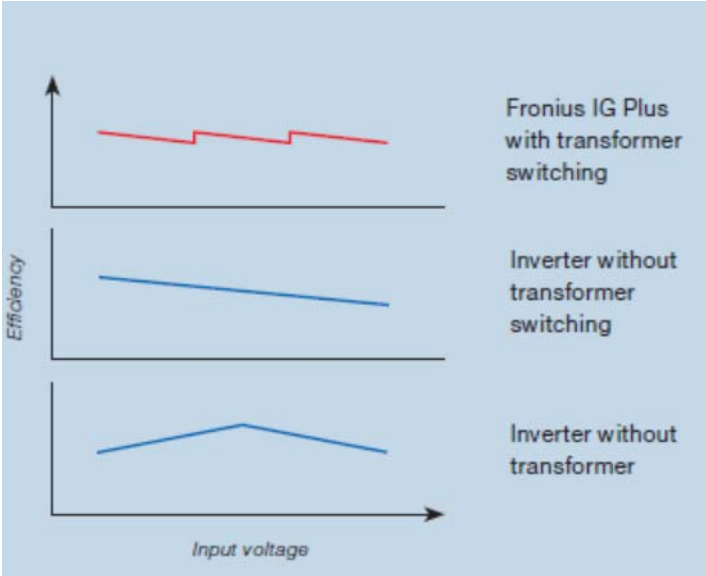

Fig. 3. 35. Comparison of conversion efficiency depending on voltage input voltage between traditional systems and Fronius IG Plus inverter with MIX system [130]

From the MIX system, authors in [129] presents a new reconfiguration that uses the MIX system, but with two inverters of different sizes connected in parallel and removing the master-slave concept.

A lot of others innovative structures exist and each day, new one is created showing the dynamic of this scientific field and the challenge to improve globally performances.

3.5 Conclusion

In this chapter, the photovoltaic conversion chain structures have been introduced. Beginning from the different topologies using in PV installation, we have finished by introducing the distributed DC-DC conversion structures.

During the history of PV installation, many topologies have been used. Nevertheless, last structures tend to distributed PV exploitation systems. It is the case of AC modules, and DC optimizers. We has focused the analysis in DC optimizers, DC-DC power converters that maximize the PV energy extraction and are connected to an DC-AC inverter in its output port to grid-tied applications.

The most of analyzed structures show a big voltage gain. Nevertheless, they are deficient in terms of efficiency and cost. Indeed, they are complex structures with big amount of components, that require complex control systems and have high cost. Moreover, the high quantity of components involves also losses in each of them, which decrease considerably the efficiency.

The boost converter still remain a good structure for PV applications as it present low complexity either in structure or control, low cost and high efficiency. It has a voltage-step up characteristics, needed for a correct match with inverters inputs ports. Moreover, it is a simple and stable structure, and in the laboratory, there is an acquired knowledge in this subject, due to previous works [109]-[110].

However, it still presents drawback. For this reason, it is important to evolve the structure to more efficient systems. The inter-connection of conversion structures allow to reach power converter with improved and even new characteristics. The three main connections are the cascaded, series and parallel structure. The cascaded converters are mainly used to increase the degree of liberty or the power transfer capability. The series connections are used to increase the voltage. They allow achieving big transformation ratio by means of output series connection. However, these structures are instable and request for complex control system. Finally, the parallel connected are the more popular and used structures. Indeed, these structures allow the improvement of efficiency and are normally. In addition, they can be used to lifetime improvement since they can easily become in redundant systems.

The following chapter 4 is dedicated to a presentation of a new structure based in boost converters, but that improves power converters increasing the efficiency and lifetime prediction by the parallel interconnection of converters.

CHAPTER 4

4 MULTI-PHASE ADAPTIVE CONVERTER

4.1 Introduction

As shown in previous chapters, photovoltaic systems are exposed to very changeable weather working conditions. The temperature and irradiance are not controllable variables, and they induce high changes in PV energy production which cannot be easily and exactly predicted. In the other hand, at each moment, the PVG productions affect the PV power converter structure with high variations of the operating point. Thus, a simple cloud can involve the passage from a maximum power production to a minimal power production.

The design of a power conversion structure dedicated to a PV source which guarantees high conversion efficiency for all of operating points became difficult. The efficiency of a classical power converter presents a maximum value (η_{MAX}) to a given input power (nominal power, P_{nom}). The converter efficiency decreases when the input power is lower or higher than this nominal power value. In many power management applications, the design of the converter is made by referring to a fixed operating point (nominal power), set with the maximum efficiency.

High efficiency systems in several applications are designed to match their nominal operating point with η_{MAX}. In the case of PV systems, the working points can vary in a large range of power values from zero to P_{MAX}. Thus, this type of design is not possible for PV systems, as the power production changes constantly and it is impossible to fix an operating point.

Moreover, a simple power conversion structure cannot assure a high efficiency for all the operating point of a photovoltaic system. More sophisticate ones must be designed in the goal to guarantee high conversion efficiency for long power ranges. The field of these new researches is named “flat efficiency” ones.

Nevertheless, complexity in power structures, if they are not designed with a lot of optimisation can involve more costs, losses, lack of robustness and reliability, instabilities and even not efficient complex controls.

As the photovoltaic systems are still expensive, the goal to improve performances of power productions must be coupled with a constant research to reduce costs. To increase globally the use of PV sources around the world, it is important for the photovoltaic global installation to be efficient, robust and long-lifetime system.

In this chapter, we present the main results we have obtained in this field, and in particular, a new multi-phase converter with an instantaneous adaptive number of phases named MPAC. It was designed to achieve flat efficiencies. Main simulation and experimental results are presented in this chapter. This type of multi-phase presents high conversion efficiency for a large power range and as the thermal constraints are reduced, a higher life-time can be achieved.

The MPAC is composed by a minimum of two similar structure converters connected in parallel. Each phase can be considered as an independent SC. Many structures can be used depending on applications. Advanced control laws specific of PV arrays allow an optimal working mode of the system in terms of efficiency and life time, adapting the number of phases connected to the PVG at each moment, depending principally on the instantaneous power level of the PV generator, but also on other many criteria as we shown in this chapter.

In this way, the number of working phases at each moment corresponds to the optimal configuration to achieve the instantaneous maximum conversion efficiency.

The problem of low electronic life-time in photovoltaic system could be partially resolved with a MPAC associated to advanced control laws. In this way, the algorithm of the MPAC, in addition to adapt number of phases at each time to maximize power production, manage the working time of each phase with a special sequence (specific timing rotation) to reach equal stress and aging of all the phases.

Thermal and electric stresses have been reduced into the power components with a MPAC. The average temperature of the SC can be maintained homogeneous, moreover the maximum temperatures of components can be controlled to be lower compared to ones working in same conditions but belong to a single converter. First results obtained in the laboratory and confirmed by experimental tests based in component temperature studies show a better global aging of each component. Then, a longer life-time reliability rates can be obtained, reducing indirectly global cost of this type of structure.

4.2 Study of Different control strategies

In the precedent chapter, the interconnections of power converters have been explored to show their potential performances through several examples. Indeed, the interconnected converters present new interesting characteristics that simple converters do not have. This way, beginning from simple and robust converters, more advantageous ones can be achieved by interconnecting them.

Parallel connection of converters offers the possibility to integrate different control strategies in order to improve the power transfer efficiency or increase the life-time of the system. Most of these techniques consist on the current distribution strategies. In fact, many works of research have been carried out in this field and there are many current control strategies, each one with its advantages and its drawbacks [113]-[114]. We studied two strategies based in paralleled converters to improve the efficiency of a power conversion structure. The first one is based in interleaving control methods. The second one consists on a multi-phase adaptive converter (MPAC), which adapts the number working phase to optimize the exploitation of the power converter.

4.2.1 Efficiency improvement by Interleaving control mode

Our main goal is to use interleaving control on paralleled converter structures and to study how we can increase the European efficiency, the reference used to compare performances of PV converters and MPPT control laws. We focused our effort in improving the efficiency in the range of power where statistically the system works most of the time. It corresponds to the power between 30% and 100% of its nominal or maximal power.

From the losses analysis carried in the chapter 3, the switching components are considered to involve their most important losses. These losses are dependent on the current, voltage and internal characteristics like temperature, but also on the switching frequency. Control techniques can be used to improve the energy transfer by taking advantages of this effect.

MOSFET losses have been defined as the sum of switching and conduction losses as illustrated in the fig. 4. 1. [131]. The conduction losses are dependent on component crossing current, the duty cycle and the resistor at on-state of the MOSFET, called $R_{DS(on)}$:

$$P_{MosFet_{conduction}} = D.R_{ds(on)}.I_g^{\,2} \tag{4.1}$$

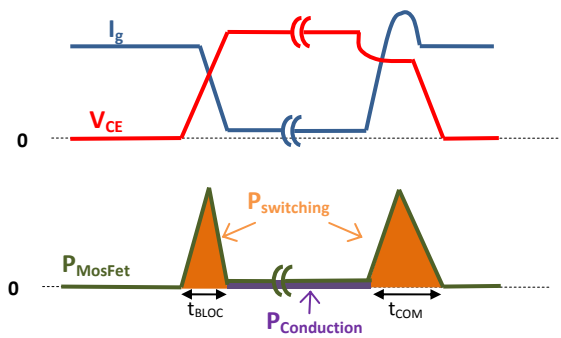

Fig. 4. 1. Simplest evalutaion of losses in a MOSFET

Switching losses are dependent on voltage, frequency, crossing current and switching time:

$$P_{MosFet_{switching}} = \frac{1}{2}U_{DC}.(I_g + I_{RM}).t_{COM}.f + \frac{1}{2}U_{DC}.I_g.t_{BLOC}.f \tag{4.2}$$

When 3 boosts are working in parallel (three phases converter), the components number and its associated losses become more important (*3) compared to a classical structure, however the current going through each commutation cell is divided by 3.

Generally, the MOSFET resistor value depends especially on the silicon area and it is inversely proportional to current though the component. The MOSFET used in the three phase converter has been dimensioned to support a third part of current of the simple converter; in consequence its resistor will be approximately three times higher. The evaluation of MOSFET conduction losses of the proposed structure shows that any conduction losses are added by parallel connection, as the equation (4.3) demonstrates:

$$P_{MosFet_{conduction}} = 3 \cdot D \cdot (3 \cdot R_{ds(on)}).\frac{I_g^{\,2}}{3^2} = D.R_{ds(on)}.I_g^{\,2} \tag{4.3}$$

A similar analysis shows that the MOSFET switching losses of the parallel converters are identical to the classical structure (equations (4.4) and (4.5)):

$$P_{MosFet_{swithcing}} = 3 \cdot \left(\frac{1}{2}U_{DC}.(\frac{I_g + I_{RM}}{3}).t_{COM}.f + \frac{1}{2}U_{DC}.\frac{I_g}{3}.t_{BLOC}.f \right) \tag{4.4}$$

$$P_{MosFet_{swithcing}} = \frac{1}{2}U_{DC}.(I_g + I_{RM}).t_{COM}.f + \frac{1}{2}U_{DC}.I_g.t_{BLOC}.f \tag{4.5}$$

In final, we have demonstrated in a first approach that the parallel solution doesn't amplify the MOSFET losses, despite the increase of commutation cells.

The other switching element is the diode. Conduction losses in a diode can be evaluated with the following equation:

$$P_F = (1-D).V_{COND}.I_g \tag{4.6}$$

Where,

$$V_{COND} = R_{COND}.I_g + V_F \tag{4.7}$$

If we consider that R_{COND} is very small, the losses caused by it can be considered negligible and we only considered the voltage drop in conduction state.

As switching losses of diode are included in the evaluation of switching losses of the MOSFET, it is not needed to evaluate this part.

In our system, the diode number and the current crossing them are respectively multiplied and divided by three. In consequence, the diode losses of the parallel connection are identical to the classical structure, as it is demonstrated by the following equations:

$$P_F = 3 \cdot (1-D).V_F.\frac{I_g}{3} \tag{4.8}$$

$$P_F = (1-D).V_F.I_g \tag{4.9}$$

This simple analysis, ignoring the evolution of the value of the MOSFET resistor according to the temperature and the commutation time variations, shows that the classical and the proposed structure which operates with the same switching frequency have approximately the same commutation cell losses. These losses can be improved by means of the interleaved mode.

4.2.1.1 Interleaved mode

One of the techniques for current distribution in paralleled power converters is the interleaved mode. Interleaved mode requires that the *n* parallel connected converters operate at constant switching frequency, but each phase must be shifted with respect to one another by *2π/n* radians.

Interleaved mode allows multiplying by *n* the switching frequency. This mode gives two alternatives: First, filters dimension can be reduced; and second, we can achieve better energy transfer by means of switching losses attenuation. This last solution consists in the switching frequency reduction by *n* in each cell, preserving initial filters.

Fig. 4. 2. illustrates the waveforms of the current and the voltage in both a classical Boost and a three phase Boost. Switching frequency being the same in two systems, we realize that switching frequency of both input current and input voltage ripple have multiplied by three. In consequence, the ripple amplitudes have also decreased.

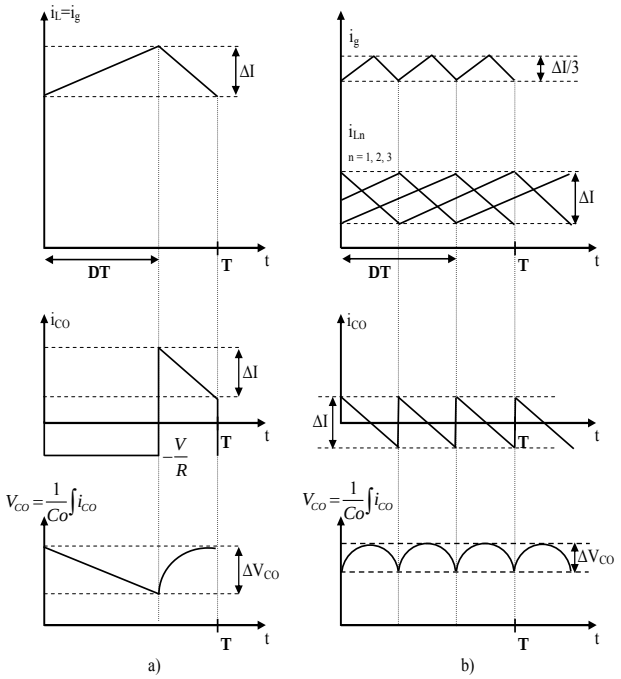

Fig. 4. 2. Waveforms of the output capacity tension and the inductor current for a classical Boost (a) and three Boost operating in interleaving mode.

In the aim of reducing switching losses, one solution consists of divide the switching frequency since these losses are dependent of the frequency. In our system of three boosts in parallel working in interleaving mode, the frequency can be divided by three. By the input and output point of view, the switching frequency will not be changed because of interleaving working mode, but in contrary, switching components will support lower frequencies. The switching losses equation (4.2) can be rewritten as:

$$P_{MosFet_{switching}} = \frac{1}{2}U_{DC} \cdot (I_g + I_{RM}) \cdot t_{COM} \cdot \frac{f}{3} + \frac{1}{2}U_{DC} \cdot I_g \cdot t_{BLOC} \cdot \frac{f}{3} \tag{4.10}$$

To sum up, the MOSFET switching losses can be reduced and converter efficiency improved by the use of three parallel connected boost and operating in interleaving mode. This result is guaranteed only if the power is correctly shared between each converter. In this case, a current distribution control must be inserted in the system. We describe in the next part an example of currant sharing method.

4.2.1.2 Current distribution control

In the case of association of several cells in parallel, a correct current distribution between cell is needed to ensure an optimum conversion yield, as well as to avoid reliability and ageing problems [113]-[114],[132]-[133].

The reference current I_{ref} which represents the global current of the parallel structure is done by:

$$I_{ref} = K(I_{L1} + I_{L2} + I_{Ln}) = \mu_1 I_{L1} + \mu_2 I_{L2} + \mu_n I_{Ln} \tag{4.11}$$

Where I_{Li} corresponds to the currents though each phase, K the function which calculate the I_{ref} value and μ_i represents the percentage of each current that is taken into account to define the reference current.

One type of regulation in which the variable μ_1 takes the value of 1 and the other variables (μ_2, μ_n, …) are affected by 0, is called "master-slave". In this regulation mode, the output current of a conversion cell which is identified as the master, is the reference for others, which are called slaves. The master is the cell that owns the highest current. When the variables μ_1,… μ_n are affected by the value of 1/n, democratic current sharing strategy is used. In this case, I_{ref} is calculated by mean of the sum of all currents [113]-[114].

This last solution has been kept for our system, ensuring the same charge in each the power cell.

4.2.1.3 Experimental prototype and control laws

A 100 W experimental prototype with parallel connection of three cells interleaved Boost converter was developed to validate the losses analysis. Each phase has been made to support a third of total power, which is 33W. For the one phase classical boost, reference of the diode is MBRD640CTT4G and for the MOSFET, we have used the reference IRFR024N. The diode and the MosFet used for the new structure of three phases in parallel are respectively the reference 50WQ04FN and the reference NTD3055-094.

As our system being composed by three boosts in parallel, and we use a democratic current sharing control, each phase is affected by *1/3* of the total current and so, the reference current I_{ref} is generated by the following equation:

$$I_{ref} = \frac{1}{3}(I_{L1} + I_{L2} + I_{Ln}) \tag{4.12}$$

For photovoltaic applications, this current regulation must be imperatively compatible with the used MPPT control to ensure the working in the maximal power point. The MPPT control is used is an extremum seeking based MPPT control that has been previously developed in the laboratory [134].

In the fig. 4. 3., the schema of the system of three paralleled boost converters with interleaved current control for PV applications is showed. The system is supplied by current control in the output of the PVG and in the input of each boost converter. PV voltage generation is also measured. PV current and voltage are used to determine the PV power generation. Using these two data, the MPPT control determines the voltage reference.

For the democratic current distribution, the current of the three phases is added, and divided by three and in this way, the current reference is obtained. The difference between the current of each phases and the current reference determines the error. From the voltage reference, the last reference is obtained by adding the error to the voltage reference. The control signal for the switching devices or the duty cycle is lastly got by PWM method. That is, comparing the last reference with triangular signal. In this case, the three triangular signals have the same frequency of 180 kHz. However, they are phased in 0°, 120° and 240° to achieve the interleaving effect.

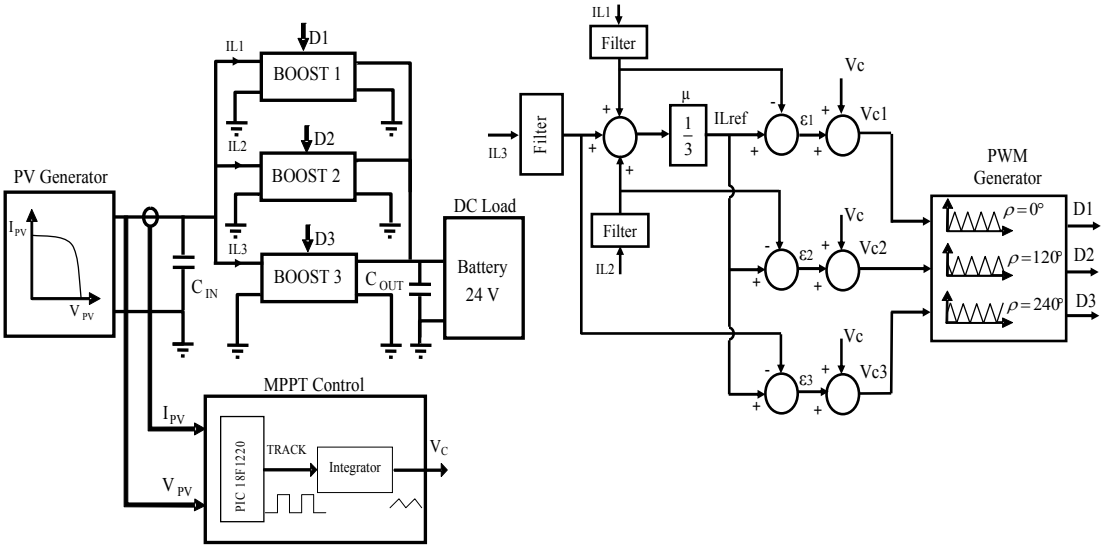

Fig. 4. 3. Schema of the three paralleled Boost system with interleaved current control for PV application

4.2.1.4 Validation of the experimental prototype

A set of real measurements has been made in order to investigate the performances of the proposed structure. The electrical features of the PV array are reported in the table 4.1., and a lead storage battery with a nominal voltage of 24V is used as a DC load. Steady state waveforms of the photovoltaic conversion chain for a constant radiation level are illustrated in fig. 4. 4.a. These waveforms show the achievement of the MPP, characterised by the oscillations around the PV maximal power point and the uniformly photovoltaic current distribution among the different converters. It is shown in this figure the compatibility between the MPPT control and current-sharing control. The current control guarantees 1/3 of PV current for each cell. The phase difference inserted by the interleaved mode is observable on the fig. 4. 4.b.

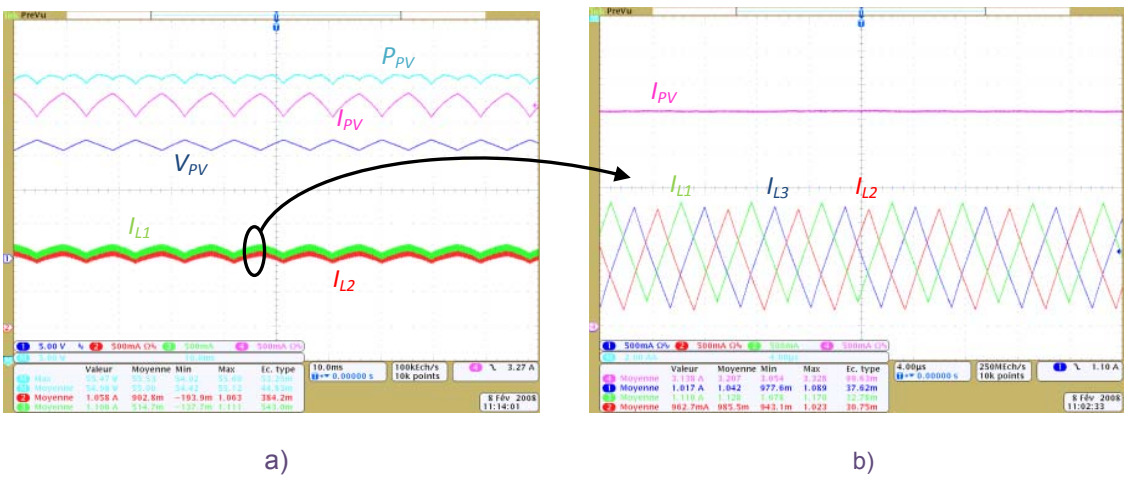

Fig. 4. 4. Steady state behaviour of photovoltaic conversion chain (a), zoom on inductor currents (IL1, IL2 and IL3) and photovoltaic current (IPV).

Table 4.1. Electrical features of the photovoltaic array:

Maximum power (Pmax)	85 W
Voltage at Pmax (Vmp)	18 V
Current at Pmax (Imp)	4.72 A
Short Circuit current (Isc)	5.0 A
Open circuit Voltage (Voc)	22.1 V

The fig. 4. 5. shows the dynamic response of the system to sudden PV power generations steps. In the first figure, the system is affected by an increasing power step. In the second one, a sudden power diminution is tested. The changes in power are simulated by increasing and decreasing current steps. The power changes do not disturb the stability of the system. The democratic current-sharing is able to maintain equally the distribution of current. Moreover, the MPP tracking is not perturbed when the system is submitted to this abrupt variation.

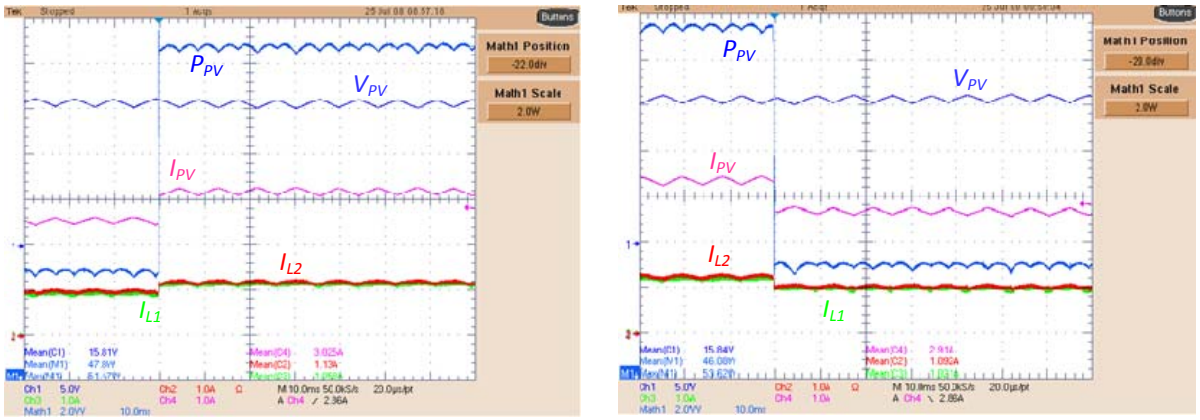

a) b)

Fig. 4. 5. Dynamic response during a solar radiation increase (a), and decrease (b).

4.2.1.5 Comparatives experimental results

New structure has been compared to a classical solar Boost converter. This classical solar converter has been designed to support the same power of the new structure and it has been provided with the same filtering elements.

The energy performances of both structures have been compared during a day. The test conditions scheme is exposed on the fig. 4. 6. Classical Boost has worked in the switching frequency of 540 kHz, while the new structure has worked three times slower, in a frequency of 180 kHz due to interleaving mode. The different electrical variables have been measured by means of the automatic measurement system developed in our laboratory [135].

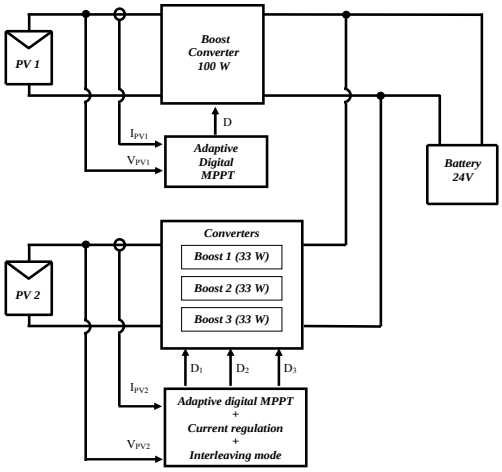

Fig. 4. 6. Scheme of paralleling 3 Boost converter and a classical Boost converter for the realisation of the tests

The results of this test are represented on the fig. 4. 7. The PV power and the Battery power represent respectively the day round evolution of the delivered power by the PV panel and the transferred power to the load. This information is essential to obtain the converter efficiencies evolution of each structure. This one decreases when the PV power increases. In contrary, the parallel structure maintains a high efficiency when the PV power is superior to 30% of its power range. In low power, the efficiency of three phase converter is poor. This phenomenon is principally induced by the operating in discontinuous mode of the proposed structure. This operating mode is directly dependent on switching frequency and the supplied PV current. Thus losses increase and the efficiency decreases. However, the power converter efficiency of the proposed structure is about 92% between 30 and 100% of rated power. Because of the effect of this long range of high efficiency, the global result implies an energy transfer gain compared only to a classical Boost converter. The principal results of this test are reported in the table 4.2.

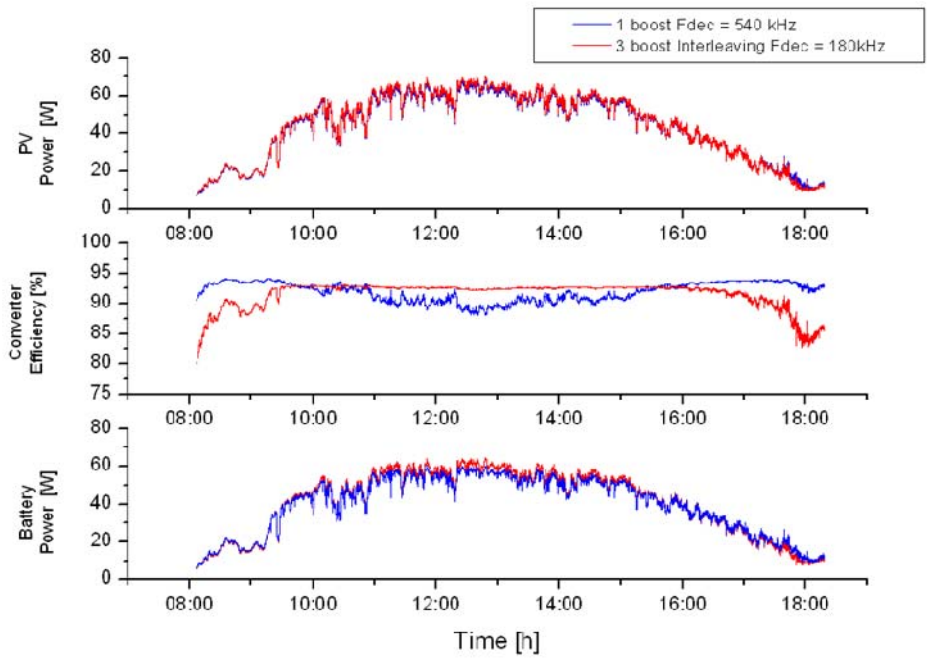

Fig. 4. 7. Daily comparison of power an efficiency between three cells interleaved Boosts converter and a classical Boost converter

Table 4.2. Synthesis of one day of measures:

		Produced energy (Wh)	Transferred energy (Wh)	$\overline{\eta}_{CONV}$(%)
Measures of 03 may 2009	Classical structure (V_{BAT} =24 V)	428	387,9	90.6
	Proposed structure (V_{BAT} =24 V)	430,9	397,1	92.1

4.2.2 Multi-Phase Adaptive Converter

Using paralleled interleaved converter has been achieved a better European efficiency. Nevertheless, this system presents a major drawback: a lower efficiency in low power ranges than a classical simple structure. For this reason, other methods must be envisaged to obtain better energy transfer efficiency in all the power range. We have designed during our PhD a new type of parallel structure named Multi-Phase Adaptive Converter (MPAC) which is presented in this part. The MPAC integrates an advanced control law which adapts the number of working phases of the converter depending on the PV power generation of each moment. This way, the efficiency of the power converter is more optimal for every power production. But the phase adaptation is not the only function that integrates the MPAC. Besides, other functionalities as phase rotation or security functions are also integrated in order to improve aging and increase life-time.

4.2.2.1 Efficiency improvement by Phase adaptation

As the parallel connection of power converter is a good option to improve power transfer efficiency in PV applications as shown by [122] and by taking into account the advantages of the parallelisation of power converters, the Multi-Phase Adaptive (MPAC) solution was designed in the context of this PhD. The principle of this structure is presented in fig. 4. 8. The MPAC is constituted by *n* converters in parallel. Using advanced Control laws to activate and deactivate the converters phases, this structure is adapted to the source characteristics as the PVG which present changeable input power conditions. Our goal with this type of structure is to achieve not only a higher efficiency for a larger input power range, nearer to the ideal efficiency, but also manage the electric and thermal stress of components which could be traduced as a larger life-time, a high reliability and, in its global life-cycle duration, a relative reduction cost.

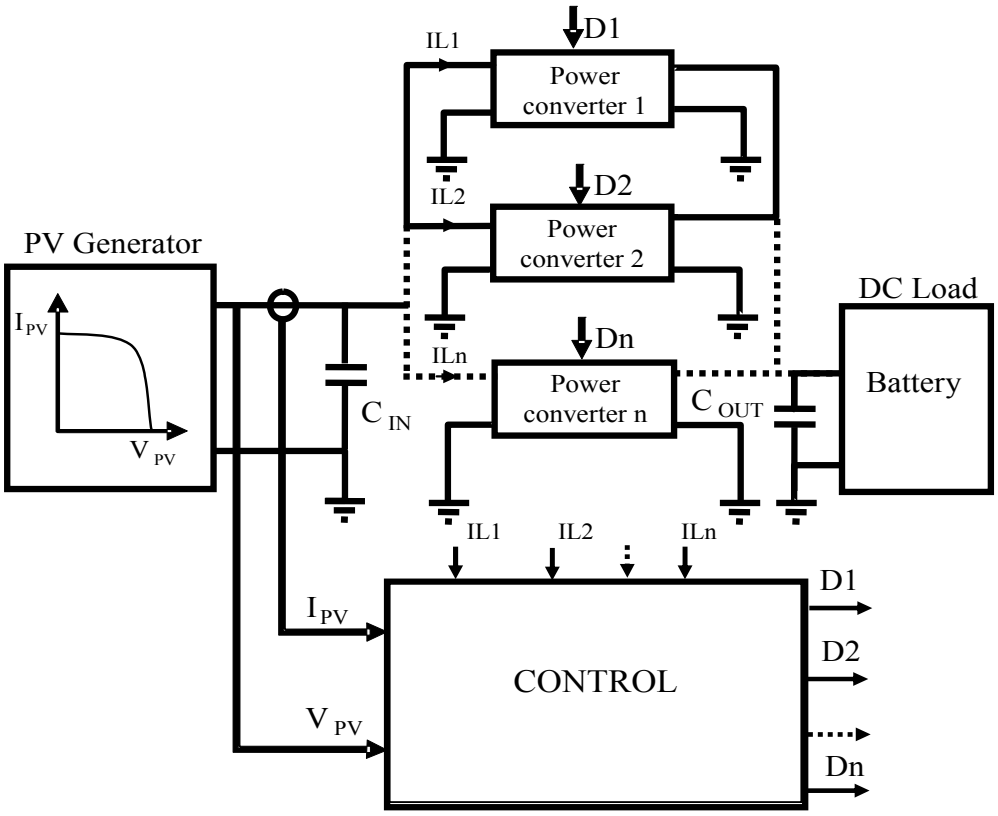

Fig. 4. 8. Schema block of the n parallelized converters

With the aim to adapt the number of phases in order to achieve the best efficiency possible, the criteria of optimal power values for each adaptation moment have to be chosen precisely.

As *n* converters are connected in parallel, this could bring to think that the turn on and turn off of the phase must be done by keeping power proportionality with the nominal power of individual converters, that is, in the power corresponding to *1/n*, *2/n*, *3/n*,…values. Nevertheless, in this way, there is not possible to take advantage of all the conversion efficiency of the power converter because the behaviour of efficiency is not proportional with the power crossing converters.

In the cases of paralleling connection of power converters with adaptation systems, this adaptation of phase is carried out by establishing adaptation points proportional to nominal power of the individual converters.

In order to illustrate this effect, the efficiency curves for the efficiency test of 3 phase power converter will be analysed. In fig. 4. 9., the efficiency curves for 1,2 and 3 phases mode of functioning for a 100W_P prototype are shown for typical conditions of functioning (V_{in}=15V and V_{out}=24V). $P_{1/3}$ and $P_{2/3}$ represent respectively the power level where the phase number must be changed. We name this type of control: a linear phase adaptation. The theoretical efficiency of the power converter in this case of adaptation is also shown by a red line. In this curve, we can see drastic drops in the efficiency at each modification, and thus the conversion efficiency is not really improved by using this adaptation method.

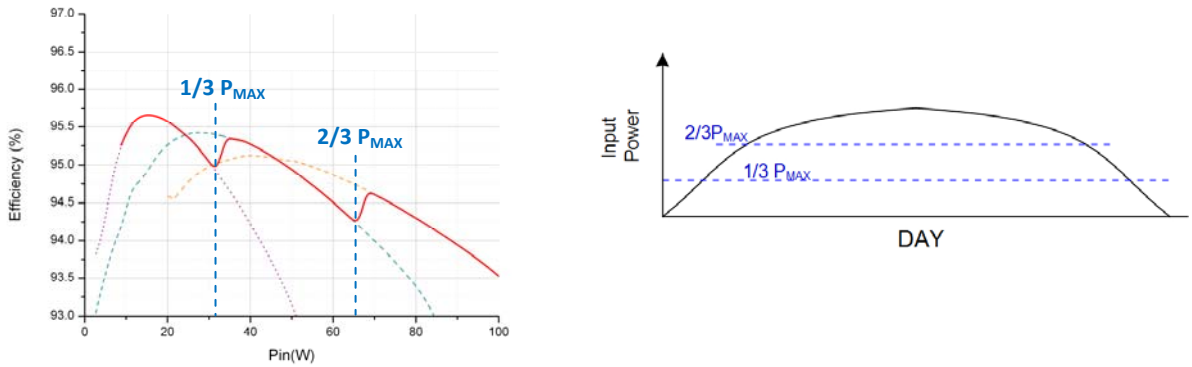

a) b)

Fig. 4. 9. Efficiency curves for 1,2 and 3 phases operating mode and for an algorithm based on the adaptation done for 1/3 and 2/3 of nominal power.

Thus, if we examine precisely behaviours of 1, 2 and 3 phases, it can be shown that to achieve better efficiency, the adaptation of the phase must be made in precise intersection points of the efficiency curves. These points are defined as P_n. They correspond to power levels where the change of number of phases is made optimally. The first intersection point is called P_1, the second, P_2, and successively depending on the number of paralleled phases of the system.

These points are used to adapt the number of active phase of the system in each moment. Thus, when the photovoltaic power production is lower than P_1, only one phase is active and the other phases are kept in off state. For PV power production between P_1 and P_2, two phases will be active; and for power productions higher than P_2, three phases will be active. The theoretical efficiency of the power converter using this adaptation mode is shown by the red line. In this case, the efficiency curve does not suffer drastic drops and it follows the maximum possible efficiency for all the power range.

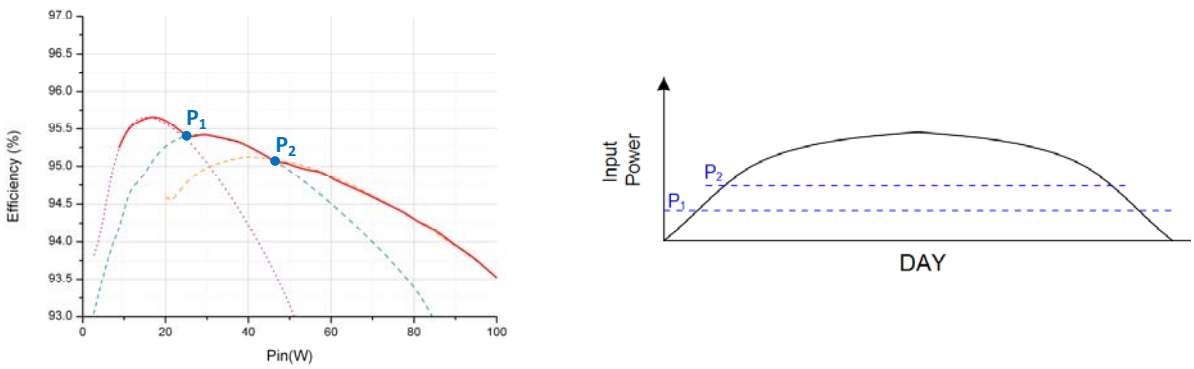

a) b)

Fig. 4. 10. Efficiency curves for 1,2 and 3 phases operating mode and for the adaptation using predetermined optimal points.

Finally, in fig. 4. 11., the comparison between both methods can be appreciated. The use of predetermined points P_1 and P_2 shows better efficiency. To resume, it is important to adapt the number of phases in an exact moment. This moment corresponds to a particular

power level called P_n which can be defined as the intersection between the efficiency curves of *n* and *n+1* phases operating modes.

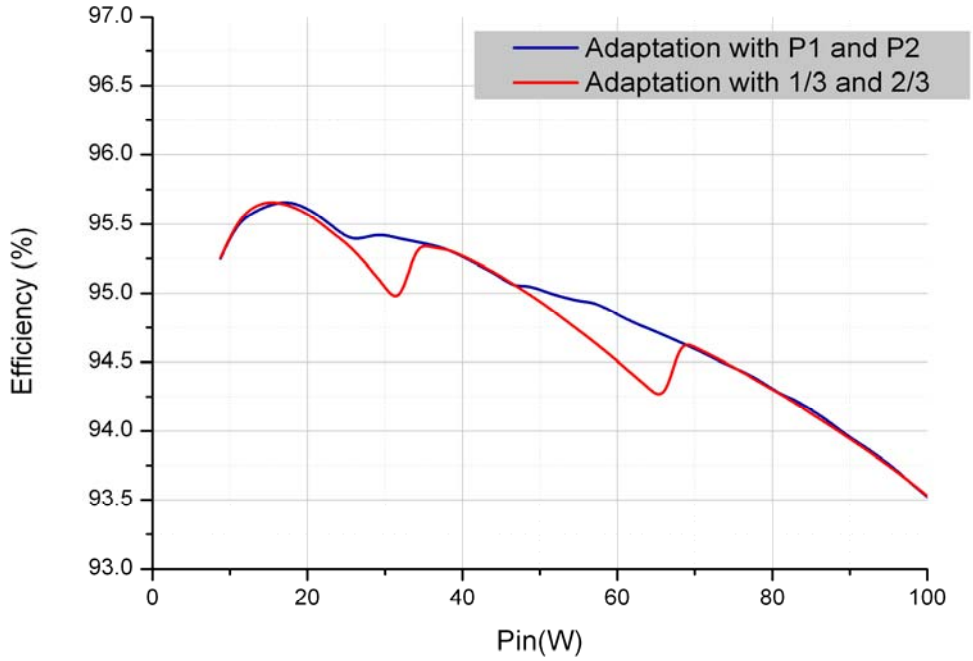

Fig. 4. 11. Comparison of efficiencies with the two algorithms.

Thus, the working mode for N paralleled phases power converter can be defined by a sunny day as in the fig. 4. 12. The values from P_1 to P_n have been measured. Looking the intersection of efficiency curves, the optimal number of active phases corresponds to the number of phases that have the highest efficiency for the instantaneous power value. The values P_1 to P_n represent the intersection in which the number of active phases changes. The number of phases that are active in each moment of the day are also represented.

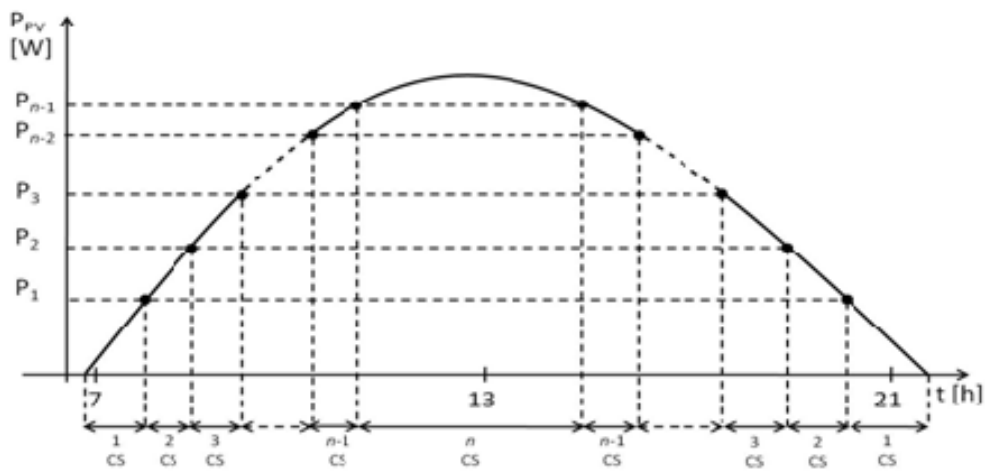

Fig. 4. 12. The working mode of N paralleled converter for a sunny day.

4.2.2.2 Example of design of a MPAC

A simple power conversion structure has been envisaged to carry out this research and its experimental validation. Thus, a simple structure was chosen with a unique PV panel in the input port of the MPAC and a lead acid battery for a load. This choice has been made above all due to installation availability as well to the possibility to carry out practical test for validate the system. Moreover, in the laboratory, there is an already acquired knowledge with this structure as they have been used in previous works. Good results have been obtained in of boost prototypes with associated MPPT controls [136]-[137].

Nevertheless, these researches could be expanded to more complex DC-AC grid connected systems since the type of losses of almost all the converters presents the same nature.

In this way and in order to improve the efficiency of a power converter, it is important to understand the origin of losses and their behaviour linked to several constraints.

4.2.2.2.1 A boost converter for the elementary phase

The analysis of the losses of a power converter will be carried out taking the boost converter as the practical example. The electrical schema of the boost converter is reminded in the fig. 4. 13. The boost converter is one of the simplest DC-DC converters. It is a switched mode converter that is capable to produce a DC output voltage which is greater in magnitude than the DC input voltage. For testbench and practical test prototypes, the switch cell is constituted with a MOSFET and a diode. An inductor is used as intermediate to store energy. The inductor acts as a load when it is being charged and it absorbs energy. When it is being discharged, it acts as an energy source.

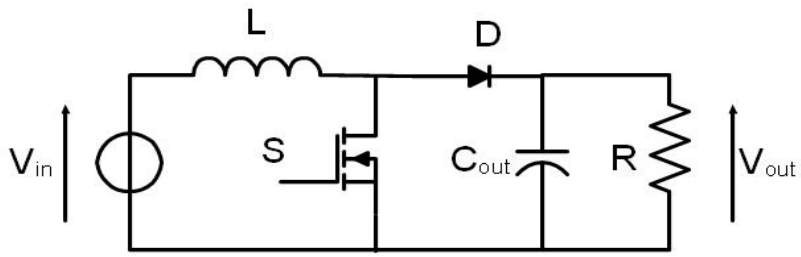

Fig. 4. 13. The electrical schema of a boost converter

As we have detailed in the previous chapter, the efficiency of a power converter can be defined as the ratio between the output power and the input power and the output power will be determined by the losses of the system in the power transfer:

$$\eta_{PV} = \frac{P_{out}}{P_{in}} = \frac{P_{in} - P_{Losses}}{P_{in}} \tag{4.13}$$

For a continuous operating mode, the ratio between the input and output voltage is defined by the following equation.

$$\frac{V_{out}}{V_{in}} = \frac{1}{1-\alpha} \tag{4.14}$$

The losses analysis carried out in the chapter 3 showed that the total losses come from switching losses, conduction losses and losses produced by the supply of the components. This analysis has shown that they depend on the input current, or even in the input power if the input voltage is considered constant, and can be represented with a second level equation. This formula is reminded in the equation (4.15).

$$P_{Loss_T} = a \cdot i_{PV}^{\ 2} + b \cdot i_{PV} + c \tag{4.15}$$

Where,

$a \propto P_{Ldc} + P_{On}$;

$b \propto P_{sw} + P_{D_{on}}$;

and $c \propto P_{Lac} + P_{Qg} + P_{Qds} + P_{CTRL}$.

This losses equation involves a presence of a maximum in the efficiency of converters which correspond to a given input current. For working condition with lower or higher current than this value, the efficiency decrease considerably.

4.2.2.2.2 Loss evolution in a multi-phase converter

In order to evaluate the interest of a *n* phases converter, a similar analysis must be also done for this structure. In fig. 4. 14, the structure of *n* phases boost converter is shown. Their inputs and output ports are connected in parallel. One global control is used to all of the converters in parallel.

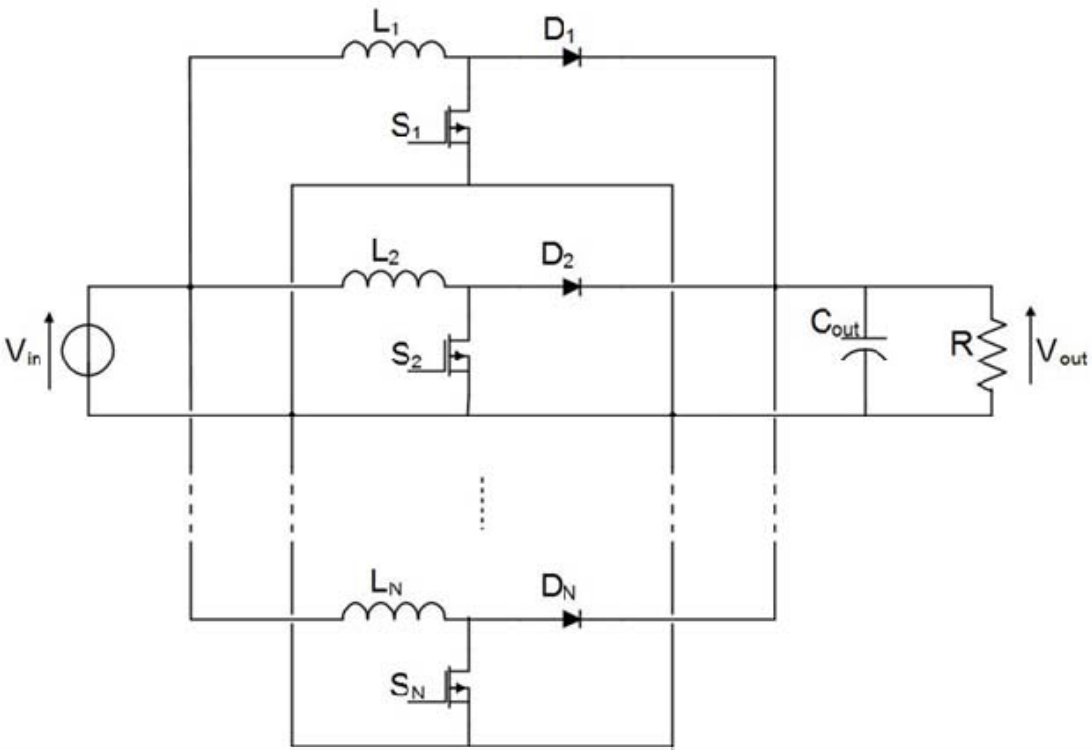

Fig. 4. 14. Electric schema of N paralleled boost converters

In equation (4.15), losses for a simple boost converter are defined. From this analisys and this formula the losses in *n* phases converter can be deducted.

Two loss associated effects take place in paralleled power converters. In one hand, as the number of converters or phases is multiplied, the number of components is also multiplied and, in this way, the total losses of the paralleled converter will be also multiplied. On the other hand, considering that all the phases are identical and a homogenous current distribution is assured, the current though each phase will be also divided. In this case, the PV voltage and the temperature are considered unchanged as their variation is not as important as the current and it has a slower time constant. Thus, the following simplified equation can be obtained, which represents the loss in a multi-phase converter:

$$P_{Loss_n} = n \cdot \left(a \cdot \left(\frac{i_{PV}}{n} \right)^2 + b \cdot \frac{i_{PV}}{n} + c \right) \tag{4.16}$$

$$P_{Loss_n} = \frac{a}{n} \cdot i_{PV}{}^2 + b \cdot i_{PV} + nc \tag{4.17}$$

Where

$a \propto P_{Ldc} + P_{On}$;

$b \propto P_{sw} + P_{D_{on}}$;

and $c \propto P_{Lac} + P_{Qg} + P_{Qds} + P_{CTRL}$.

This result allows the realization of a comparison between a single one phase power converter and multi-phase converter. Two points will be compared: the null currents or losses tendency when the input or PV current goes toward zero; and high values or the losses tendency when the PV current increases toward infinite values.

When PV current values go toward null values, that is, in low PV current cases, the *c* value determines the losses:

1 phase $\lim_{I_{PV} \to 0} Loss_{TOTAL} = c$ (4.18)

(4.19)

n phase: $\lim_{I_{PV} \to 0} Loss_{TOTAL_n} = nc$ (4.20)

(4.21)

As $c < nc$, losses are bigger for multi-phase converter in low current values, that is, in low PV power productions.

The losses increase in parabolic way with increasing input current. The increasing speed of a curve is measured by the derivate of its curve equation. In this way, the increasing speed of both structures can be defined in the following way:

1 phase: $$\frac{d\left(Loss_{TOTAL}\right)}{dI_{PV}} = \frac{d\left(a \cdot i_{PV}{}^{2} + b \cdot i_{PV} + c\right)}{dI_{PV}} = 2a + b \tag{4.22}$$

n phase: $$\frac{d\left(Loss_{TOTAL_n}\right)}{dI_{PV}} = \frac{d\left(\frac{a}{n} \cdot i_{PV}{}^{2} + b \cdot i_{PV} + nc\right)}{dI_{PV}} = 2\frac{a}{n} + b \tag{4.23}$$

As $2a + b > 2\frac{a}{n} + b$, losses are smaller for multi-phase converter in high current values, that is, in higher PV power productions.

Fig. 4. 15. show the losses of one phase converter and three phase converter by MatLab simulation of the (4.17.) equation. The simulations parameters are the same that has been used in the boost converter efficiency simulation showed in fig. 3. 20. and they are given in table 3.3. and table 3.4. The losses are lower for a single converter in low power, as the analysis has shown. In contrary, they are lower for the three phase converter in lower power as, the losses increases faster for the single converter. Thus, there is an intersection in the losses and efficiency curves.

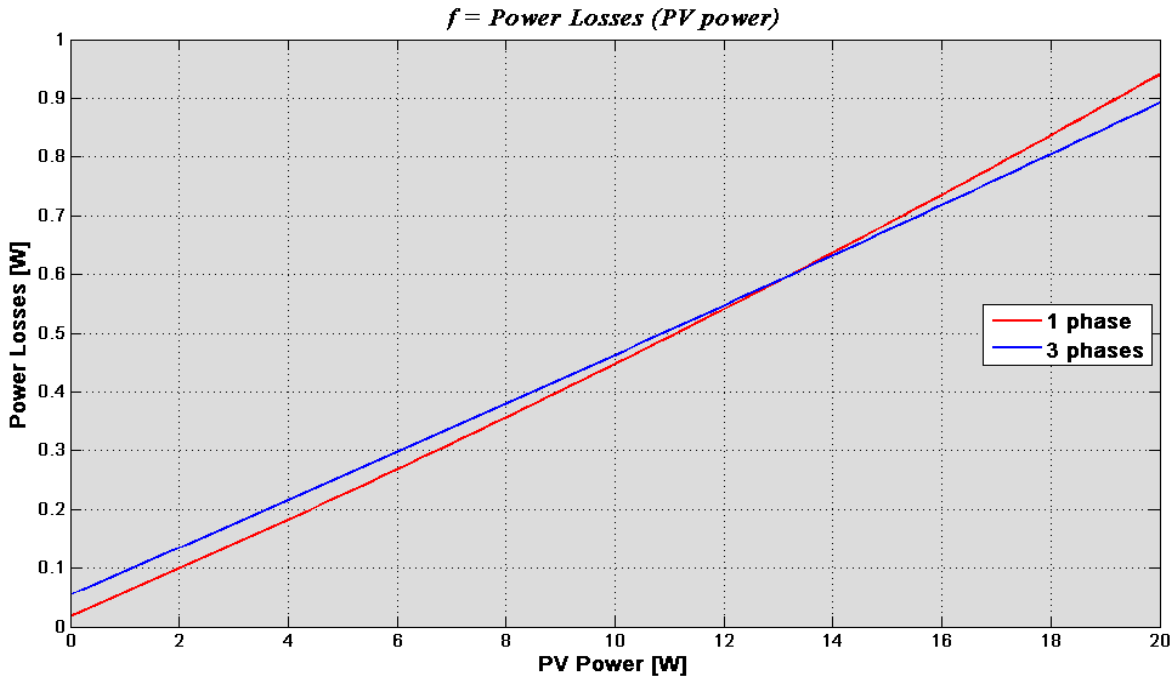

Fig. 4. 15. Power loss evolution for 1 and 3 phases parallelised boost converter.

The losses analysis has also demonstrated the interest of the main function of the MPAC that consist on the adaptation of phases depending in instantaneous power level.

4.2.2.3 Determination of power ranges

Power ranges for each functioning mode are first determined. These ranges are based in efficiency curves of each mode. The crossing between this curves define the low value and high value of power ranges for each functioning mode. The intersections point of efficiency curves are named P_n, determining this point the power level in which the power

converter change the number of working phases. The intersection between one phase efficiency curve and two phase efficiency curve will be named P_1. P_1 determines the power level to pass from one phase working mode to two phase working mode. For the intersection between two phase and three phase efficiency curves, the crossing point is named P_2 and it determines the power level where the converter changes from two to three phases. Thus, to resume, the intersection between *n* phases working mode and *n+1* working mode is named P_n, and it determines the power level in which the power converter change the number of phase from *n* to *n+1*.

These points are determined by experimental tests. In fact, to adapt correctly the phases the adaptation point must correspond to the intersection of efficiency between efficiencies of each working mode. An experimental prototype has been used to determine these points.

Efficiency test has been carried out for this purpose. For each of the working modes, the efficiency has been measured by a current sweeping. The input and output voltages have been kept constant in the entire test. Fig. 4. 16. represents the efficiency evolution of the MPAC designed to be connected to the PV module of 85 W_P. Here, the MPAC is constituted by three power converters of 100W. The input voltage has been defined as 14V, which correspond to the maximum power point voltage level. The output voltage simulates a 24V battery. The intersection of the efficiency curves of one and two phase working modes determines the first power level (P_1). In this power level, the MPAC change the working mode from 1 to 2 phases if the power is increasing and from 2 to 1 phase if the PV power generation is decreasing. In the same way, the intersection of the efficiency curves of two and three phase (P_2) determines the transition point between two phases and three phases working mode.

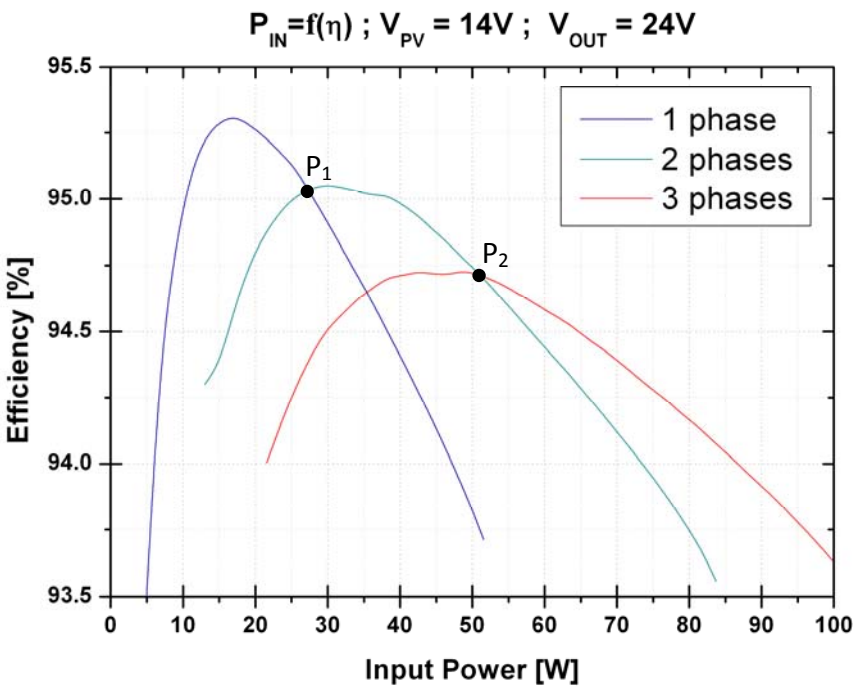

Fig. 4. 16. Behaviour of the conversion efficiency of the MPAC operating during different configurations

The number of converters inserted in the MPAC can vary depending on the PV generator power and the efficiency curves evolution of the MPAC operating modes (1, 2… until *n* phases connected). For this structure and power level three converters are used. The efficiency gain of the third phase is still visible; however, another phase would increase the price and complexity of the converter but without any obvious gain in efficiency. For other applications, other theoretical studies and methodology analysis must be predicted.

4.2.2.4 Phase adaptation control law

Once the transition points, *Pn*, are determined, the values of these points are saved. The adaptation algorithm uses this information to adapt the number of phases depending on the PV power production of each instant.

The system is equipped by captors that measure the input current and voltage. By its multiplication, the PV power is calculated. This PV power is compared with pre-determined power ranges and the optimum number of active phases is determined. The determined number of phases is connected. The algorithm of the converter adaptation law is reported in the Fig. 4. 17. for *n* converters.

The adaptation of phases is made by a micro controller that controls the working state of all the phases. The phases are activated or deactivated by a control signal from the micro controller that actives the MOSFET or the active switching component of each phase. Fig. 4. 17. shows the algorithm used to the phase adaptation.

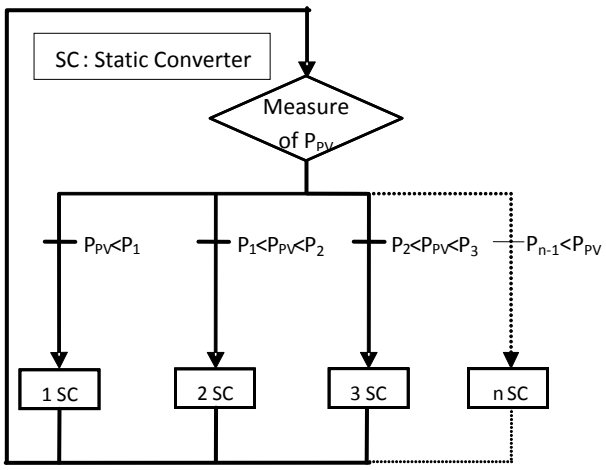

Fig. 4. 17. Algorithm for the converters number activation.

4.2.2.5 Life-time improvement by phase rotation

Nevertheless, the improvement of efficiency is not the only factor that must be improved in a photovoltaic system.

However, this mode of working could involve the premature aging of the phase number 1, which is active during all the different operating modes. In order to avoid this phenomenon, another control law has been integrated: the rotation of phases of the power converter.

The rotation of converter phases has been incorporated to the system to homogenize working time of each phase. That will guarantee uniform aging in the phases and increased

the average life time of the system, avoiding that one phase break down much faster than the other ones.

In order to perform the rotation of the converter, a control law has been implemented in the system. This control law is based in the assignation of priorities according to the total working time of each phase. The activation order of the phases will depend in this priority.

The algorithm consists in registering the total working time of each phase. Each 10 seconds this total time will be checked and the different phases will be assigned with respective priority levels. The converter that has worked less time will be assigned with the highest priority and the one that has worked more time with the lowest priority. Then, the phase or phases will be activated according to priority level. The algorithm of converter phase rotation must be integrated taking into account the adaptive phase algorithm, explained in the previous section. The simplified schema of the rotation and adaptation algorithm is shown in the fig. 4. 18.

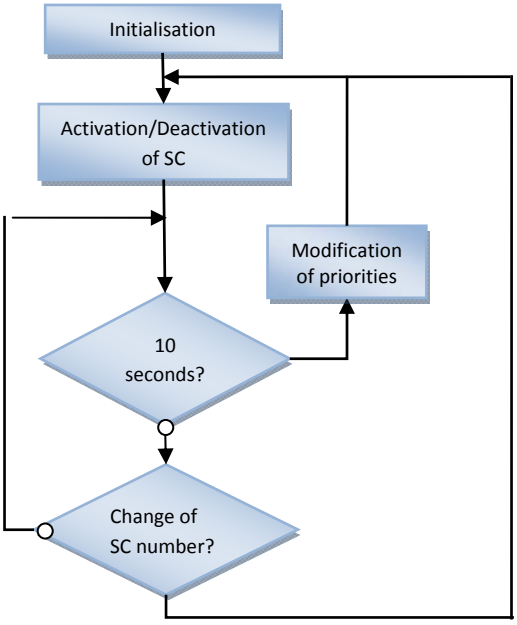

Fig. 4. 18. Algorithm of the rotation law of phases

4.2.2.6 Other functionalities

In addition to the adaptation and the rotation of phases, the system also needs additional functions or control laws to its optimal working. It is the case of security functions that will assure its functioning even in case of phase failures and the MPPT control, necessary in PV system to get the maximum available power in the PVG.

4.2.2.6.1 Security and failure detection

Although, the rotation of the phase has been integrated to achieve a homogeneous aging of all the phase, the failure of one of the phase cannot be completely prevented. Thus as security function, the different power converters are checked constantly in order to verify if their operating state is in accordance with the commanded state. The method to detect the default consists in measuring the currents through the different converters. In the case of the presence of current in a deactivated phase or the absence of current in an activated phase, the presence of a failure is detected. In this case, priority level of this broken phase will be

set to null, disallowing the option of its activation. This monitoring mode is represented in the fig. 4. 19. by the security and fault blocks.

After the system initialization, where the initial priorities will be defined in accordance with the total worked time of each converter, the activation of number of phases is carried out according to the PV power production and the priorities of the moment. Then the security test is carried out, as well as the verification of possible changes of static converter number due to a PV power evolution. These verifications are constantly carried out, and the same configuration mode is maintained, while there are no failure detected or power changes happened.

Each 10 seconds, the priority will be modified with the purpose of maintain the same operating time for all the phases and avoid the premature aging of one of them. This will carry on the activation or the deactivation of the phase or phases of the lower priority.

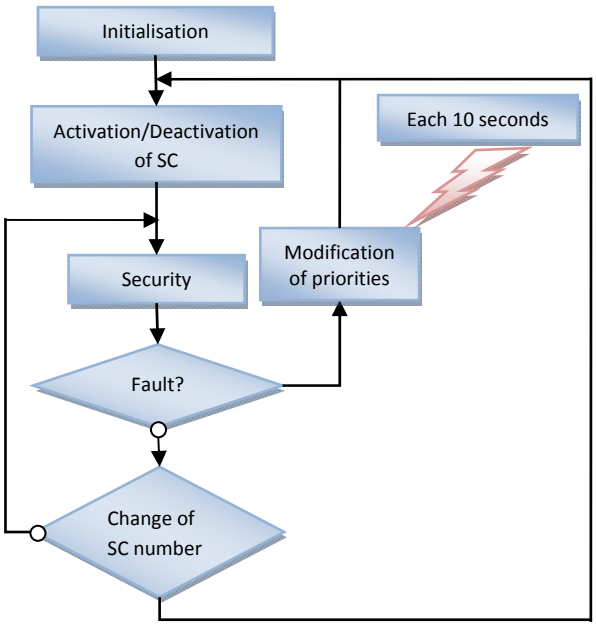

Fig. 4. 19. Principle algorithm of the multi-phases converter.

4.2.2.6.2 MPPT Control

As this system is dedicated to photovoltaic applications and due to its non lineal characteristic, the control of the converter is associated to Maximum Power Point Tracking (MPPT) control which tracks permanently the maximum power point (MPP) of the panel. As explained in chapter 2, many researches have been made about MPPT control; many kind of control has been studied and developed. In this system a MPPT control developed in our laboratory in previous works is used, which is based on the Perturb&Observe principle and carried out in digital way [134].

4.2.2.7 Design of complete algorithm and its integrations

In the fig. 4. 20, the whole system has been represented: from the power processing part to the representation of the control laws and the interactions between all the system. Each part will be defined in the following lines:

Parts A, B and C represent the power processing part. The adaptation stage (A), which consists of a switching structure of three boost in parallel, transfers the power from photovoltaic array (B, source) to the battery (C, load).

All the part in D corresponds to the circuit representation of the control laws. All this controls are implemented in a FPGA. All the functions block interact between them, and the task are carried out in parallel.

A MPPT control identified by (1) in the fig. 4. 20. adjusts the duty cycle value (α) of the converter in order to permanently track the maximum power point.

In parallel, the phase adaptive algorithm, where is placed inside bloc number 2, will establish the number of phases to activate according to power of the photovoltaic array and the predefined power levels (P_1,P_2).

Block 3 represents the rotation algorithm, where the priority of the phases is defined. According of the signal with the information of number of phase to activated coming from (2), this block will set to 1 (on state) or reset to 0 (off state) the signals B1,B2 and B3, corresponding simultaneously to the working states of phase number 1, number 2 and number 3.

Security block (4) will recover the real state of phases by means of the current through each phase and will inform if they are faulty or not. This information will be send to the block (3), which will set to null the priority of the faulty phase, avoiding its activation.

Finally, the switching box (5), will define the duty cycle for each converter (d1, d2, d3) using the information received from the MPPT (1) and the signals B1, B2 and B3.

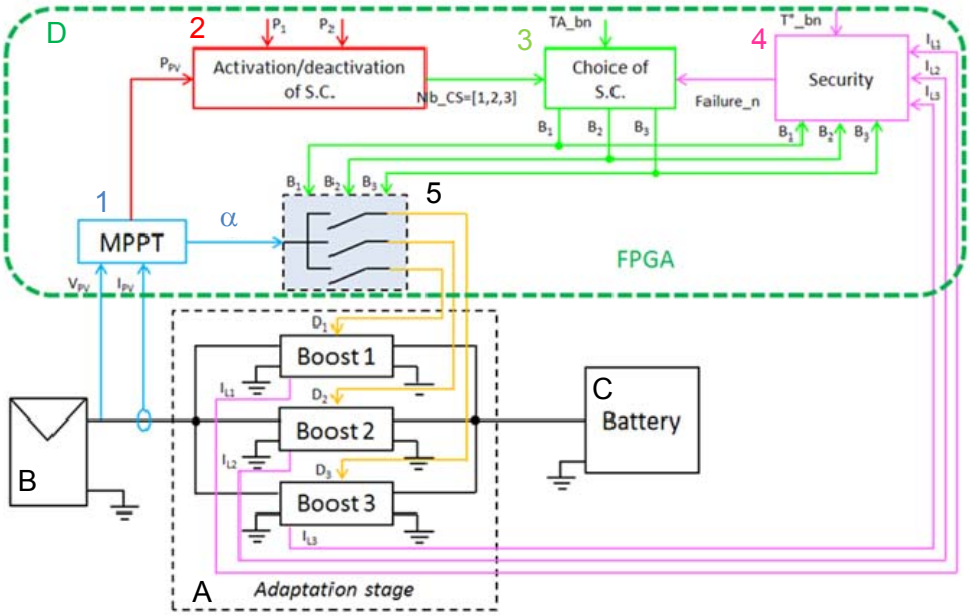

Fig. 4. 20. Implementation of the function on the system for three static converters

4.2.2.8 Experimental prototypes

A demonstrator of three dc-dc boost converters has been designed and implemented, as shown in fig. 4. 21. To validate the operating of our demonstrator, we have used a PV

module of 85 W_P couple to a 24V battery. At first time, the control laws are integrated in a FPGA AGLN250-VQG100 [res_ICREPQ6]. A set of supplementary function has been added to the system, as a date storage memory, an USB connection to a computer and a user interface. They allowed an easier analysis of the system and treatment of data.

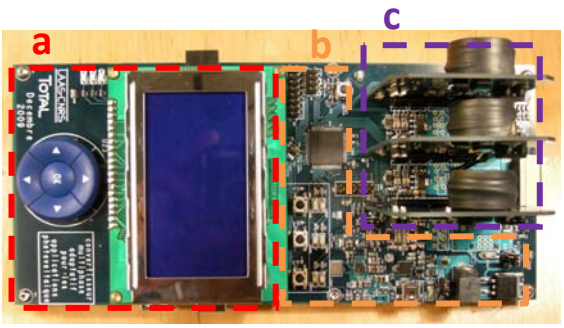

Fig. 4. 21. Prototype of MPAC: a) User interface; b) Control; c) Power

This prototype has been used to carry out the first tests as the validation of functionalities and first efficiency test. In a second version, the control device has been substituted. A PIC microcontroller has been used. In difference of the FPGA, this microcontroller cannot be carried out functions in parallel. Nevertheless, the system works correctly also, carrying out all the function in time to answer system characteristics. Moreover, the second version has been optimized also in size and weight and it can be incorporate in the junction box below the PV modules.

4.2.2.9 Experimental results

Different tests have been carried out to validate all the functions of the MPAC converter.

The first tests have been achieved in order to validate the rotation algorithm and the phase adaptation function, as well as the stability of the system in the presence of the continuous changes in the state of the converter. At first time, we have made the tests without the MPPT control, using as source a constant DC supply. The fig. 4. 22. and fig. 4. 23. show these first tests.

Fig. 4. 22. shows the results of the rotation algorithm tests for a constant input power corresponding to operating mode with two static converters. The signals 1, 2 and 3 represent the working state of three different phases, being the high state, the activated condition and the low state, the non-activated condition. Each 10 seconds, the working phase will change. From t_1 to t_2, the phases number 1 and 2 work; from t_2 to t_3, the phase number 3 takes the place of the phase 2, in order to equilibrate the working time of all the phases.

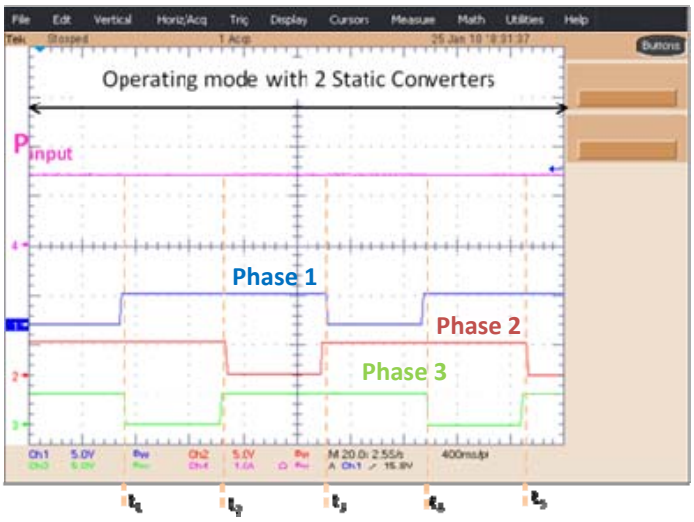

Fig. 4. 22. Test of phase rotation algorithm

In fig. 4. 23., the interaction of the rotation algorithm and the phase adaptation function is shown for an increasing and decreasing input power generate by a DC supply. Like in the previous test, the signals 1, 2 and 3 represent the working states of the phases 1, 2 and 3 corresponding to the power evolution: from t_0 to t_1, only one phase is activated (phase 2). In t_1, as the power become higher than P_1, a second phase is activated (phase 3). From t_2, the phase rotation algorithm can be noticed: the phase 1 takes the place of the phase 2, to equilibrate the operating times of all the phases. In t_3, the limit of P_2 is passed and all the three phases are activated. In decreasing power, the deactivation of phases is carried out, following also the rotation of the converters. In t_4, the third phase is disconnected. In t_5, the rotation algorithm take place, deactivating the first phase and activating the third phase. In t_6, the power become lower than P_1 and the second phase is deactivate. Between t_6 and t_7, the phase number 3 is the only phase that is operating, to give place to the phase number one in t_7.

These two pictures validate the functionality of the phase adaptation and the rotation algorithms.

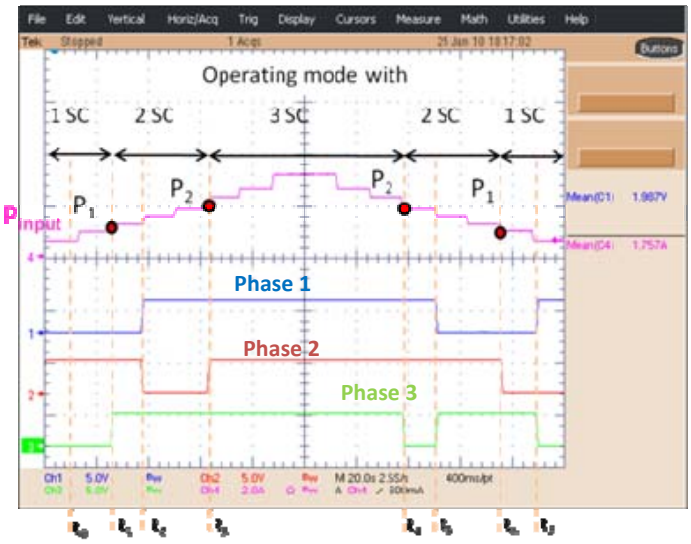

Fig. 4. 23. Test of the algorithm for the converter number activation in interaction with the phase rotation algorithm. (SC : Static Converter)

In a second time, as shown in fig. 4. 24, we test the compatibility of our system with the MPPT control. The AG E4360A [138] solar simulator of Agilent Technologies have been used to simulate the PV input and the PV power changes. The system reaches the maximum power point (MPP) and oscillates around this one. In fig. 4. 24.a., the system suffers a decreasing power change. Before the perturbation, we can see that the PV Current (I_{PV}) is uniformly shared between the converter 1 and 2 ($I_{L1}=I_{L2}=I_{PV}/2$.) The answer of our system to this change is fast and stable: it follows oscillating around the new MPP. Moreover, we can see that the first phase is deactivated, since the second phase current (I_{L2}) is equal to the PV current. Although the impact of this change is visible in the currents of the phases, it is invisible from the view of the input voltage and current. With the decreasing power change, the operating point has been changed from two to one active converter. In the fig. 4. 24.b., a increasing power change occurs. Previous to perturbation, only one phase is active as the phase number two takes all the PV current ($I_{L1}=I_{PV}$). We can also see that the system stay stable after the change, oscillating around the MPP and as in the falling change, the response is fast. In this case, we can distinguish the activation of the phase 2; as the power has passed the P_1 limit, a second phase is activated and the input current is distributed uniformly between both phases ($I_{L1}=I_{L2}=I_{PV}/2$).

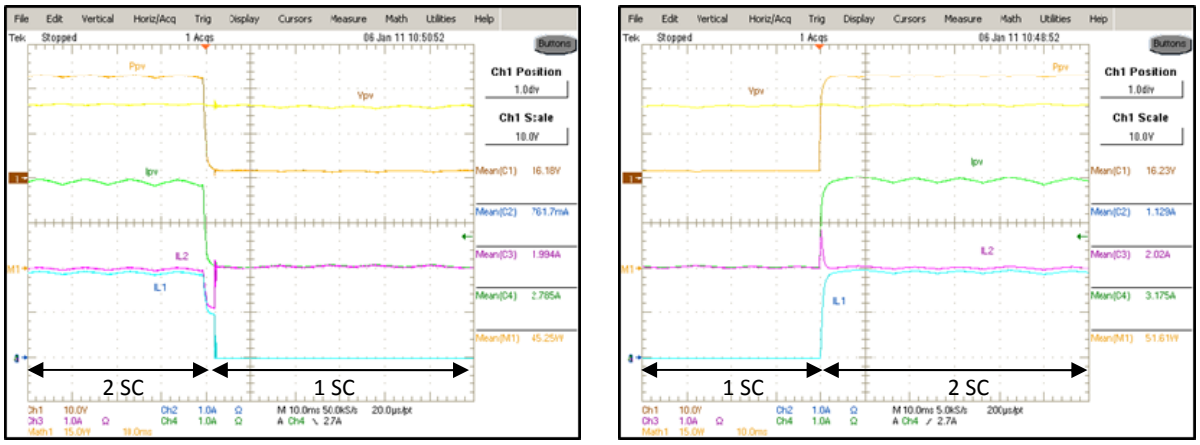

a) b)

Fig. 4. 24. Experimental results: a) Phase adaptation in decreasing power: from 2 to 1 active phase; b) Phase adaptation in power: from 3 to 2 active phases

4.2.2.10 Comparatives tests

In order to validate the gain in the produced energy provided by this new system (MPAC) in comparison to a classical structure, a set of indoor measurement has been made. The electrical features of 85Wp PV array are simulated with AG E4360A solar simulator in order to supply the same PV energy to both structures. In the output port, a battery has been connected.

The tests have been realized by simulating three different daily profiles in 4 hours simulations for both structures. Three different profiles have been chosen. The first profile simulates a sunny day. The other profiles give two different cloudy days with different levels of irradiation and sudden changes.

The equivalent of one day solar power production has been simulated in 4 hours for both structures. The transferred energy to the load and the converter efficiency have been measured [135].

The fig. 4. 25. shows the results of the first simulation. A sunny day is simulated here. The input power characteristic, the output power characteristic and the energy production are shown in this figure for a simple phase boost converter, and for the MPAC. Comparing the efficiency curves of both structures an important difference can be seen. In effect, the efficiency decreases for the simple converter at noon, when the PV power production is higher. Meanwhile, for the MPAC, the efficiency is kept higher for a bigger power range.

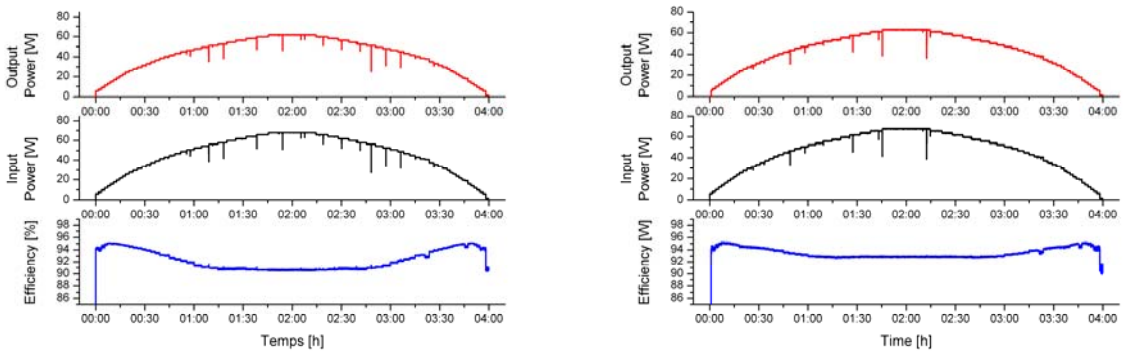

a) b)

Fig. 4. 25. Comparison of one phase boost converter (a) and MPAC (b) energy production in a sunny day.

If a zoom is made (fig. 4. 26), this difference can be seen more precisely. Indeed, there is a 2% of difference in efficiency between both structures in almost half of the total PV production time. Moreover, the efficiency of the MPAC is higher in 2/3 of the time, and in the rest of the time, the both structures present the same efficiency.

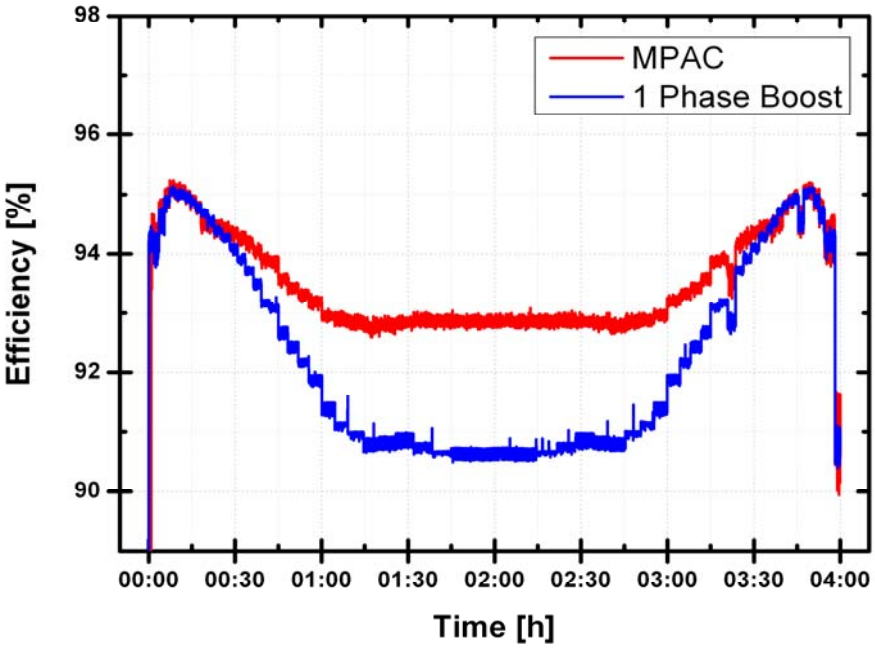

Fig. 4. 26. Comparison of efficiencies of one phase boost converter and three phase MPAC

In a second test, a perturbed sunny day is simulated. That is, some clouds or shadows have been added along the day. In the fig. 4. 27. are shown the input and output power and the efficiency of both structures.

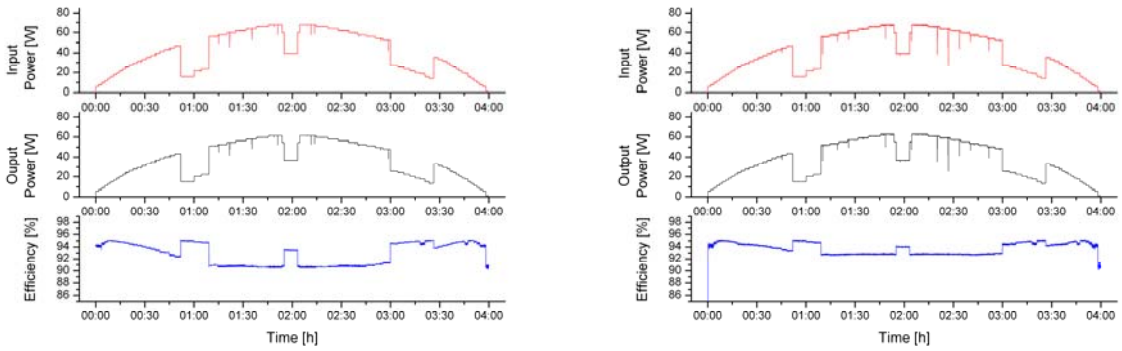

a) b)

Fig. 4. 27. One phase boost converter (a) and MPAC (b) energy production in a sunny day.

In the fig. 4. 28., a zoom is made for the comparison of efficiencies of both structures. The efficiency of the MPAC is for all the power range higher than the one phase boost convert, arriving to have efficiency difference of 2%.

Other conclusions can be also found in the analysis of the efficiency curve comparison:

- When the input power is low and the MPAC is working with only one phase, the efficiency curves are superposed.

- When the power is higher, the difference in efficiency between both structures is the higher on, arriving to values of 2%.
- When the power is in middle, the efficiency difference is not as high, and we conclude that the phase two phase are working in the same time for the MPAC structure.

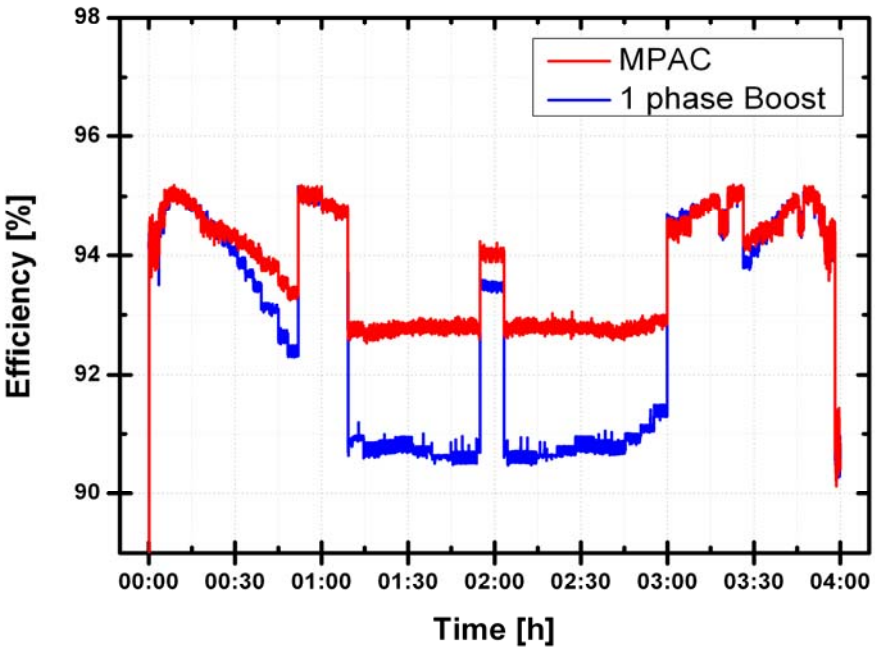

Fig. 4. 28. Comparison of efficiencies of one phase boost converter and three phase MPAC

The third profile is a cloudy day profile with sudden change in solar irradiation. Two parts can be seen in this profile. In the morning and the beginning of the afternoon, sudden and fast clouds or shadows pass in front of the PVG. In the afternoon, a cloudy climatology is simulated, that is, reduced irradiation conditions.

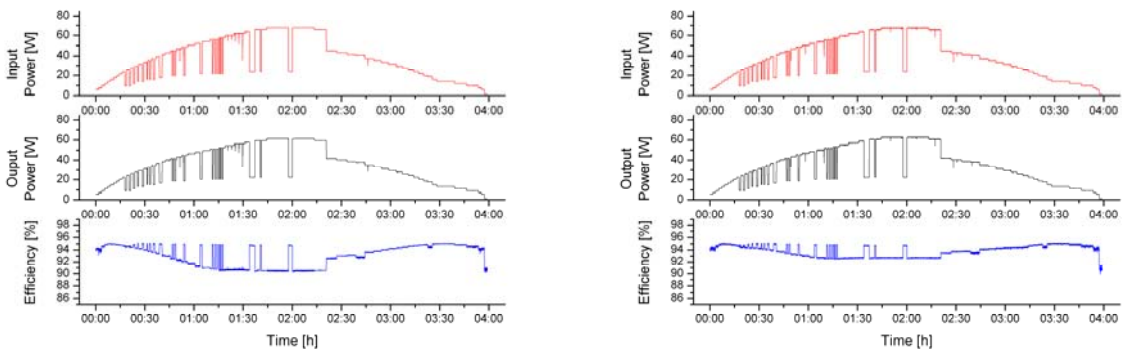

a) b)

Fig. 4. 29. One phase boost converter (a) and MPAC (b) energy production in a sunny day.

As in the previous test, an improvement in efficiency can be appreciated with the MPAC. Indeed, the efficiency of this structure is all the time higher or equal of the simple boost structure.

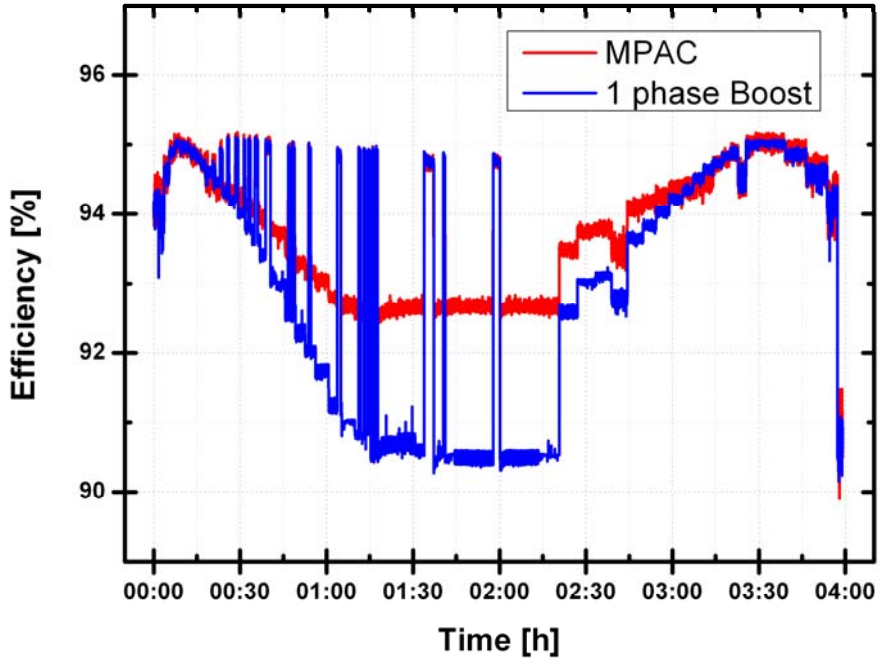

Fig. 4. 30. Comparison of of efficiencies between one phase boost converter and a three phase MPAC prototypes.

Finally, a set of experimental tests in real conditions has been carried out during several days. Our MPAC structure has been compared to a classical boost during five days. Both structures have been connected to 85W_P PV panels with similar electrical characteristics. In addition, the energy supplied to the load has been measured. The fig. 4. 31. shows the results obtained for this five day of tests. The energy produced by our MPAC structure during these experimental tests was superior than the classical one (table 4.3.). We can notice 2.9% higher energy produced by the MPAC compared to the single converter.

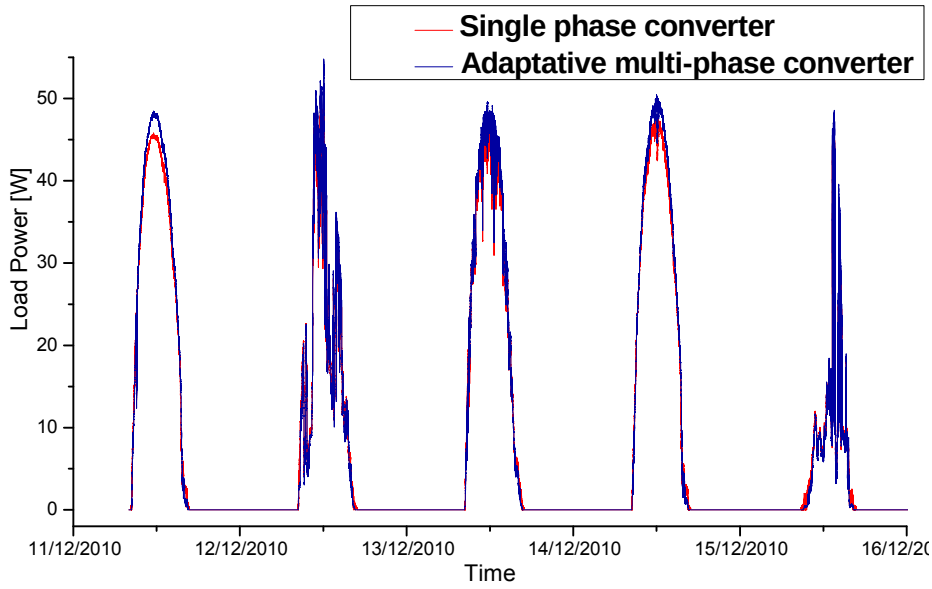

Fig. 4. 31. Experimental measurements of power production for a classical boost and for our MPAC converter.

Table 4.3. Energy production of 5 days in December.

	Day 1	Day 2	Day 3	Day 4	Day 5	**Total**
Classical Structure	248 Wh	164.1Wh	238.4Wh	249.7Wh	66.4Wh	**966Wh**
MPAC	258.5Wh	166.1Wh	247Wh	259.66Wh	62.97Wh	**995Wh**

Outdoor experimental test has been carried out several days. These tests must be made for longer periods and in different seasons in order to evaluate more accurately the real performances of the MPAC. Nevertheless, after some days of tests, the efficiency gain was superior for our MPAC and we considered that this gain was enough promising to follow the research within this kind of structure without waiting other scientific and experiment proofs. Indeed, the efficiency gain between 2 and 3% between a classical boost and the MPAC is important in term of economical point of view if it is compared with the cost for the same percentage of the efficiency improvement carried out in the optimisation of materials of PV cells and modules.

Moreover, this kind of prototype is not designed for long duration tests. We preferred to concentrate our effort in the conception of more optimized and appropriated algorithms for the realization of more performing and reliable prototypes able to support long duration tests. We expose in the following paragraphs our research work in terms of algorithms and difficulties in the conception of version of pre-industrialized prototypes.

4.2.3 Control of a MPAC based on a Look-up Table integrating an adaptive control law

The MPAC had shown a good improvement on its own efficiency compared to a classical power converter. Nevertheless, in our previous tests, we didn't take into account the influence in the efficiency linked to the changes in the input and output voltage levels and the temperature. The effect of these parameters is not so important to change the global tendency of a good % gain in favour of our MPAC. However, their effects must be analyzed to achieve best optimization in future prototypes. For example, the new algorithms to improve their performances must be taken into consideration these influences on the global electrical behaviour of a MPAC.

4.2.3.1 Effects in efficiency due to working parameter of the system

At first time, the effects in the efficiency of other parameter than the input current and power will be analyzed. In effect, the efficiency of power converters is affected by other parameters like temperatures and input and output voltages. Based on the equations of losses of power components, the effect of other parameter can be appreciated in the efficiency of the power converters.

The analysis of the MOSFET losses through the following equations shows the influence of several technological and external parameter:

$$P_{Q_{DS}} = \frac{1}{2} \cdot C_{DS_H} \cdot V_i^2 \cdot f \tag{4.24}$$

$$P_{sw} = \frac{1}{2} \cdot V_o \cdot f \cdot \left(\left(t_f + t_r\right) \cdot I_{PV} + \frac{\left(t_r - t_f\right)}{2} \cdot \Delta I_L \right) \tag{4.25}$$

$$P_{ON} = \frac{V_o - V_i}{V_o} \cdot R_{ds(on)} \cdot \left(i_{PV}{}^2 + \frac{\Delta I_L^2}{12} \right) \tag{4.26}$$

Three elements Vi, Vo and $R_{DS(on)}$ are identified as the major factors on the influence of MOSFET losses. In real cases, they can vary and affect in a large range the efficiency.

The losses in the diode components are reminded too:

$$P_D = \frac{V_i}{V_o} \cdot V_f \cdot I_{PV} \tag{4.27}$$

Here, a new parameter to be mainly taken into account appears: V_f.

In both switching components losses we can estimate the losses dependences with input and output voltages (V_i and V_o). Both parameters can depend on exterior conditions as irradiation, battery charge level, the temperature or even the control of the same system.

The input voltage is mainly dependant on the PVG and its PPM when there is an adequate control law. Globally, the power generated by a PVG is dependent on irradiation, temperature but also on the control.

This effect can be seen in an experimental test as shown in fig. 4. 32. For this, we used the prototype described previously. Efficiency tests have been carried out for different working conditions. Fig. 4. 32. shows the efficiency measured for one phase working in different conditions tests for different input power and voltage levels. A new efficiency behaviour can be distinguished for each set global condition tests.

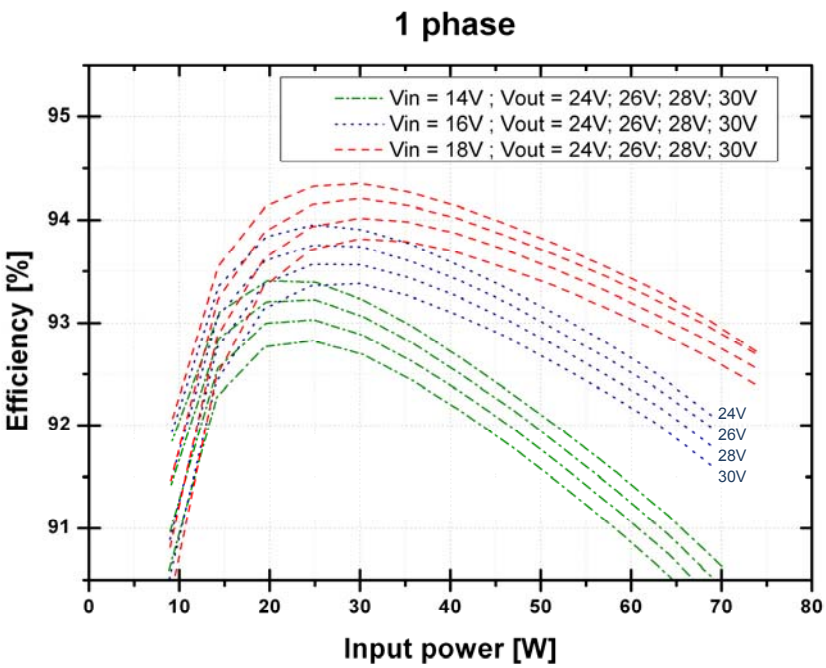

Fig. 4. 32. Efficiency evolution for on phase for different inputs and outputs voltage levels.

In the previous tests, we didn't take into account temperatures. We had decided to study more in detail their influences before design new algorithms because we though temperature effects must also been taken into account by them.

The operating temperature of the components has a direct relation with the electrical characteristics of the electronic components. As well as a temperature increase as a temperature decrease influences the electrical characteristics of the components like the MOSFET and the diode. $R_{DS(on)}$ and V are two characteristics of the MOSFET and the diode simultaneously, which affect directly in the losses of these components.

$R_{DS(on)}$ is an internal characteristic of the MOSFET component. The effects of the temperature in this resistance are given by the component constructor in their data sheets. The fig. 4. 33. from a MOSFET datasheet [139] shows the change in the internal resistance of a diode in relation of the temperature. For example, in a working temperature of 100ºC, it has a resistance that is 1,5 times bigger than in working conditions of 20ºC.

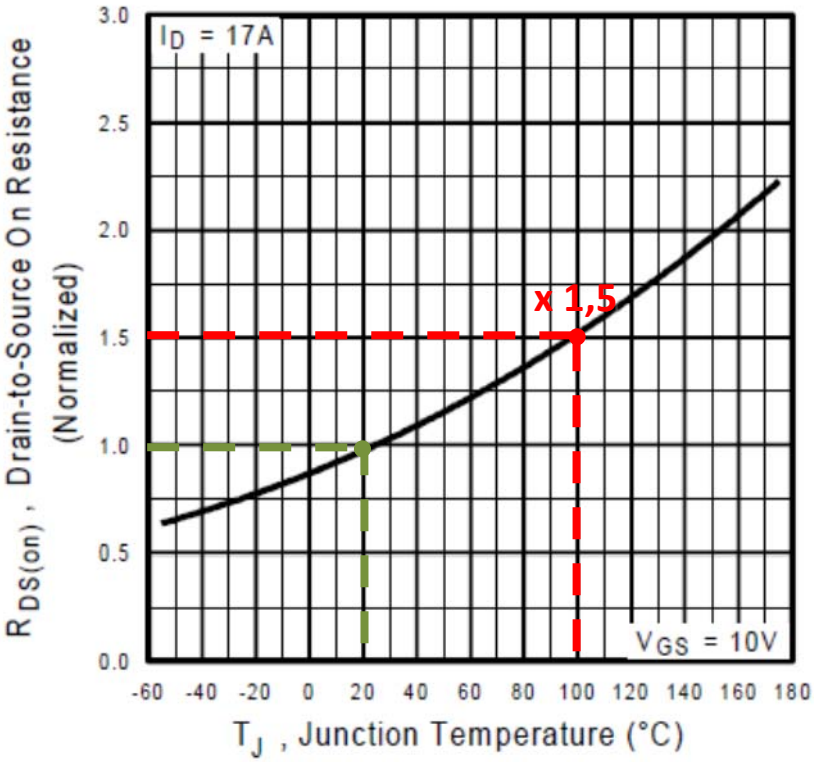

Fig. 4. 33. Effects of the temperature in the value of RDS(on) resistance for IRFR024N MOSFET [139]

For the diode, the temperature increasing is traduced as a decrease in the voltage drop (V_f) as is seen in the fig. 4. 34. [140]

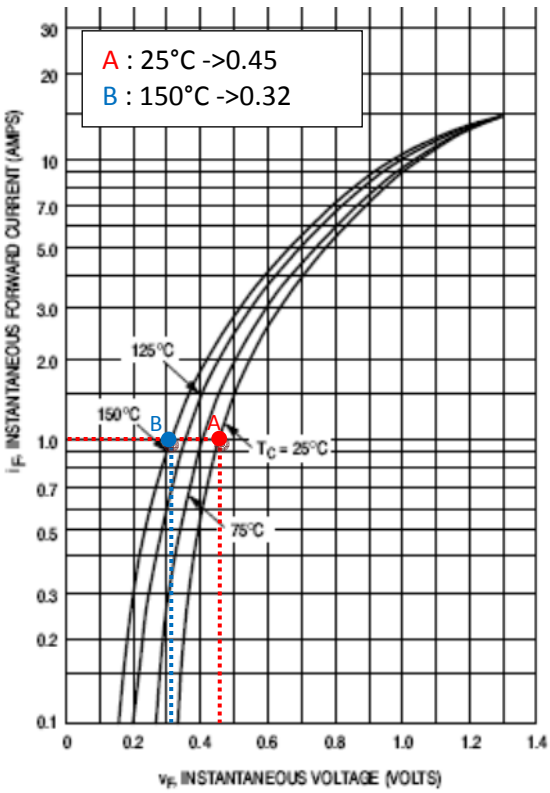

Fig. 4. 34. Effects of the of the temperature in the value of Voltage drop (Vf) for MBRD620CT Diode [140]

Passive components as the capacitors, inductors and resistances are also influenced by the temperature. These components do not support the auto-heating phenomena, but in contrary, they are exposed to temperature increase by mean of thermal convection and radiation of other elements.

The capacitor is one of the components that support the most constraint. It capacitance decrease considerably in extreme temperatures and it deteriorates rapidly in limit temperatures. Although there are capacitors that can support high temperatures, their prix is very high.

Unfortunately, tests in for different constant temperatures are more difficult to carry up. A special thermal enclosure is need, which is not accessible for as for us. This way, only input and voltage effects will be taken into consideration in future test. Nevertheless, the system will keep open to include of temperature effects in future works.

4.2.3.2 Definition of a look up table

For this effect, an MPAC which adapts the P_n points is presented. This adaptation is made by look up tables.

The look-up tables can be defined as the predetermined data tables easily accessible to the control system. The look up table is in informatics a data structure. Normally, it is an array that replaces runtime computation with a simpler array indexing operation. The look up table are very useful to save processing time, since to take a data value from the memory is faster than an complex computation or input/output operation. The tables are normally pre-calculated and stored in static program storage. The control laws accede to this table when it needs any of its values without excessive time calculations.

4.2.3.3 Determining optimal Pn values.

In the same way that the efficiency curves itself are affected as seen previously, the position of P_n intersection points are impacted too by these parameters variations. Thus, in order to increase the efficiency and adapt the MPAC phase in the most optimal way, we propose to use an algorithm based on a look-up table that modifies the values for P_1 and P_2 depending on the voltage and temperature changes.

As the efficiency for one phase converter has been characterized, the same process has been carried out for the other two phases. The results for different output voltages levels are shown in the fig. 4. 35.The input has been maintained constant for this test.

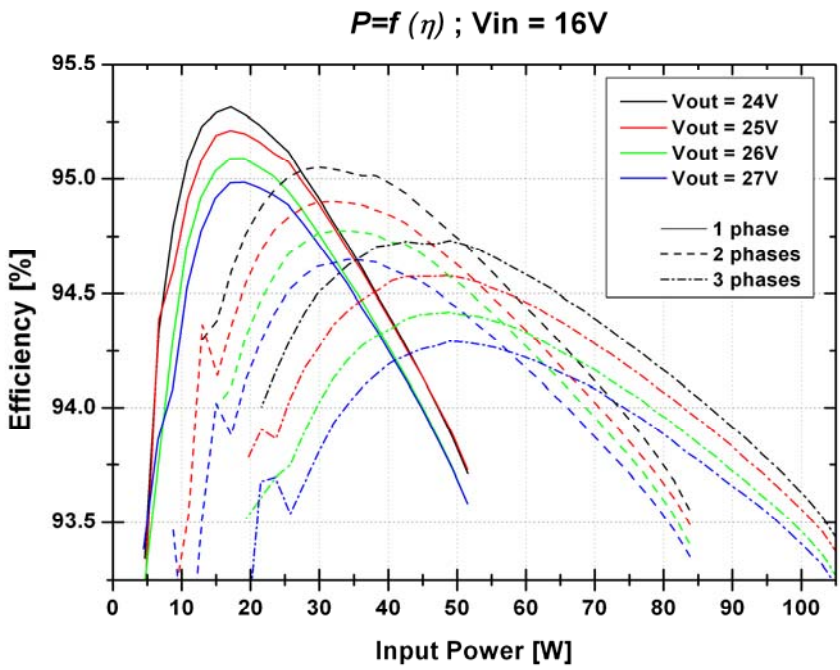

Fig. 4. 35. The experimental evolution of efficiency for different output voltage levels for respectively one, two and three phases working modes for three 100W phase paralleled converter.

From the characterization test can be deducted different P_n values. From this characterization set of measures, we can deduce different crossing P_n values and their range of variation depending on V_{out} for a fixed V_{in}. We can see some strange variations in efficiencies curves at low input power for example. It is probably linked either to values instability in discontinuous mode, which makes difficult the measure; or to temperature variations, which can change the behaviour of losses. These phenomena are very difficult to analyze with the state of our test bench. For a first analysis, we don't take into account these variations. It simplifies our method but we reserve some possibilities to add the temperature influence in our future work.

In the fig. 4. 36., the P1 (fig. 4. 36.a) and P2 (fig. 4. 36.b) of the MPAC converter values are represented for different input and output voltage levels.

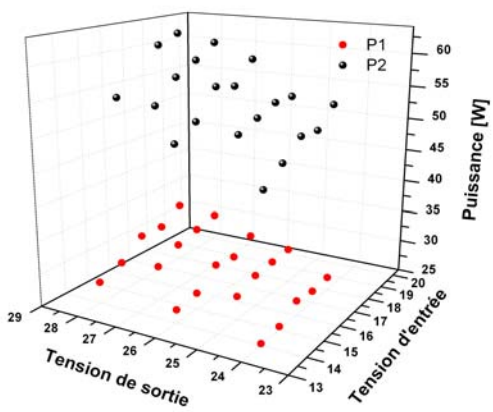

Fig. 4. 36. Distribution of P_1 and P_2 values for different input and output voltage levels

4.2.3.4 Design of optimal look-up tables dedicated for a PV multi-phase converter like the MPAC

The determination of the P_n values computationally asks for complex model and equations systems. This way, the look up table allows, with only a previous characterization task, to determine and adapts the number of working phase in more precise way.

Once, P_n values have been determined, a table with these values can be defined. From this table, the principle proposed consists on an introduction of a look-up table into the adaptation algorithm to dynamically change the points P_n depending on the input voltage, the output voltage and the temperature.

A tri-dimensional look up table is proposed here. The three variables are the input voltage, the output voltage and the temperature. Fig. 4. 37. shows the principle of the used table. Experimental test must be made to determine each of the values.

In three phase converter, two tables will be needed, one for the P_1 and another to the P_2 values. For each additional converter connected in parallel, another table is needed.

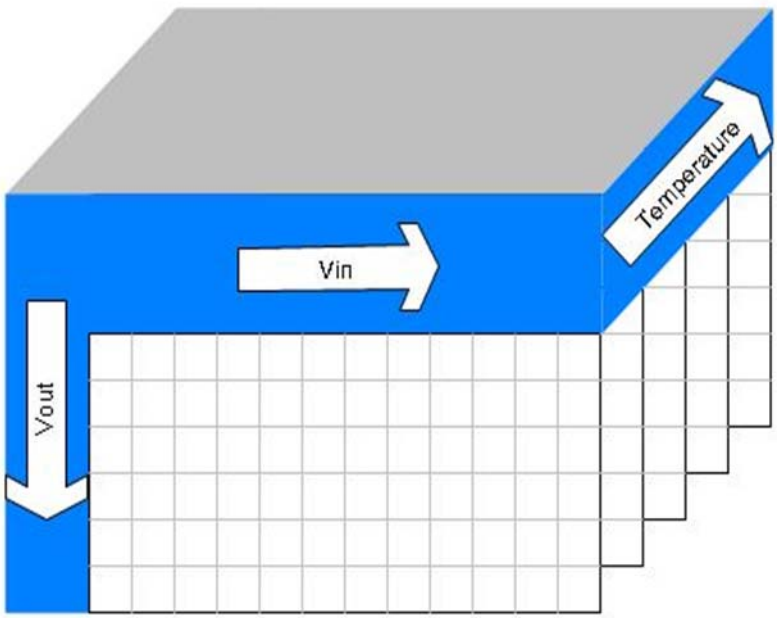

Fig. 4. 37. The structure of the Look-up table used for the MPAC takes into account three variables: input voltage, output voltage and temperature.

Simulations done by Matlab and PSIM have been performed in order to demonstrate the feasibility of this kind of control. The power stage is carried out in PSIM (fig. 4. 38.), the control stage in Matlab (fig. 4. 39.) and the library named Simcoupler is used as interface between both programs for co-simulation. The state variables for this simulation are the input and output voltages, the input current and the output of MPPT (Maximum Power Point Tracking) control block based on a P&O (Perturb&Observe) algorithm. The different values of P_1 and P_2 are stored in the look-up table. This table defines the instantaneous values for P_1 and P_2 for different input/output voltage values. The primary function defines which converters have to be enabled. A counter is used to record the operating time of the

converters and a control algorithm ensures homogeneous aging of each phase to increase the global life-time of the power system.

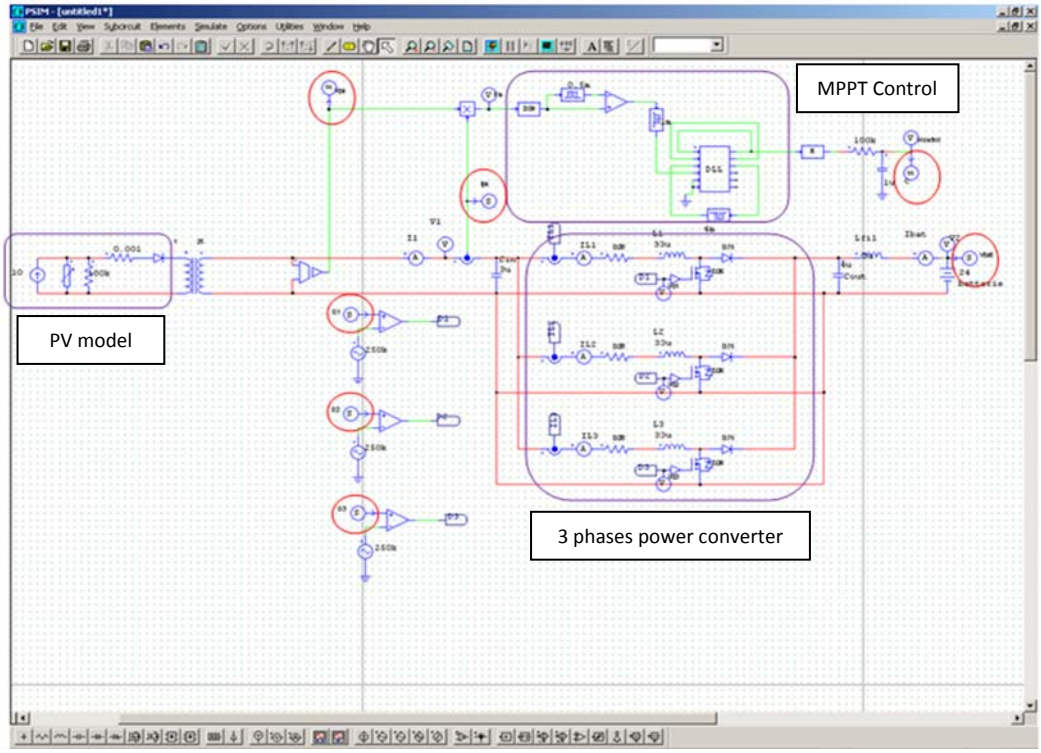

Fig. 4. 38. Schema of the simulated power of the power part in PSIM

Fig. 4. 39. Schema of the MPAC using a look-up table as shown in fig. 4. 37

The simulation results in fig. 4. 40. are performed with the following parameters: V_{bat}=24V, L=47µH, R_L=8Ω, C_{in}=25µF and C_{out}=4uF. We can observe the behaviour of the system for an input power and input voltage variation. A change in input voltage implies a modification of the crossing points P_1 and P_2. The variations of these values are not updated until they are stabilized. Two cases are presented. In the first part of the simulation, the PV

module power value is more important to P_2 level. In the second one, after a reduction of the input voltage, the input power is between the P_1 and P_2 levels.

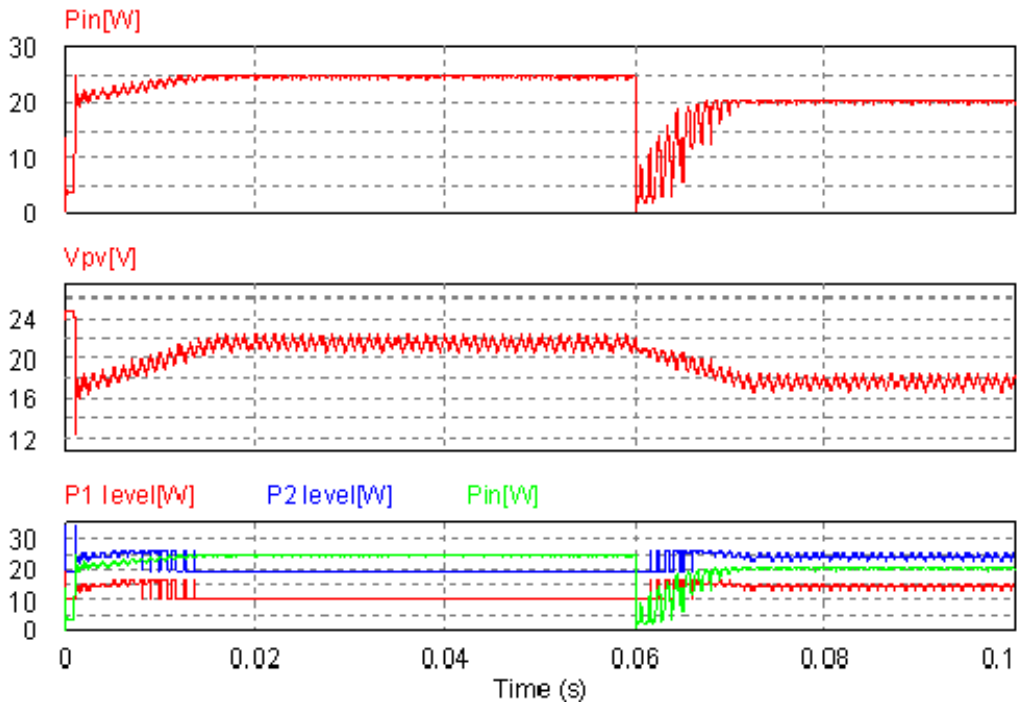

Fig. 4. 40. Simulation results of the adaptive control for multi-phase converter based on look-up tables.

4.2.3.5 Experimental results done with a tri-phase boost MPAC

Experimental tests have been performed to verify the feasibility and the improvement on the efficiency of the new method of control. First, a characterization off the system was needed to determine different P_1 and P_2 values for different input voltages. Fig. 4. 41. shows some experimental results test where the variations of the P_1 and P_2 points according to the input voltage are seen. The results are summarized in table 4.4.

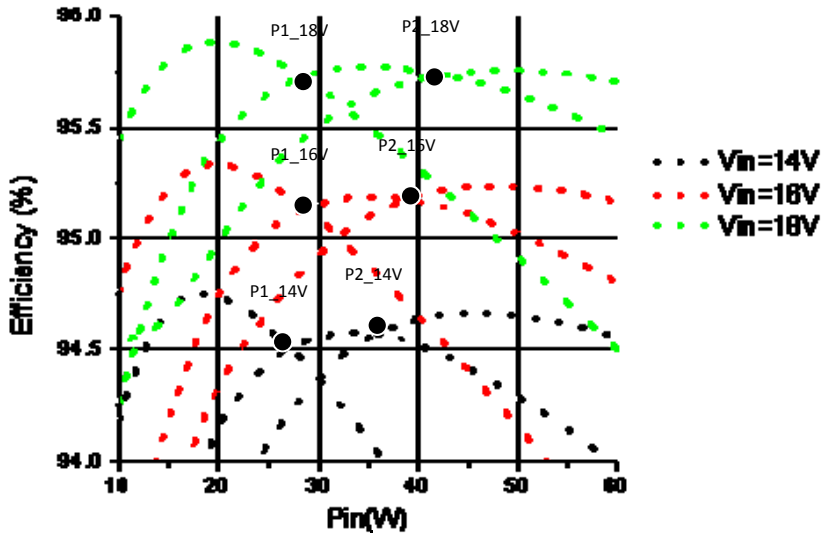

Fig. 4. 41. P1 and P2 variation according to the input voltage

Table 4.4. P1 and P2 turning points variations Vs. VIN

Input Voltage V_{IN}	14V	16V	18V
P_1 [W]	27	28.5	28
P_2 [W]	37	41	44

Fig. 4. 42. shows a comparison between efficiencies for the two different control schemes. Two efficiency tests have been carried out under same operating conditions (V_{IN}=14V and V_{OUT}=24V). With the first test (blue), the number of operating phases has been adapted in a fixed and predisposed way that corresponds to average working conditions (V_{IN}=16V and V_{OUT}=24V). In the second test (red), the number of operating phases has been adapted in the adaptive way, using the look-up table to dynamically compute the values of P_1 and P_2 corresponding to the actual working conditions.

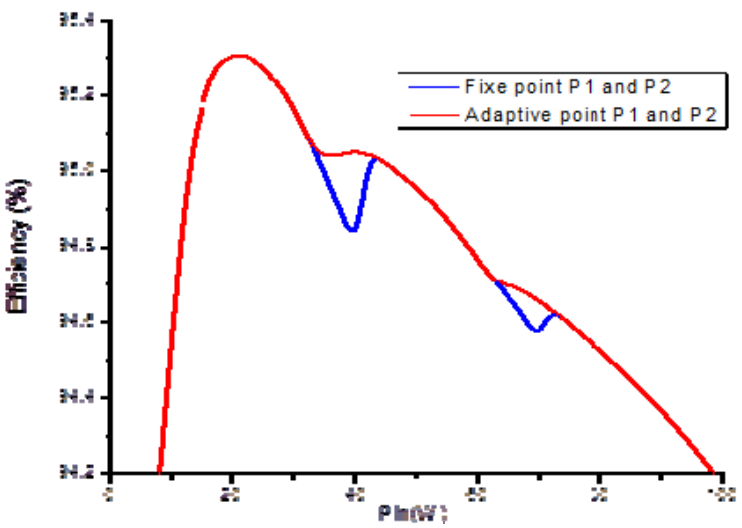

Fig. 4. 42. Comparison between a fix and adaptive crossing points algorithms

Efficiency obtained by adapting P_1 and P_2 values with the look-up table is always above the efficiency of the converter with fixed turning points. The difference between both efficiencies is up to 0.5%. Although this difference is not very high, it must be taken into account that every working conditions causing changes in the efficiency, lead to an efficiency decrease when fixed adaptation mode is used. The use of a look-up table allows a global improvement of the conversion efficiency with an easily implementable control law. In addition, this implementation has been tested in a low power photovoltaic system (85W_P). The gain obtained for a high power structure would be even better as the differences in efficiency will be more important.

The adaptation of P_n values is taken into account in the patent about the MPAC [5] whatever the origin of influence in the parameter affecting in their value. The use of the look-up table for their adaptation is a simplified example of its application. Thus, other innovations are still possible to become the algorithm implementable in a micro-controller or in a FPGA.

4.3 Advanced control strategies

As we have already indicated, the efficiency is an important issue in photovoltaic applications, but it is not the only important matter to take into account. In effect, the reliability, maintainability and life-time of the system are also issues to consider seriously. The PV modules are normally guarantee for 20 years or more. This is not the case of PV applied power electronics. The average lifetime of power system is lower, and therefore the electronic system must be repaired or changed to guarantee a correct exploitation of the PVG. This way, it is important to focus also in the lifetime and maintainability when power converter is designed.

4.3.1 Meteorological effects

One of the constraint that must continuously follow a photovoltaic system is the sudden changes in working condition, above all, linked to the change in the solar irradiation and therefore in PVG power production. In effect, the sudden shadows and clouds involve an rapid variation in energy production. The fig. 4. 43 shows an example of one of this kind of days. Thus, these perturbed days involve a constant adaptation of number of phases. These numerous and fast change shall have a negative impact in the life-time and reliability of electronics components of the power converter.

An anticipation algorithm has been proposed to avoid this kind of changes [6]. It was an important contribution of the join work done by Total and the LAAS. Its goal resides in reducing maximally the thermal and electrical stress of active components in unexpected power variations. The idea of the algorithm is simple : when a sudden decreasing power variation is happen, the algorithm will wait and will not change the number of working phases. If the power is stabilised after defined *t* duration time, the number of active phases will be changed. In contrary, if the power is suddenly increased, the system will follow working with the same number of converters. The fig. 4. 43.b and c shows the principle of this algorithm. The waiting time value must be defined by analysing the temperature change caused in the power converter by sudden power changes.

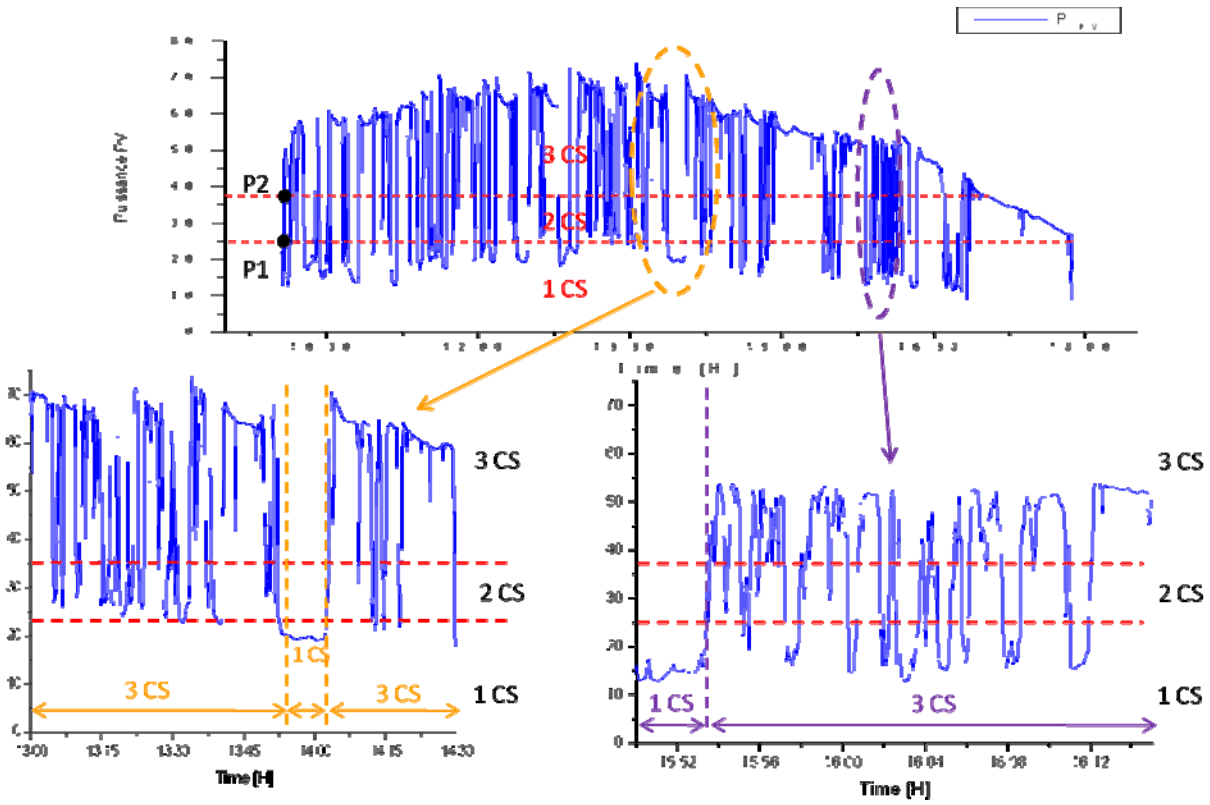

Fig. 4. 43. Evolution of photovoltaic power production in a perturbed working day (a) and the principle of working of the anticipation algorithm (b and c).

One of the drawbacks of the proposed anticipation algorithm is the degradation in power transfer efficiency. In effect, the adaptation of phases is not made in the most optimum way if the system works with more active phases than the PV power generations asks.

In addition, it is difficult to determine how many time must be waiting until the system is stable. Indeed, the clouds size can be enormously variable and there are not studies about their size. This way, it is not assured that the algorithm is useful all the time, as the system can support a variation just in the moment that the system consider itself stable and just make the change of number of phases.

4.3.2 Converter redundancy and over-sizing

The redundancy is the effect of duplicate the critical components of functions of a system with the intention of increasing reliability of the system or the life-time. It is a widely used technique in many safety-critical systems, such as fly-by-wire and hydraulic systems in aircrafts or in not easily or impossible accessing and long life-time asking systems, such aerospace ones.

In redundant system, an error in one component or function may be out-voted by the redundant one. This way, all the redundant component must fail before the entire system fails. This is traduced by bigger reliability and longer life-time to the system.

Photovoltaic systems are sensed to be long life-time product. Indeed, the PV modules are guarantee to life 20 years. Nevertheless, it is not the case of electronic devices as power

converters linked to these PV installations. The normal and affordable electronics do not resist as long as the PV generators. Military and aerospace products could resist the constraint to which they are exposed. However, the cost of PV installation will not be affordable to normal user.

Redundant systems give the possibility of increasing life-time. The MPAC offers an ideal occasion to apply this redundancy. In effect, the MPAC is already composed by paralleled converter. Over-sizing each of the phases in the way that each of them support the maximal power produced by the PV power, the redundancy is guarantee. This way, the life-time of the system is considerably increased, as the all the phase must be fails before the entire system stop working and producing energy. Moreover, a higher efficiency is assured with an MPAC. Thus, although the initial investment is higher, the higher efficiency and longer life-time of the system assures a bigger energy transfer to the user.

In this way, each phase of the converter is designed to support the total power of the photovoltaic source, guaranteeing the operating of our system, even if one of the converters is in default.

The control laws of the system take into the account this effect by the integration of security function which controls the state of each phase. This security task is included just before the activation of phases. In case of one of the phases is considered faulty, it is automatically disconnected, and alarm signal is send to the user.

The state of the phases is checked by looking the current though each phase. The presence of current through each phase is looked. If it is agree with the theoretical state or the order of the control system, the phase is considered ok. If it is not agreed, the phase is considered faulty, it is automatically disconnected and its priority is set to null. Then, it is not taken into account for the rotation and the rotation is carried out with the other phases that work correctly.

The system is deliberately designed with changeable phases. Indeed, each phase is an individual part of the system which can take off and put in by the user in an easy way. This way, when an alarm is set off because of a faulty phase the user has two options:

- Replace the faulty phase: after the replacement, the system will follow working correctly and with all the functions actives. Nevertheless, while the phase is still faulty, the production and transfer of the energy to the load is not stopped.
- Do not replace the faulty phase: the system will be working without take into account the faulty phase, that is, in a degraded mode. Nevertheless, the system will follow producing and transferring energy to the load until all the phases of the converter fail.

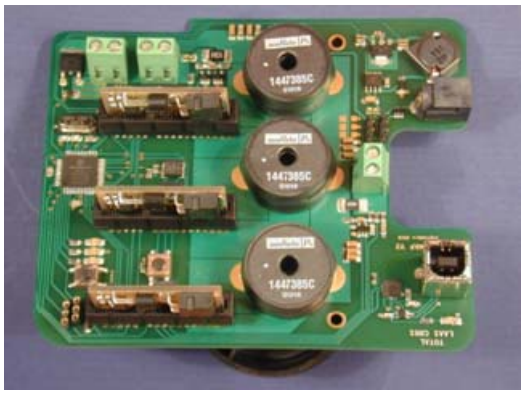

Fig. 4. 44. Experimental prototype of MPAC where each phase is easily changeable in case of failure of one of them

In both cases, the photovoltaic energy conversion is assured for longer time. In the first case, it is not stopped, that it is possible to carry on the same procedure until the damage and production stop of the photovoltaic power generator. In the second case, the life-time of MPAC will be longer than a simple converter, and even if the conversion efficiency is not as high as the beginning of its life, the energy production is assured for more time. Consequently, the benefits of the systems are higher.

4.3.3 Effects of temperature in electronics lifetime

The working temperature of the system has a fundamental importance on the lifetime or reliability of power electronics systems. Some experiences shows that the failure rate will double for every 15-20°C increase during normal temperature [141]. The temperature influence on the reliability can be described as an exponential function.

The variation in the temperature has also lot of importance in the aging of an electronic component. The thermal variations produce mechanical constraints in the semiconductor components, above all, caused by the dilatation coefficient difference of the used materials (fig. 4. 45).

a) b)

Fig. 4. 45. Electronic power device working in a) 25°C and b) 100°C

These constraints can be originated by two principal sources:

- Variable ambient temperature
- Variation in working charges, for instance, variation in PV power production.

Fig. 4. 46. shows the influence of many thermal cycles in an electrical contact. It supports mechanical constraint that makes reveal micro-fissures, which can even arrive to break down the component.

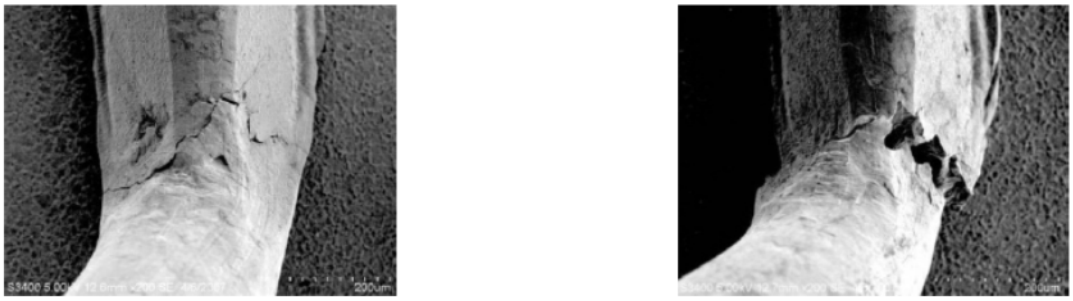

Fig. 4. 46. Micro-fissures in a wire bonding after N thermal cycles.

It is important to keep the working temperature and temperature variation of the system as low and small as possible. Any improvement on these variables can be traduced in reliability and life-time increasing, which is an important issue in PV applied power electronics as they life-time prediction is still much lower than PV module ones.

4.3.4 Experimental tests: temperature profiles

With the intention of verify the improvement in the working temperature, thermal measures have been carried out. For that, a FLIR thermal camera [142] has been used. Different input power profiles have been simulated by the PV simulator. For each test, the temperature of the electronic device has been recorder. From this recording the temperature of the components can be extract.

One phase converter and three phases MPAC have been used to the comparison. The temperature of the area of each diode has been utilised to the temperature comparison.

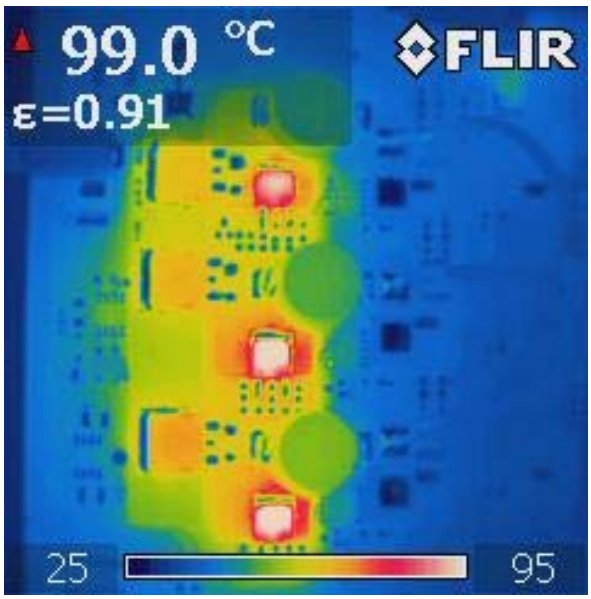

Fig. 4. 47. Image of power converter by thermal camera where the temperatures has been measured

The first test simulates a sunny day four hours. In the fig. 4. 48., the applied input power and the mean media of each of the diodes is shown. The difference in temperature of both structures is obvious. In effect, the one phase structure achieves temperatures over 80°C. In contrary, the three phases structure reaches only 55°C. The difference between two structures is about 25°C.

The total difference in temperature of the minimum and maximum value of one phase structure is about 50°C during the day. For the three phase structure, each of the diodes support an difference in temperature of about 30°C during the day. Taking in consideration that one of the most constraints in the life-time on electronics components is the thermal stress, this diminution in working condition temperature is a big improvement for its life-time prediction.

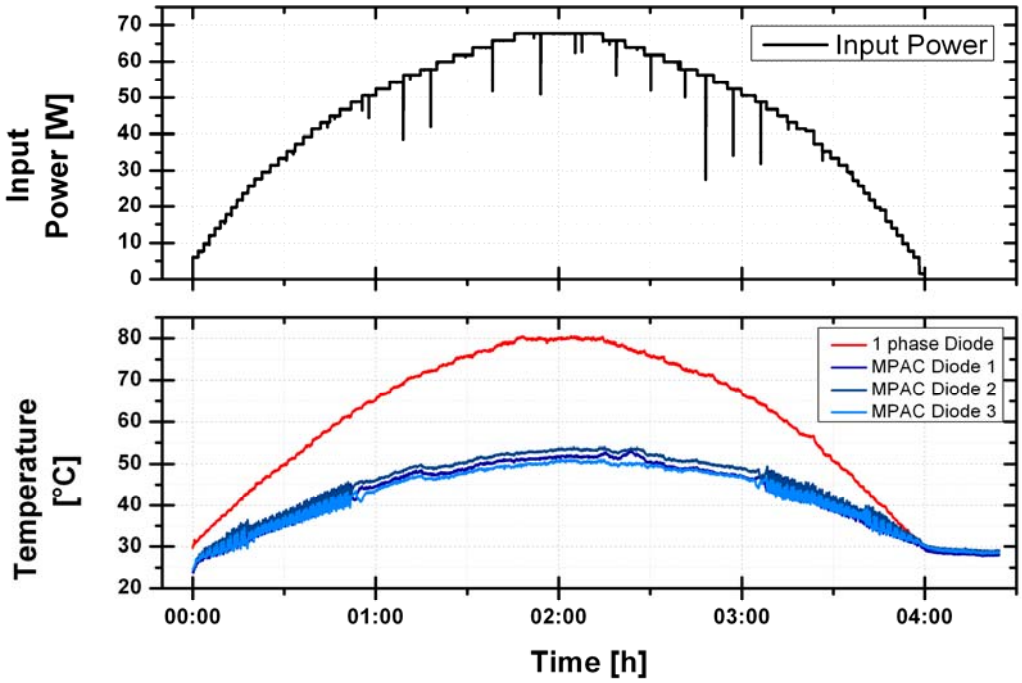

Fig. 4. 48. Temperature comparison between the diodes of one phase structure and three phase structure for a simulated sunny day.

In a second test, a perturbed sunny day is simulated, that is, some drastic clouds or shadows has been included in sunny day (fig. 4. 49.). The input power changes involved temperature changes in power device components. The maximum temperatures are similar to which the first sunny day simulation test has reach for both of the structures. Nevertheless, the sudden power changes involve different temperature changes in both structures. A simulated shadow, corresponding to 30W decreasing change (from 55W to 25W) in input power level, involves 20°C decrease (from 60 to 40°C) in one phase converter structure. However, the temperature change for three phase structure is about 10°C (from 40 to 30°C) which is the half comparing to the first structure.

The same conclusion can be obtained analyzing the other power changes. The changes in temperature are more important for the one phase structure than the three phases MPAC. This way, the effect of big clouds is considerably more important and dangerous for the one phase structure. Indeed, for each big shadow or voltage drop, the system supports a big changes in temperature, which reduces considerably its life-time prediction.

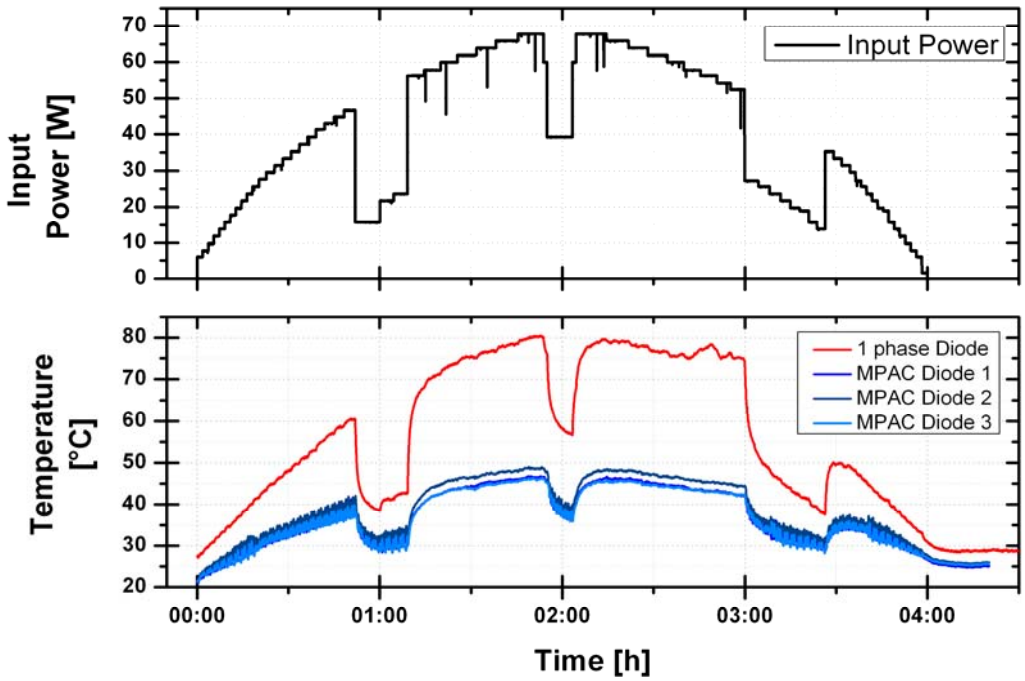

Fig. 4. 49. Temperature comparison between the diodes of one phase structure and three phase structure for a simulated sunny day with sudden clouds or shadows.

A third profile has been tested. This profile is characterized by sudden change in solar irradiation in the morning and a reduced irradiation conditions in the afternoon. During the morning, sudden irradiation changes has been simulated, which involved power change from 10 to 45W. This is translated in temperature changes in the power structure. This temperature changes varies between 5°C to 25°C in one phase structure. Nevertheless, the temperature variations in three phases MPAC are lower, taking values from 5°C to 10°C. As in the precedent cases, the temperature variation are softer in the case of the MPAC, which benefits for its life-time prediction.

During the afternoon, when the solar irradiation, and therefore, the PV power production is lower, the difference in temperature is not as evident as in sunny conditions moments. Nevertheless, the temperature of the diode of 1 phase converter is all the time higher than the diodes of the MPAC structure.

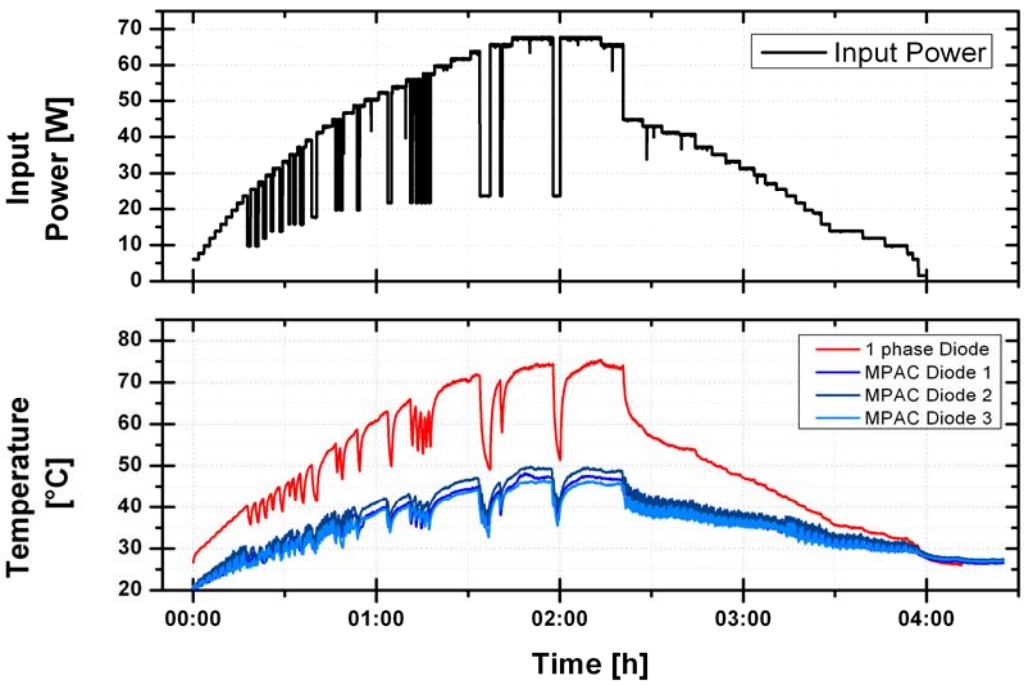

Fig. 4. 50. Temperature comparison between the diodes of one phase structure and three phase structure for a simulated day.

4.4 Conclusion

A new structure based in paralleled converters dedicated to photovoltaic systems has been presented in this chapter named MPAC. This new structure improves globally the efficiency and life-time of the power conversion structure by its optimal structure associated to the use of specific control algorithms. Firstly, the interleaving current method has been studied to improve the efficiency but face to major difficulties to design correspondent SC this type of algorithm did not be used in our system. New and important studies must be done to evaluate the real potential of them. Secondly, the MPAC has been presented. The main function of this structure is to adapt the number of active phases to optimize the energy conversion efficiency. In addition, it carries out the rotation of phases in order to guarantee homogeneous aging of converters, to decrease the thermal stress of components and to improve the life-time prediction. Experimental prototypes allowed demonstrating the important benefits of these structures in different working conditions. Examples of improvements in efficiency and thermal stress had been exposed in this chapter by means of experimental tests.

Although, the electronic devices must be carefully designed to avoid additional cost, too big size or contra-performances, this work has demonstrated the influence of control algorithms to improve not only the efficiency but also the temperature and stress of components. Easily implementable control laws were designed, answering our first goal to improve conversion efficiency, adapting the conversion to specific characteristics of photovoltaic sources and presenting new optimized prototypes. This part can be today included in several existing inverters without a lot of technical problems. For Total, it can be the major result of this global work.

Since almost all the power converter are designed with the same components but in different quantity and placement, this work is thought to be extensible to other power conversion structures. For this reason, for future works, a deeper study in losses must be envisaged. The adaptation of algorithms to other different structures can be easily done based on results obtained in this work either of DC-DC type structures or DC-AC ones for grid connection systems.

CHAPTER 5

5 CONCLUSION AND FUTURE WORKS

CONCLUSION AND FUTURE WORK

The main work of this thesis was focused in the optimisation of electric energy conversion of photovoltaic systems. Nowadays, the photovoltaic energy is becoming a popular energy source, induced by more and more demanded either in domestic installations or big photovoltaic central camps. Nevertheless, the photovoltaic installations still present many drawbacks in terms of efficiency, life-time and cost.

The chapter 2 presents the main elements of photovoltaic installations and their characteristics. A special emphasis is made in performance evaluations modes. The efficiency of the elements of PV systems is not easy to define and measure. Some new normative efficiencies are proposed like the European one. Face of the importance of the efficiency of power converters and its need to present high efficiency levels in a large range of working conditions due to the changeable characteristic of photovoltaic power sources, it is important to have the same reference to have a good comparison of performances.

The third chapter introduces the state of art of different types and structures of on-grid PV installations, with a special focus in topologies with DC optimizers. These structures consist of DC-DC power converters linked to one PV module. They are in charge of extracting the maximum power from the PVG and transfer it to the load or the inverter in the most efficiency way. They are becoming the substitute of classical diode protections, as they make possible the failure detection, and in addition, they can optimize the PV energy extraction. We propose in this part a comparative study to help the future designer the choice of the more adapted static converter for his applications.

The main work of this thesis has been focused in the improvement of a photovoltaic power conversion structure in terms of efficiency and life-time with some new solutions proposed in the chapter four. Paralleled power converters structure has been used in this goal, using redundancy properties and improving also the robustness. The base of this work has been a power converter loss and efficiency analysis. Beginning from this analysis, the power conversion structure must be adapted to special conditions of PV systems, above all, to the power production variability linked to irradiation changes. However, in addition to be efficient, this structure must have long life-time prediction in order to approach to PV sensors life-time that is guarantee for more than 20 years.

In all the analysis, prototype and experiences carried out in this work, boost DC-DC converters has been used. With this type of structure, we can globally improve its efficiency but also connect PV array to inverters through this structure with a large different range of voltage. The structure is thought to be connected to one PV module and make the function of DC optimizers.

The main improvements have been carried out by means of advanced control laws. Different control has been implemented which has allowed the optimisation of efficiency and life-time duration of the structure. Firstly, the efficiency improvement has been carried out by means of the interleaving control method. Nevertheless, this technique only improves the structure for high input power conditions.

Secondly, the multi-phase adaptive converter has been presented. This structure improves the efficiency in all the power range by adapting the number of working phase depending on the input power level of the PVG which can change at each moment. Using

this control, the transfer to the load can be improved in 2.9%, as outdoor test during 5 days has been showed. In addition, phase rotation function has been integrated to limit stress in active components and then improve life time of each elementary SC. The rotation of phases allows the homogeneous aging of all the phase but also a lower working temperature and smaller temperature variation during the day, either in sunny or cloudy and perturbed days. This improvement has been showed by temperature profiles, measured by thermal cameras. This work has allowed the publication of several articles [143]-[145] but also the publication of two patents [5]-[6] within the parts more innovative of algorithms.

Finally, an easy adaptation of the MPAC has been presented by integrating Look-up tables to optimize the phase adaptation. By means of these tables, the adaptation points can be modified depending in the external conditions that support the power converter such as the PV voltage level, the output voltage lever and the temperature.

Nevertheless, the end of this work also shows some perspective and ideas for the progression in future work. They are some of them proposed in the following lines:

Firstly, the efficiency improvement by means of interleaving power paralleled converters has been carried out. As it does not reach high efficiencies in low power, and for photovoltaic systems all power ranges are important, the multi-phase adaptive converter has been presented. Both ideas could be integrated in the same structure in future works: the adaptation of phases depending on the power level, but also the introduction of interleaving to improve efficiency or reduce filter elements. The difficulty of this technique is linked to the adaptation of frequencies and phase differences to carry out the interleaving method in a correct way. In effect, the interleaving method asks for phase difference of 360°/n, corresponding *n* to the number of active phases. In the same way, the adaptation of frequency must be made to keep the same filtration level and the output and input ports do not notice any changes in oscillations frequencies. The stability of the system must be analyzed before its integration but also its real realisation with by-pass draw-back of losses in passives elements.

The improvement of the life-time of power converters must become a priority in the future. That has been done by reducing the electric and thermal stress of components by including the rotation algorithm. Indeed, the rotation of phases guarantees a homogeneous aging off all the phase. This works reach the reduction of the working temperature and the temperature variations that are the main factors of component stress. The reliability of the system will increased, and therefore, it will present higher life-time prediction if temperature and globally transfer power are more optimised through the different SC. However, it is important to improve our knowledge on behaviour of SC and their intrinsic losses. A more precise loss model will be a real progress in new optimised algorithms. Actually, our loss model does not take into account the temperature effect and it could be really improved by integrating this aspect. In effect, the temperature affects in the internal characteristic of many electronic components. Moreover, some other losses lied to the circuitry, wire losses or power layout losses are not taken into considerations. A continuation of this study must envisage a more complex and exact model of power converter losses. This analysis would also help to automate the adaptation of P_n values depending in working conditions. Depending in the complexity of this result and it equations, a choice between and predetermined look-up table with P_n values or the utilization of these equations can be done.

The mains electronic elements of power conversion structures do not change from Boost DC-DC converters. Diodes, MOSFET or IGBT switches and passive storage elements as the capacitors and inductances are present in all converters although they are in different proportion and quantities and connected in a different way. For this reason, the effect of the losses in efficiencies for different numbers of phases are thought to be similar to the boost converter paralleled systems. Thus, the works presented in this thesis can be extended and generalised either to other DC-DC structures or DC-AC inverters and even on globally to all power applications and sources. For instance, this function could be integrated in the inverters that are already used in nowadays photovoltaic installation. A little extra investment in control systems and extra material could allow an optimization of power conversion efficiency and life-time of the installations. Nevertheless, a real analysis and study adapted to inverters must be done to guarantee that fact.

Finally, looking the industrial context of this thesis, since it has been carried out in contractual collaboration between Total S.A. and the laboratory LAAS-CNRS, a future integration of this work in industrial prototype must be envisaged. Nevertheless, before a possible integration of the system in an industrial prototype and its commercialization, a socio-economical study is pending. In fact, even if this new structure improves the efficiency and life time of the converter, it needs a higher initial investment. This way, before its commercialization, the final economical advantage must be calculated, not only measuring the real life-time prediction and total gain in transferred energy, but also, analyzing consumer habitudes and if whatever they are ready to replace the faulty converter or they wait for total breakdown. We hope this work can be connected to other works carried out by Total. In fact, in the same contractual context of the collaboration between LAAS and Total, other works are accomplishing. It is the case of the photovoltaic reconfigurable architecture in which these structures could be integrated to achieve more competitive PV products in the future.

6 REFERENCES:

[1] “UNFCCC and the Kyoto Protocol” United Nations, 1998 ; Available in : www.un.org.

[2] www.rggi.org

[3] www.pv-magazine.com, 28 January 2013.

[4] "La production d'électricité d'origine renouvelable dans le monde" ; Observ’ER ; Available in : www.energies-renouvelables.org;

[5] C.Alonso, A.Berasategi, C.Cabal, B.Estibals, S.Petibon and M.Vermeersch. "System for the Electronic management of photovoltaic cells as a function of meteorology”. French patent WO 2010055757, 16 June 2011

[6] C.Alonso, A.Berasategi, C.Cabal, B.Estibals, S.Petibon and M.Vermeersch. "System for the Electronic management of photovoltaic cells with adapted thresholds”. French patent WO 2010055756, 16 June 2011

[7] F. Lasnier, T. G. Ang, “Photovoltaic Engineering Handbook”; IOP Publishing Ltd. 1990; ISBN 0-85274-311-4.

[8] D. M. Chapin, C. S. Fuller, and G. L. Pearson. "A New Silicon p-n Junction Photocell for Converting Solar Radiation into Electrical Power". Journal of Applied Physics; Vol.25; pp.676–677; May 1954.

[9] "The History of Solar," U.S. Department of Energy, 2004.

[10] K.W. Mitchell, K. J. Touryan; “Amorphous Silicon Alloys for Solar Cells”; Annual Review of Energy, vol. 10, pp. 1-34; Nov. 1985

[11] T. Couture, Y. Gagnon; “An analysis of feed-in tariff remuneration models: Implications for renewable energy investment”; Energy Policy, vol. 38, issue.2, pp. 955-965; 2010.

[12] A. Luque, S. Hegedus.; “Handbook of Photovoltaic Science and Engineering”; 2nd ed., ISBN 978-0-470-72169-8; John Wiley and Sons Ltd. 2001.

[13] www.photowatt.com

[14] www.nrel.gov

[15] J. Zhao, A. Wang, M.A. Green; “24.5% Efficiency Silicon PERT Cells on MCZ substrates and 24.7% Efficiency PERL Cells on FZ Substrates”; Prg. In Photovoltaic: Research and Apllications; Vol. 7, pp. 471-474; 2009.

[16] www.sunpowercorp.com

[17] Fan Jiang; Wong, A., "Study on the performance of different types of PV modules in Singapore," 7th International Power Engineering Conference, 2005. IPEC 2005, pp. 104-109. Nov. 2005.

[18] www.mitsubishielectric.com

[19] A. Hinsch, J.M. Kroon, R. Kern, I. Uhlendorf, J. Holwbock, A. Meyer, J. Ferber. "Long-term Stability of Dye-Sensitised Solar Cells"; Progress in Photovoltaics: Research and Applications, vol. 9, pp. 425-438. 2001.

[20] M. Nikolaeva-Dimitrova, R.P. Kenny, E.D. Dunlop; "Long Term Stability of a-SI: H thin film modules"; 21st European Photovoltaic Solar Energy Conference, Sept. 2006.

[21] S. Hegedus; "Thin Film Solar Modules: The Low Cost, High Thoughput and Versatile Alternative to Si Wafers"; Progress in Photovoltaics: Research and Applications, vol. 14, pp. 393-411. 2006.

[22] N. Rome, A. Bosio, A. Romeo; "An innovative process suitable to produce high-efficiency CdTe/CdS thin-film modules", Solar Energy Materials and Sola Cells, vol. 94, issue 1, pp. 2-7. Jan. 2010.

[23] K. L. Chopra, P. D. Paulson, V. Dutta; "Thin-film solar cells: an overview"; Prg. In Photovoltaic: Rechearc and Apllications; Vol. 12, Issue. 2-3, pp. 69-92, 2004.

[24] H. Fritzsche; "Amorphous and Heterogeneous Silicon Thin Films"; Collins R W, et al (eds); Materials Research Society, Symposium Proceeding Vol. 609, p. A17.1 Warrendale. 2001.

[25] M. Bär, I. Repins, M. A. Contreras, L. Weinhardt, R. Noufi, and C. Heske; "Chemical and electronic surface structure of 20%-efficient Cu(In,Ga)Se_2 thin film solar cell absorbers"; Applied Physics Letters, 2009; Vol. 95.

[26] Y. Tanaka, N. Akema, T. Morishita, D. Okumura, K. Kushiya; "Improvement of Voc upward of 600mV/cell with CIGS-based absorber prepared by Selenization/Sulfurization"; Proc. of 17th EC Photovoltaic Solar Energy Conference, Munich, October 2001; pp. 989–994.

[27] R.D. Wieting; "CIS product introduction: Progress and challenges"; American Institute of Physics Conference Proc. 1999; March 1999; Vol. 642; pp 3-8.

[28] C. Brabec, V. Dyakonov, U. Schert U, "Organic Photovoltaics: Materials, Device Physics, and Manufacturing Technologies", ed. Wiley-Vch, 2008, ISBN 3-52731-675-2

[29] S. Sun, L. Dalton, "Introduction to Organic electronic and Optoelectronic Materials and Devices", ed. CRC Press/Taylor Francis, 2008, ISBN 0-84839-284-5.

[30] T.A. Skothein , J.R. Reynolds, "Handbook of Conducting Polymers", 3rd edn, ed. CRC Ress: Boca Raton, 2007, ISBN 1-57444-665-7.

[31] D. Forbes, S. Hubbard, "State-of-the-art, triple-junction, quantum-dot-enhanced photovoltaic devices exhibit increased output current and increased efficiency", International Society for Optics and Photonics, SPIE Newsroom, 26 July 2010.

[32] M.A. Green, K. Emery, Y. Hishikawa, W. Warta. "Solar cell efficiency tables (Version 36); Prg. In Photovoltaic: Research and Applications; Vol. 18, pp. 346-352; 2010.

[33] www.photovoltaique.info

[34] T. Esram, P.L. Chapman, "Comparion of Photovoltaic Array Maximum Power Point Tracking Techniques"; IEEE transactions on Energy Conversion, vol. 22, issue: 2, pp. 439-449; June 2007.

[35] P. Assis Sobreira, M.Gradella Villalva, P.Gomes Barbosa, H.A. Carvalho, J.R. Gazoli, E. Ruppert, A.A. Ferreira; "Comparative analysis of current and maximum voltage-controlled

photovoltaic Maximum Power Point tracking"; Power Electronics Conference, COBEP, Brazil, 2011.

[36] C.T. Pan, J.Y. Chen, C.P. Chu , T.S. Huand; "A fast maximum power point tracker for photovoltaic power systems"; in 25th Annual Conf. of the IEEE ind. Electron. Society, 1999, pp. 390-393.

[37] M. Bodur, M. Ermis; "Maximum power point tracking for low power photovoltaic solar panels"; in Proc. 7th Mediterranean Electrotechnical Conf., 1994, pp. 758–761.

[38] A. Hussein, K. Hirasawa, J. Hu, J. Murata,; "The dynamic performance of photovoltaic supplied dc motor fed from DC-DC converter and controlled by neural networks"; Porc. 2002 international Joint Conf on Neural Networks, 2002; pp. 607-612.

[39] L. Zhang, Y. Bai, A. Al-Amoudi, "GA-RBF neural network based maximum power point tracking for grid-connected photovoltaic systems"; International Conf. on Power Electronics, Machines and Drives, 2002; pp. 822-826.

[40] A. Bouabana, A. Al-Diab,C. C. Sourkounis; "Influence of a high precision current sensor for improving the efficiency of PV power systems"; Compatibility and Power Electronics (CPE), 2011 7th International Conference-Workshop; pp. 196-201. June 2011.

[41] A. F. Boehringer, "Self-adapting dc converter for solar spacecraft power supply," IEEE Trans. Aerosp. Electron. Syst., vol. AES-4, no. 1, pp. 102–111, Jan. 1968.

[42] T.-Y. Kim, H.-G. Ahn, S. K. Park, and Y.-K. Lee, "A novel maximum power point tracking control for photovoltaic power system under rapidly changing solar radiation," in IEEE Int. Symp. Ind. Electron., 2001, pp. 1011–1014.

[43] K.Kobayashi, I. Takano, andY. Sawada, "A study on a two stage maximum power point tracking control of a photovoltaic system under partially shaded insolation conditions," in IEEE Power Eng. Soc. Gen.Meet., 2003, pp. 2612–2617.

[44] W. J. A. Teulings, J. C. Marpinard, A. Capel, and D. O'Sullivan, "A new maximum power point tracking system," in Proc. 24th Annu. IEEE Power Electron. Spec. Conf., 1993, pp. 833–838.

[45] A. Safari, S. Mekhilef; "Simulation and Hardware Implementation of Incremental Conductance MPPT With Direct Control Method Using Cuk Converter"; Industrial Electronics, IEEE Transactions on; vol: 58 , Issue: 4; 2011.

[46] O. Hashimoto, T. Shimizu, and G. Kimura, "A novel high performance utility interactive photovoltaic inverter system," in Conf. Record 2000 IEEE Ind. Applicat. Conf., 2000, pp. 2255–2260.

[47] E. Koutroulis, K. Kalaitzakis, and N. C. Voulgaris, "Development of a microcontroller-based, photovoltaic maximum power point tracking control system," IEEE Trans. Power Electron., vol. 16, no. 21, pp. 46–54, Jan. 2001.

[48] W. Xiao, W. G. Dunford, "A modified adaptive hill climbing MPPT method for photovoltaic power systems," in Proc. 35th Annual IEEE Power Electron. Spec. Conf., 2004, pp. 1957–1963.

[49] N. Femia, G. Petrone, G. Spagnuolo, M. Vitelli; "Optimization of Perturb and Observe Maximum Power Point Tracking Method"; IEEE transactions on Power Electronics, Vol. 20, Issue: 4, pp.: 963-973; 2005.

[50] W. Wu, N. Pongratananukul, Weihong. Qiu, K. Rustom, T. Kasparis, I. Batarseh “DSP-based Multiple Peak Power Tracking for Expandable Power System”; Eighteenth Annual IEEE Applied Power Electronics Conference and Exposition, APEC '03, feb. 2003.

[51] C.C. Hua, J.R. Lin, “Fully digital control of distributed photovoltaic power systems”; in IEEE International Symp. on Ind. Electron., 2001, pp. 1-6.

[52] N. S. D’Souza, L. A. C. Lopez, S. Liu; “An intelligent máximum power point tracker using peak current control”; in 36th Annual IEEE Power Electron. Specialists Conf., 2005, pp. 172-177.

[53] M. Veerachary, T. Senjyu, K. Uezato; “Maximum power point tracking control of IDB converter supplied PV system”; in IEE Proc. Elect. Power Applicat., 2001, pp. 494-502.

[54] N. Kasa, T. Lida, L. Chen, “Flyback Inverter Controlled by Sensorless Current MPPT for Photovoltaic Power System”, IEEE Trans. Ind. Electron., vol.52; pp. 1145-1152, Aug. 2005.

[55] Y.H. Kim, Y.G. Ji, C.Y. Won, T.W. Lee; “Flyback inverter using voltage sensorless MPPT for AC module systems”; International Power Electronics Conference, IPEC, 2010. pp. 948-953.

[56] MA.S. Masoum, H. Dehbonei, E.F. Fuchs; “Theoretical and experimental analyses of photovoltaic systems with voltage and current-based maximum power-point tracking”; IEEE Trans. Energy Conversion, vol.17, pp. 514-522, Dec. 2002.

[57] J. Ahmad, “A fractional open circuit voltage based maximum power point tracker for photovoltaic arrays”; 2nd International Conference on Software Technology and Engineering (ICSTE), 2010.

[58] T. Noguchi, S. togashi, R. Nakamoto; “Short-current pulse based adaptive maximum power point tracking for photovoltaic power generation systems”; in 35th Annual IEEE Power Electron. Specialists Conf., 2002, pp. 1125-1129.

[59] B. M. Wilamowski and X. Li, "Fuzzy system based maximum power point tracking for PV system," in 28th Annual Conf. of the IEEE Ind. Electron. Society, 2002, pp. 3280-3284.

[60] M. Veerachary, T. Senjyu, and K. Uezato, "Neural-network-based maximum-power-point tracking of coupled-inductor interleaved-boostconverter-supplied PV system using fuzzy controller," IEEE Trans. Ind. Electron., vol. 50, pp. 749-758, Aug. 2003.

[61] A. M. A. Mahmoud, H. M. Mashaly, S. A. Kandil, H. El Khashab, and M. N. F. Nashed, "Fuzzy logic implementation for photovoltaic maximum power tracking," in Proc. 9th IEEE International Workshop on Robot and Human Interactive Commun., 2000, pp. 155-160.

[62] N. Patcharaprakiti and S. Premrudeepreechacharn, "Maximum power point tracking using adaptive fuzzy logic control for grid-connected photovoltaic system," in IEEE Power Eng. Society Winter Meeting, 2002, pp. 372-377.

[63] N. Khaehintung, K. Pramotung, B. Tuvirat, and P. Sirisuk, "RISCmicrocontroller built-in fuzzy logic controller of maximum power point tracking for solar-powered light-flasher applications," in 30th Annual Conf. of IEEE Ind. Electron. Society, 2004, pp. 2673-2678.

[64] C.-Y. Won, D.-H. Kim, S.-C. Kim, W.-S. Kim, and H.-S. Kim, "A new maximum power point tracker of photovoltaic arrays using fuzzy controller," in 25th Annual IEEE Power Electron. Specialists Conf., 1994, pp. 396-403.

[65] F. Bordry, “Power converters: definitions, classifications and converter topologies”; CAS - CERN Accelerator School and CLRC Daresbury Laboratory : Specialised CAS Course on Power Converters; pp 13-42; May 2004.

[66] H. Haeberlin, L. Borgne, M. Kaempfre and U.Zwahlen. “New Tests at Grid-Connected PV Inverters: Overview over Test Results and Measured Values of Total Efficiency ηtot.”. 21st European Photovoltaic Solar Energy Conference, Dresden, Germany, Sept. 2006.

[67] www.energy.ca.gov

[68] www.fronius.com

[69] www.sma.de

[70] M. Valentini, A. Raducu, D. Sera, R. Teodorescu; , "PV inverter test setup for European efficiency, static and dynamic MPPT efficiency evaluation," 11th International Conference on Optimization of Electrical and Electronic Equipment, 2008. OPTIM 2008., pp.433-438, 22-24 May 2008

[71] M. Nikolic, H. Zimmermann; "Photovoltaic energy harvesting for hybrid/electric vehicles: Topology comparison and optimisation of a discrete power stage for European Efficiency," 9th International Multi-Conference on Systems, Signals and Devices, SSD 2012, pp.1-7, 20-23 March 2012

[72] L. Zhang; H. Hu; L. Feng; Y. Xing; H. Ge; K. Sun; , "A weighted efficiency enhancement control for modular grid-tied photovoltaic generation system," 37th Annual Conference on IEEE Industrial Electronics Society, IECON 2011, pp.3093-3098, 7-10 Nov. 2011

[73] B. York, W. Yu, J.S. Lai; "An Integrated Boost Resonant Converter for Photovoltaic Applications," Power Electronics, IEEE Transactions on , vol. 28, issue:3, March 2013.

[74] M. Cacciato, A. Consoli, V. Crisafulli; "A high voltage gain DC/DC converter for energy harvesting in single module photovoltaic applications," IEEE International Symposium on Industrial Electronics, ISIE 2010, pp.550-555, 4-7 July 2010.

[75] “Trends in photovoltaic applications: survey report of selected IEA countries between 1992 and 2009”, International energy agency – photovoltaic power systems programme, Report IEA-PVPS, T1-19:2010. Available in: www.iea-pvps.org.

[76] EN 50160, “Voltage characteristics of electricity supplied by public distribution systems, European committee for electro-technical standardization”, CENELEC, 1999.

[77] “Utility aspect of grid connected photovoltaic power systems, International energy agency – Photovoltaic power system programme” International energy agency – photovoltaic power systems programme, Report IEA PVPS, T5-01: 1998. Available in: www.iea-pvps.org.

[78] www.epsma.org

[79] “Evaluation of islanding detection methods for photovoltaic utility-interactive power systems”, International energy agency – photovoltaic power systems programme, Report IEA PVPS T5-09:2002, 2002. Available in: www.iea-pvps.org

[80] F. Bordry, “Power converters: definitions, classifications and converter topologies”; CAS - CERN Accelerator School and CLRC Daresbury Laboratory : Specialised CAS Course on Power Converters; pp 13-42; May 2004.

[81] M. N. Mather, M. Malengret, J.C. Le Claire; "110 W low cost, efficient PV-grid interface for rural electrification," 8th International Conference on Power Electronics and Variable Speed Drives, 2000. No. 475 , pp.136-139, Sept. 2000.

[82] C. Meza, J.J. Negroni, F. Guinjoan, D. Biel; "Inverter Configurations Comparative for Residential PV-Grid Connected Systems," 32nd Annual Conference on IEEE Industrial Electronics, IECON 2006, pp.4361-4366, 6-10 Nov. 2006.

[83] J. Imhoff, J.R. Pinheiro, J.L. Russi, D. Brum, R. Gules, H.L. Hey; "DC-DC converters in a multi-string configuration for stand-alone photovoltaic systems," Power Electronics Specialists Conference, PESC 2008, pp.2806-2812, 15-19 June 2008.

[84] A.M. Pavan, S. Castellan, S. Quaia, S. Roitti, G. Sulligoi; "Power Electronic Conditioning Systems for Industrial Photovoltaic Fields: Centralized or String Inverters?," International Conference on Clean Electrical Power, 2007. ICCEP '07, pp.208-214, 21-23 May 2007.

[85] G. Sheppard; “Energy Efficiency Technology to Take Solar Market by Storm”, February, 2011. Available in: www.isuppli.com

[86] G. Sheppard; “Where Moore’s Law Impacts the Solar Market”, November, 2010.Available in: www.isuppli.com

[87] L.E. Weldemariam, P. Bauer, E. Raijen, P. Kumar; “Connecting Topologies of Stand alone Hybrid Power Systems”, International Exhibition & Conference for Power Electonics, Intelligent Motion and Power Quality 2011, PCIM Europe 2011. May 2011.

[88] P. Petit, M. Aillerie; “Integration of individual DC/DC converters in renewable energy distributed architectures” 2012 IEEE International Conference on Industrial Technology , ICIT 2013, pp.802,807, 19-21 March 2012.

[89] R.W. Erickson, D. Maksimović; “Fundamentals of Power Electronics” 2nd Edition, ed. Springer, 31 janv. 2001, 883 pages, ISBBN: 0-79237-270-0.

[90] M. Yamadaya, H. Matsuo; “Control Method for Autonomous Changing the Number of DC-Dc Converters to Improve Efficiency.” 31st International Telecommunications Energy Conference, INTELEC 2009, pp. 1-5, 18-22 Oct. 2009.

[91] N. Garcia; “Determining Inductor Power Losses”, Coilcraft, Available in: www.inductors.ru

[92] B.R. Lin and H.H. Lu; “*Single phase three-level PWM rectifier”*. In *Proc. IEEE APEC,* 1999, pp. 63-68.

[93] B.R. Lin, H.H. Lu and Y.L. Hou; “Single-phase power factor correction circuit with three-level boost converter”. in Proceeding of the IEEE International Symposium on Industrial Electronics 1999, ISIE’99, vol. 2, pp. 445-450.

[94] M.T. Zhang, Y. Jiang, F.C. Lee, M.M. Jovanovic; “Single-phase three-level boost power factor correction converter”, 10th Conf. Proc. In Applied Power Electronics Conference and Exposition, APEC 1995, vol. 1, pp. 434-439.

[95] H. Wu and X. He, “Single phase three-level power factor correction circuit with passive lossless snubber”, IEEE trans. Power Electron, vol. 17, n°.6, pp.946-956, Nov. 2002.

[96] T. F.Wu and T. H. Yu; “Unified approach to developing single-stage power converters,” IEEE Trans. Aerospace and Electronic Systems, vol. 34, no. 1, pp. 211– 223, Jan. 1998.

[97] B. R. Lin, J. J. Chen; “Analysis and implementation of a soft switching converter with high-voltage conversion ratio,” Proc. IET-Power Electron., vol. 1, no. 3, pp. 386–394, Sep. 2008.

[98] S. Y. Tseng, S. H. Tseng, and J. G. Huang, “High step-up converter with partial energy processing for livestock stunning applications,” 21st Annual IEEE Applied Power Electronics Conference and Exposition, 2006, pp. 1537–1543, March 2006.

[99] S. Y. Tseng, S. H. Tseng, and J. Z. Shiang; “High step-up converter associated with soft-switching circuit with partial energy processing for livestock stunning applications,” 5th Power Electronics and Motion control conference, IPEMC, 2006, pp. 1–5, Shangai, Aug. 2006.

[100] L.H.S.C. Barreto, E.A.A. Coelho, V.J. Farias, L.C. de Freitas, J.V. Vieira Jr.; “An Optimal Lossles Commutation Quadratic PWM Boost Converter”, 17th Annual IEEE Applied Power Electronics Conference and Exposition, 2002. APEC 2002., vol.2, pp.624-629, 2002.

[101] R. Kadri, J.P. Gaubert, G. Champenois, M. Mostefaï, “Performance Analysis of Transformless Single Switch Quadratic Boost Converter for Grid Connected Photovoltaic Systems”, XIX International Conference on Electrical Machines, ICEM, 2010, pp.1-7, 6-8 Sept. 2010.

[102] R.-J. Way, C.-Y. Lin; "High-efficiency, high-step-up DC-DC convertor for fuel-cell generation system," Electric Power Applications, IEE Proceedings, vol.152, no.5, pp. 1371- 1378, 9 Sept. 2005.

[103] H. C. Shu; “Design and analysis of a switched-capacitor-based step-up dc/dc converter with continuous input current,” IEEE Trans. On Circuits Systems I: Fundamental Theory and Applications, vol. 46, no. 6, pp. 722–730, Jun. 1999.

[104] H. S. Chung, A. Ioinovici, and W. L. Cheung; “Generalized structure of bi-directional switched-capacitor dc/dc converters,” IEEE Trans. Circuits Systems I Fundamental Theory and Applications, vol. 50, no. 6, pp. 743–753, Jun. 2003.

[105] K. K. Law, K. W. Cheng, and Y. P. Yeung; “Design and analysis of switched-capacitor-based step-up resonant converters,” IEEE Trans. Circuits Systems I Fundamental Theory and Applications, vol. 52, no. 5, pp. 1998–2016, May 2005.

[106] F. Z. Peng, F. Zhang, Z. Qian; “A magnetic-less dc–dc converter for dual voltage automotive systems,” IEE Trans. Ind. Appl., vol. 39, no. 2, pp. 511–518, Mar./Apr. 2003.

[107] Bangyin Liu; Shanxu Duan; Tao Cai; "Photovoltaic DC-Building-Module-Based BIPV System—Concept and Design Considerations," IEEE Transactions on Power Electronics, vol.26, no.5, pp.1418-1429, May 2011.

[108] L. Linares, R.W. Erickson, S. MacAlpine, M. Brandemuehl; "Improved Energy Capture in Series String Photovoltaics via Smart Distributed Power Electronics," Twenty-Fourth Annual IEEE Applied Power Electronics Conference and Exposition, 2009. APEC 2009. pp.904-910, 15-19 Feb. 2009.

[109] A. Cid-Pastor, “Conception et réalisation de modules photovoltaïque électronique”, Ph.D. of Institut National des Sciences Appliquées, INSA. Toulouse 2006.

[110] C. Cabal, "Optimisation énergétique de l’étage d’adaptation électronique dédiéà la conversion photovoltaïque", Ph.D. of Université Paul Sabatier, Toulouse 2008.

[111] R. Haroun, A. Cid-Pastor, A. El Aroudi, L. Martinez-Salamero; "Cascade connection of DC-DC switching converters by means of self-oscillating dc-transformers," 15th International Power

Electronics and Motion Control Conference, EPE/PEMC, 2012, pp.DS1b.14-1-DS1b.14-5, 4-6 Sept. 2012

[112] Yeong Jia Cheng; E.K.K. Sng; "A novel communication strategy for decentralized control of paralleled multi-inverter systems," IEEE Trans. on Power Electronics, , vol.21, no.1, pp. 148-156, Jan. 2006

[113] K. Siri, C. Q. Lee, T. F. Wu, "Current distribution control for parallel connected converters: part I," IEEE Trans. Aerospace and Electronic Systems, vol. 28, July 1992, pp. 829-840.

[114] K. Siri, C. Q. Lee, T. F. Wu, "Current distribution control for parallel connected converters: part II," IEEE Trans. Aerospace and Electronic Systems, vol. 28, July. 1992, pp. 841-851.

[115] J.A. Abu-Qahoug, H.Mao, S. Deng, I. Batarshe. “Interleaved Current Doublers with Parallel Connected Transformers’ Primary and Secondary Sided”. Applied Power Electronics Conference and Exposition, APEC 2004, vol. 4, pp. 641-646, 2004.

[116] F.P. Singh, A.M. Khambadkone, “Giant Magneto Resistive (GMR) Effect Based Current Sensing Technique for Low Voltage/High Current Voltage Regulator Modules”. IEEE Transactions on Power Electronics, vol.23, pp. 915-925, March 2008.

[117] P. Alou, J. A. Cobos, O. García, R. Prieto, J. Ucedav “Input Voltage influence on Voltage Regulator Modules based on Multiphase Buck and Multiphase Half Bridge topologies”. Applied Power Electronics Conference and Exposition, APEC 2004. Vol.2, pp. 1282-1288. 2004.

[118] J.M. Guerrero, L. Hang, J. Uceda; "Control of Distributed Uninterruptible Power Supply Systems," IEEE Transactions on Industrial Electronics, vol.55, no.8, pp.2845-2859, Aug. 2008

[119] T. Hosi, “Control circuit for parallel operation of self-commutating inverters” Japanese Patent S56-13101, Apr.10, 1975.

[120] Jingtao Tan; Hua Lin; Jun Zhang; Jianping Ying, "A novel load sharing control technique for paralleled inverters," IEEE 34th Annual Power Electronics Specialist Conference, PESC 2003., vol.3, no., pp.1432,1437 vol.3, 15-19 June 2003.

[121] Daolian Chen, "Parallel inverters with high frequency pulse dc link," 23rd Annual IEEE Applied Power Electronics Conference and Exposition, 2008. APEC 2008., pp.1623,1627, 24-28 Feb. 2008.

[122] L. Luo, Z. Ye, R.-L. Lin, F. C. Lee, “A classification and evaluation of paralleling methods for power supply modules”. IEEE Power Electronics Specialists Conference, PESC 1999, pp. 901-908, Jul. 1999.

[123] R. Giral, L. Martinez-Salamero, S. Singer. “Interleaved converters operation based on CMC”, IEEE Trans, vol 47, pp.1330-1339, Sept. 2000.

[124] R. Crews, K. Nielson, “Interleaving is Good for Boost Converters, Too”. Available in: www.powerelectronics.com, May 1, 2008.

[125] D. J. Perreault, J. G; Kassakian, “Distributed interleaving of paralleled power converters”, IEEE Transaction on Circuits and Systems I: Fundamental Theory and Applications, vol 44, Aug.1997, pp 728-734.

[126] S. C. Babu, M. Veerachary, “Predictive controller for interleaved Boost converter”, IEEE International symposium on Industrial electronics, ISIE 2005, vol 2, pp. 577-581, June 2005.

[127] www.solarmax.com

[128] J.M.A. Myrzik, M. Calais, “String and Module Integrated Inverters for Single-Phase Grid Connected Photovoltaic Systems – A Review”, Power Tech Conference Proceedings, 2003 IEEE Bologna, Vol.2, Pp.8, 23-26 June 2003.

[129] G. Velasco-Quesada, F. Guinjoan-Gispert, R. Piqué-Lopez. “Energy efficiency improvement in reconfiguralbe grid-connected PV systems with adjustable sizing factor”, 23rd European Photovoltaic Solare Energy Conference, PVSEC 2008, 1-5 Sept. 2008, Valencia

[130] Fronius International press releases. *“Maximum Earning – In any Weather”*. June 2007. Available online at: www.fronious.com

[131] S. Lefebvre, F. Miserey, “Composants à semi-conducteur pour l’électronique de puissance”, Editions TEC & DOC, ISBN : 2-7430-0719-2, Lavoisier 2004

[132] Y. Panov, J. Rajagopalan, and F. C. Lee, "Analysis and design of N paralleled DC-DC converters with master-slave current sharing control," Applied Power Electronic Conference and Exposition, APEC 1997, vol. 1, pp. 436-442, Feb. 1997.

[133] M. Ponjavic and R. Djuric, "Current sharing for synchronised dc-dc converters operating in discontinuous conduction mode," IEE Procedings - Electric power applications, vol. 152, no 1, pp. 119-127, Janv. 2005.

[134] Y. El Basri, S. Petibon, B. Estibals, C. Alonso “New P&O MPPT Algorithm For FPGA Implementation”, 36th Annual Conference of IEEE Industrial Electronics Society, IECON 2010.

[135] S. Petibon, C. Cabal, F. Blanc, B. Estibals, C. Alonso, “Automatic data acquisition system for testing photovoltaic conversion chains performances in real conditions”, International Journal of Metrology and Quality Enginerring, 129-139. Dec, 2010.

[136] S. Petibon, “Nouvelles architectures distribuées de gestion et de conversion de l’énergie pour les applications photovoltaïques”, Ph.D. of Université Paul Sabatier, Toulouse 2009.

[137] J.F.Reynaud, “Recherches d’optimums d’énergies pour charge/décharge d'une batterie à technologie avancée dédiée à des applications photovoltaïques”, Ph.D. of Université Paul Sabatier, Toulouse 2011.

[138] www.actel.com

[139] IRFR024N MosFet, http://www.datasheets.com

[140] MBRD620CT Diode, http://www.datasheets.com

[141] “Reliability Aspects on Power Supplies”, available in www.ericsson.net.

[142] www.flir.com

[143] A.Berasategi, C.Cabal, C.Alonso and B.Estibals. "European efficiency improvement in photovoltaic applications by means of parallel connection of power converters". 13th European Conference on Power Electronics and Applications, EPE 2009, Barcelone (Spain), 8-10 September 2009.

[144] A.Berasategi, Y.El Basri, C.Cabal, B.Estibals, C.Alonso and M.Vermeersch. "Control laws to improve efficiency and average life time of an adaptive multi-phases converter dedicated to photovoltaic applications". International Conference on Renewable Energies and Power Quality (ICREPQ'11), Las Palmas de Gran Canaria (Spain), 13-15 April 2011.

[145] A.Berasategi, Y.El Basri, C.Cabal, B.Estibals, C.Alonso and M.Vermeersch. "An adaptive multi-phases converter for photovoltaic applications." International Exhibition & Conference for Power Electronics Intelligent Motion Power Quality (PCIM Europe 2011), Nuremberg (Germany), pp.363-367, 17-19 May 2011,